

International Project Research-Workshop (I)

# Proceedings of 4<sup>th</sup> Malaysia Mathematics in Industry Study Group (MMISG2023)

Chief Editor: Zaitul Marlizawati Zainuddin, Arifah Bahar

Editors: Shariffah Suhaila Syed Jamaludin, Zaiton Mat Isa, Nur Arina Bazilah Aziz,  
Taufiq Khairi Ahmad Khairuddin, Shaymaa M.H.Darwish, Ahmad Razin Zainal Abidin,  
Norhaiza Ahmad, Zainal Abdul Aziz, Hang See Pheng, Mohd Ali Khameini Ahmad

九州大学マス・フォア・インダストリ研究所

International Project Research-Workshop (I)

**Proceedings of 4<sup>th</sup> Malaysia Mathematics in  
Industry Study Group (MMISG 2023)**

■ **Chief Editors:**

Zaitul Marlizawati Zainuddin, Arifah Bahar

■ **Editors:**

Shariffah Suhaila Syed Jamaludin, Zaiton Mat Isa, Nur Arina Bazilah Aziz,  
Taufiq Khairi Ahmad Khairuddin, Shaymaa M.H. Darwish, Ahmad Razin Zainal Abidin,  
Norhaiza Ahmad, Zainal Abdul Aziz, Hang See Pheng, Mohd Ali Khameini Ahmad

## About MI Lecture Note Series

The Math-for-Industry (MI) Lecture Note Series is the successor to the COE Lecture Notes, which were published for the 21st COE Program “Development of Dynamic Mathematics with High Functionality,” sponsored by Japan’s Ministry of Education, Culture, Sports, Science and Technology (MEXT) from 2003 to 2007. The MI Lecture Note Series has published the notes of lectures organized under the following two programs: “Training Program for Ph.D. and New Master’s Degree in Mathematics as Required by Industry,” adopted as a Support Program for Improving Graduate School Education by MEXT from 2007 to 2009; and “Education-and-Research Hub for Mathematics-for-Industry,” adopted as a Global COE Program by MEXT from 2008 to 2012.

In accordance with the establishment of the Institute of Mathematics for Industry (IMI) in April 2011 and the authorization of IMI’s Joint Research Center for Advanced and Fundamental Mathematics-for-Industry as a MEXT Joint Usage / Research Center in April 2013, hereafter the MI Lecture Notes Series will publish lecture notes and proceedings by worldwide researchers of MI to contribute to the development of MI.

October 2022

Kenji Kajiwara

Director, Institute of Mathematics for Industry

## International Project Research-Workshop (I) Proceedings of 4<sup>th</sup> Malaysia Mathematics in Industry Study Group (MMISG2023)

MI Lecture Note Vol.97, Institute of Mathematics for Industry, Kyushu University  
ISSN 2188-1200

Date of issue: March 28, 2024

Chief Editors: Zaitul Marlizawati Zainuddin, Arifah Bahar

Editors: Shariffah Suhaila Syed Jamaludin, Zaiton Mat Isa, Nur Arina Bazilah Aziz,

Taufiq Khairi Ahmad Khairuddin, Shaymaa M.H. Darwish, Ahmad Razin Zainal Abidin,

Norhaiza Ahmad, Zainal Abdul Aziz, Hang See Pheng, Mohd Ali Khameini Ahmad

Publisher:

Institute of Mathematics for Industry, Kyushu University

Graduate School of Mathematics, Kyushu University

Motooka 744, Nishi-ku, Fukuoka, 819-0395, JAPAN

Tel +81-(0)92-802-4402, Fax +81-(0)92-802-4405

URL <https://www.imi.kyushu-u.ac.jp/>

## PREFACE

Mathematics in Industry Study Group is a collaborative problem-solving platform, uniting applied mathematicians to address real-world challenges across industries. Originating at Oxford University in the 1960s, this format has been instrumental in fostering practical solutions globally. At Universiti Teknologi Malaysia (UTM), we take pride in being pioneers, having introduced this study group to Malaysia since 2011. Our commitment continues and is evident in the recent organization of the 4<sup>th</sup> Malaysia Mathematics in Industry Study Group (MMISG2023) held at Menara Razak, Universiti Teknologi Malaysia, Kuala Lumpur, from November 20<sup>th</sup> to 22<sup>nd</sup>, organized by UTM Centre for Industrial and Applied Mathematics (UTM-CIAM). It was also made possible through the joint efforts of UTM Department of Mathematical Sciences, Faculty of Science; the Institute of Mathematics for Industry at Kyushu University, Japan; and MYHIMS Solutions LLP.

In general, the primary objective of Malaysia Mathematics in Industry Study Group-MMISG is to bridge the gap between academia and industry in Malaysia. It is a platform for STEM researchers to apply their expertise to solve industrial relevant problems, fostering a collaborative spirit between the two domains.

At MMISG2023, five industries, namely Ranhill SAJ Sdn Bhd, Total Logistic Services (M) Sdn. Bhd., MYHIMS Solution LLP, Langkawi Development Authority (LADA), and Ifactors Sdn. Bhd. presented their industrial problems. The problems spanned from model reconstruction at archaeological sites to cutting-edge developments in the logistic industry, and from forecasting volatility of agricultural commodity prices to optimizing operations processes.

To tackle the array of industrial issues, five cohesive sub-groups were formed, each guided by selected domain advisors. Within each group, members (termed as contributors) comprising of mathematicians, engineers, computer scientists played crucial roles in identifying key scientific issues and mathematical challenges. More than 50 contributors from ten institutions, both local and international, including Universiti Teknologi Malaysia, Universiti Malaya, Universiti Teknologi MARA, Universiti Malaysia Sabah, Universiti Kebangsaan Malaysia, Universiti Malaysia Terengganu, Universiti Malaysia Pahang Al-Sultan Abdullah, Universiti Teknologi Petronas, Kyushu University, Japan and Universitas Negeri Malang, Indonesia participated. Online discussions were also conducted with UTM-CIAM international partner at Oxford Centre for Industrial and Applied Mathematics (OCIAM). This collaborative effort harnessed the expertise from various institutions, enriching the event with a wide spectrum of mathematical and statistical approaches, all unified in the common goal of effective problem-solving. This initiative seamlessly aligns with UTM's mission to actively engage in both local and global networks, fostering partnerships with diverse organizations and industries to drive innovation through innovative solutions. The MMISG2023 has once again proven to be a pivotal event in fostering collaboration between academia and industry and further solidifies the event's reputation as a catalyst for innovation and problem-solving. It is evidenced from the positive feedback received from the participants: industrial representatives and contributors.

In addition to the solutions and recommendations generated for the industry, MMISG2023 has also catalyzed other significant outcomes, highlighting its impact as a significant program of Mathematics in Industry. Preparations are underway for Memorandum of Understanding and Letters of Collaboration between UTM-CIAM and the participating industries. Furthermore, technical reports have been published, and the MI Lecture Note serves as another avenue for disseminating MMISG outputs. Moreover, MMISG2023 marked the beginning of a larger project focused on system development for Ifactors Sdn. Bhd. The continuation of studies initiated during MMISG2023 is anticipated, with the expectation of yielding even more impactful results for the participating industries.

Chief Editors: Zaitul Marlizawati Zainuddin, Arifah Bahar  
February 2024

## CONTENTS

	<b>Page</b>
Preface	i
History of Malaysia Mathematics in Industry Study Group	1
Organizing Committee	3
Programme Schedule	4
List of Participants	5
Event Photos	8
<b>Abstracts</b>	
Ifactors Sdn. Bhd.: Transient Modelling of Subsea Cable Laying	11
LADA: 3D Shape Reconstruction of Charcoal Chamber Monument	12
Ranhill SAJ Sdn. Bhd.: Predictive Modelling of Pipe Burst Towards Sustainable Non-Revenue Water	13
TLS (M) Sdn. Bhd.: Tackling Carbon Emissions: Strategies for Medium and Heavy-Duty Trucks	14
MYHIMS Solution LLP: Price Forecasting Model for Main Vegetables in Malaysia	15
<b>Papers and Presentations</b>	
Ifactors Sdn. Bhd.: Transient Modelling of Subsea Cable Laying	16
LADA: 3D Shape Reconstruction of Charcoal Chamber Monument	51
Ranhill SAJ Sdn. Bhd.: Predictive Modelling of Pipe Burst Towards Sustainable Non-Revenue Water	69
TLS (M) Sdn. Bhd.: Tackling Carbon Emissions: Strategies for Medium and Heavy-Duty Trucks	107
MYHIMS Solution LLP: Price Forecasting Model for Main Vegetables in Malaysia	145

## **HISTORY OF MALAYSIA MATHEMATICS IN INDUSTRY (MMISG)**

Mathematics in Industry Study Group is a collaborative problem-solving platform, uniting applied mathematicians to address real-world challenges across industries. Originating at Oxford University in the 1960s, this format has been instrumental in fostering practical solutions globally.

At Universiti Teknologi Malaysia (UTM), we take pride in being pioneers, having introduced this study group to Malaysia since 2011. The second MISG was held in 2014 and the third in 2015.

### **MMISG 2011**

The 1<sup>st</sup> MMISG was attended by 4 industries with 6 problems.

- i) Optimal Placement of Security Cameras in In-door Spaces from MIMOS Bhd.
- ii) Efficient Reasoning in Conceptual Graph Knowledge Representation Model from MIMOS Bhd.
- iii) River Pollution Problem in Iskandar Malaysia Region from J-Biotech
- iv) Cardiological Problem from KPJ Johor
- v) Fouling in Heat Exchangers of Refineries from Petronas Penapisan (Melaka) Sdn. Bhd.
- vi) Oil Refinery Water Supply from Petronas Penapisan (Melaka) Sdn. Bhd.

### **MMISG 2014**

The 2<sup>nd</sup> MMISG was attended by 6 industries with 6 problems.

- i) Mathematical Modelling and Optimization for Biological-based Treatment of Taman Timor Oxidation Pond, Johor from J-Biotech
- ii) River Pollution Attenuation in Aquifers Using Bank Infiltration Technique from National Water Research Institute of Malaysia (NAHRIM)
- iii) Development of early warning system for rice blast and brown planthopper (BPH), pest and disease of rice from Malaysian Agricultural Research and Development Institute (MARDI)
- iv) Coronary Bifurcation – Effect of Stent on Blood Flow from KPJ Johor
- v) Green Propulsion Regenerative Electromagnetic Suspension System (GPRESS) from PROTON
- vi) Cost Effective Minimum Water and Energy Networks for The Industries from PROSPECT

### **MMISG 2015**

The 3<sup>rd</sup> MMISG was attended by 7 industries with 7 problems.

- i) Modelling Thiophene and Pyran -4-ONE to Early Signs of Ganoderma Infection in Oil Palms from Agri-D Sdn. Bhd.
- ii) Optimal Stock Level and Inventory Policy from EP Manufacturing Berhad (EPMB)

- iii) Subsea Cable Laying Problem from Ifactors Sdn. Bhd.
- iv) Multi-Sensor Imaging System for Target Detection from IR Technic Sdn. Bhd.
- v) Modelling of Optimal Conservation of Giant Clam Species in Johor Islands from J-Biotech
- vi) Modelling and Optimization of Clay-based Product for Green Cleansing from MIFF Marketing Sdn. Bhd.
- vii) Magneto-Rheological Semi-Active Suspension System (MaRS) from PROTON

Our commitment continues and is evident in the recent organization of the 4<sup>th</sup> Malaysia Mathematics in Industry Study Group (MMISG2023) held at Menara Razak, Universiti Teknologi Malaysia, Kuala Lumpur, from November 20<sup>th</sup> to 22<sup>nd</sup>, 2023.

## **ORGANIZING COMMITTEE**

**Chairman:** Assoc. Prof. Dr. Zaitul Marlizawati Zainuddin  
**Co-Chair:** Assoc. Prof. Dr. Shariffah Suhaila Syed Jamaludin  
**Secretary:** Dr. Zaiton Mat Isa  
**Assistant Secretary:** Mrs. Nik Zetti Amani Nik Faudzi  
**Treasurer:** Dr. Nur Arina Bazilah Aziz  
**Assistant Treasurer:** Mrs. Siti Nur Sakinah Ahmad

### **Scientific**

Assoc. Prof. Dr. Arifah Bahar  
Prof. Dr. Sharidan Shafie  
Dr. Taufiq Khairi Ahmad Khairuddin  
Assoc. Prof. Dr. Zarina Mohd Khalid  
Assoc. Prof. Dr. Zuhaila Ismail  
Prof. Dr. Zulkepli Majid  
Dr. Koh Meng Hock  
Dr. Adila Firdaus Arbain

### **Technical and Facility**

Mr. Wan Rohaizad Wan Ibrahim  
Dr. Ahmad Qushairi Mohamed  
Assoc. Prof. Dr. Yeak Su Hoe  
Dr. Amir Syafiq Syamin Syah Amir Hamzah  
Dr. Tan Lit Ken

### **Protocol, Food, and Hospitality**

Assoc. Prof. Dr. Norhaiza Ahmad  
Dr. Syarifah Zyurina Nordin  
Ms. Siti Zulfarina Fadzli  
Dr. Noorehan Yaacob

### **Publication**

Dr. Hang See Pheng  
Assoc. Prof. Dr. Shariffah Suhaila Syed Jamaludin  
Dr. Mohd Ali Khameini Ahmad

### **Accommodation, Transportation, and Registration**

Dr. Nur Arina Bazilah Kamisan  
Dr. Mohammad Izat Emir Zulkifly  
Dr. Hafizah Farhah Saipan @ Saipol  
Dr. Dzuliana Fatin Jamil  
Mrs. Nurul Husna Mohammad Sairi  
Mrs. Wong Yah Jin  
Ms. Aniza Akaram

### **Intellectual Property**

Dr. Ahmad Razin Zainal Abidin  
Dr. Izyan Hazwani Hashim



## PROGRAMME SCHEDULE

Time	Activity	Venue
<b>20 November 2023 (Monday)</b>		
0830 – 0915	Registration & Morning Tea	Menara Razak Seminar Hall/Banquet Hall
0915 – 0945	Opening Ceremony/Photo Session	Menara Razak Seminar Hall
0950 – 1010	Ranhill SAJ Problem Presentation	
1015 – 1035	MYHIMS Solutions Problem Presentation	
1040 – 1100	Ifactors Sdn Bhd Problem Presentation	
1105 – 1125	TLS Problem Presentation	
1130 – 1150	LADA problem Presentation	
1200 – 1400	Lunch Break	Banquet Hall
1400 – 1730 1530 – 1600	Group Formation/Group Discussion Afternoon Tea	Room 2, 3, 4, 5, 7 Banquet Hall
<b>21 November 2023 (Tuesday)</b>		
0830 – 1230 1000 – 1030	Group Discussion Morning Tea	Room 2, 3, 4, 5, 7 Banquet Hall
1230 – 1400	Lunch Break	Banquet Hall
1400 – 1730 1530 – 1600	Group Discussion Afternoon Tea	Room 2, 3, 4, 5, 7 Banquet Hall
<b>22 November 2023 (Wednesday)</b>		
0830 – 1100 0930 – 1000	Group Discussion Morning Tea	Room 2, 3, 4, 5, 7 Banquet Hall
1105 – 1200	Output Presentation to The Industry	Room 2, 3, 4, 5, 7
1205 – 1215	Closing Ceremony	Banquet Hall
1215	Lunch	Banquet Hall

## LIST OF PARTICIPANTS

NO	NAME	EMAIL	AFFILIATION	AFFILIATION CODE
1.	Sharidan Shafie	<a href="mailto:sharidan@utm.my">sharidan@utm.my</a>	UTM: Universiti Teknologi Malaysia	1
2.	Zulkepli Majid	<a href="mailto:zulkeplimajid@utm.my">zulkeplimajid@utm.my</a>	UTM: Universiti Teknologi Malaysia	1
3.	Arifah Bahar	<a href="mailto:arifah@utm.my">arifah@utm.my</a>	UTM: Universiti Teknologi Malaysia	1
4.	Norhaiza Ahmad	<a href="mailto:norhaiza@utm.my">norhaiza@utm.my</a>	UTM: Universiti Teknologi Malaysia	1
5.	Shariffah Suhaila Syed Jamaludin	<a href="mailto:suhailasj@utm.my">suhailasj@utm.my</a>	UTM: Universiti Teknologi Malaysia	1
6.	Zaitul Marlizawati Zainuddin	<a href="mailto:zmarlizawati@utm.my">zmarlizawati@utm.my</a>	UTM: Universiti Teknologi Malaysia	1
7.	Istas Fahrurrazi Nusyirwan	<a href="mailto:istaz@utm.my">istaz@utm.my</a>	UTM: Universiti Teknologi Malaysia	1
8.	Zulhasni Abdul Rahim	<a href="mailto:zulhasni@utm.my">zulhasni@utm.my</a>	UTM: Universiti Teknologi Malaysia	1
9.	Ahmad Razin Zainal Abidin	<a href="mailto:arazin@utm.my">arazin@utm.my</a>	UTM: Universiti Teknologi Malaysia	1
10.	Dzuliana Fatin Jamil	<a href="mailto:dzulianafatin@utm.my">dzulianafatin@utm.my</a>	UTM: Universiti Teknologi Malaysia	1
11.	Hafizah Farhah Saipan@Saipol	<a href="mailto:hafizah.farhah@utm.my">hafizah.farhah@utm.my</a>	UTM: Universiti Teknologi Malaysia	1
12.	Mohd Ali Khameini Ahmad	<a href="mailto:ma.khameini@utm.my">ma.khameini@utm.my</a>	UTM: Universiti Teknologi Malaysia	1
13.	Noorehan Yaacob	<a href="mailto:noorehan@utm.my">noorehan@utm.my</a>	UTM: Universiti Teknologi Malaysia	1
14.	Nur Arina Bazilah Aziz	<a href="mailto:nurarina@utm.my">nurarina@utm.my</a>	UTM: Universiti Teknologi Malaysia	1
15.	Syarifah Zyurina Nordin	<a href="mailto:szyurina@utm.my">szyurina@utm.my</a>	UTM: Universiti Teknologi Malaysia	1
16.	Tan Lit Ken	<a href="mailto:tlken@utm.my">tlken@utm.my</a>	UTM: Universiti Teknologi Malaysia	1
17.	Taufiq Khairi Ahmad Khairuddin	<a href="mailto:taufiq@utm.my">taufiq@utm.my</a>	UTM: Universiti Teknologi Malaysia	1
18.	Zaiton Mat Isa	<a href="mailto:zaitonmi@utm.my">zaitonmi@utm.my</a>	UTM: Universiti Teknologi Malaysia	1
19.	Adila Firdaus Arbain	<a href="mailto:adilafirdaus@utm.my">adilafirdaus@utm.my</a>	UTM : Universiti Teknologi Malaysia	1
20.	Mohamad S.J. Darwish	<a href="mailto:sjmohamad@utm.my">sjmohamad@utm.my</a>	UTM: Universiti Teknologi Malaysia	1
21.	Mohd Hazmil Syahidy Abdol Azis	<a href="mailto:hazmil@utm.my">hazmil@utm.my</a>	UTM: Universiti Teknologi Malaysia	1
22.	Shaymaa M.H. Darwish	<a href="mailto:mdshaymaa@utm.my">mdshaymaa@utm.my</a>	UTM: Universiti Teknologi Malaysia	1
23.	Siti Mariam Norrulashikin	<a href="mailto:sitimariam@utm.my">sitimariam@utm.my</a>	UTM: Universiti Teknologi Malaysia	1
24.	Siti Rohani Mohd Nor	<a href="mailto:sitirohani@utm.my">sitirohani@utm.my</a>	UTM: Universiti Teknologi Malaysia	1
25.	Aniza Akaram	<a href="mailto:aniza.akaram@utm.my">aniza.akaram@utm.my</a>	UTM: Universiti Teknologi Malaysia	1
26.	Wan Rohaizad Wan Ibrahim	<a href="mailto:wrohaizad@utm.my">wrohaizad@utm.my</a>	UTM: Universiti Teknologi Malaysia	1

NO	NAME	EMAIL	AFFILIATION	AFFILIATION CODE
27.	Justin Chan Zhe	<a href="mailto:iczhe09@gmail.com">iczhe09@gmail.com</a>	UTM: Universiti Teknologi Malaysia	1
28.	Khalid Solaman Almadani	<a href="mailto:almadani@graduate.utm.my">almadani@graduate.utm.my</a>	UTM: Universiti Teknologi Malaysia	1
29.	Lai Kok Yee	<a href="mailto:lai931010@hotmail.com">lai931010@hotmail.com</a>	UTM: Universiti Teknologi Malaysia	1
30.	Nik Zetti Amani Nik Faudzi	<a href="mailto:nikzettiamani@utm.my">nikzettiamani@utm.my</a>	UTM: Universiti Teknologi Malaysia	1
31.	Ruzaini Zulhusni Bin Puslan	<a href="mailto:ruzainizulhusni@gmail.com">ruzainizulhusni@gmail.com</a>	UTM: Universiti Teknologi Malaysia	1
32.	Shukur Hasan	<a href="mailto:shukur.hasan@gmail.com">shukur.hasan@gmail.com</a>	UTM: Universiti Teknologi Malaysia	1
33.	Zainol Mustafa	<a href="mailto:zbhm@ukm.edu.my">zbhm@ukm.edu.my</a>	UKM: Universiti Kebangsaan Malaysia	2
34.	Zulkifli Mohd Nopiah	<a href="mailto:zmn@ukm.edu.my">zmn@ukm.edu.my</a>	UKM: Universiti Kebangsaan Malaysia	2
35.	Nor Hamizah Miswan	<a href="mailto:norhamizah@ukm.edu.my">norhamizah@ukm.edu.my</a>	UKM: Universiti Kebangsaan Malaysia	2
36.	Razik Ridzuan Mohd Tajuddin	<a href="mailto:rrmt@ukm.edu.my">rrmt@ukm.edu.my</a>	UKM: Universiti Kebangsaan Malaysia	2
37.	Ramhya Kathirayson	<a href="mailto:ramhya1311@gmail.com">ramhya1311@gmail.com</a>	UKM: Universiti Kebangsaan Malaysia	2
38.	Adibah Shuib	<a href="mailto:adibah@tmsk.uitm.edu.my">adibah@tmsk.uitm.edu.my</a>	UITM : Universiti Teknologi Mara	3
39.	Abd Manan Samad	<a href="mailto:dr_abdmanansamad@ieee.org">dr_abdmanansamad@ieee.org</a>	UITM: Universiti Teknologi Mara	3
40.	Zaharah Mohd Yusoff	<a href="mailto:zmy1208@uitm.edu.my">zmy1208@uitm.edu.my</a>	UITM : Universiti Teknologi Mara	3
41.	Ismail Ma'arof	<a href="mailto:ismailmaarof@uitm.edu.my">ismailmaarof@uitm.edu.my</a>	UITM : Universiti Teknologi Mara	3
42.	Mohd Mahayaudin Bin Mansor	<a href="mailto:maha@uitm.edu.my">maha@uitm.edu.my</a>	UITM : Universiti Teknologi Mara	3
43.	Auni Aslah Bin Mat Daud	<a href="mailto:auni_aslah@umt.edu.my">auni_aslah@umt.edu.my</a>	UMT : Universiti Malaysia Terengganu	4
44.	Roslinazairimah Zakaria	<a href="mailto:roslinazairimah@ump.edu.my">roslinazairimah@ump.edu.my</a>	UMP : Universiti Malaysia Pahang	5
45.	Nor Azuana Ramli	<a href="mailto:azuana@umpsa.edu.my">azuana@umpsa.edu.my</a>	UMP : Universiti Malaysia Pahang	5
46.	Norazaliza Mohd Jamil	<a href="mailto:norazaliza@ump.edu.my">norazaliza@ump.edu.my</a>	UMP: Universiti Malaysia Pahang	5
47.	Syahrizal Bin Salleh	<a href="mailto:syahrizal@gmail.com">syahrizal@gmail.com</a>	UMP: Universiti Malaysia Pahang	5
48.	Jamaliatul Badriyah	<a href="mailto:jamailatul.badriyah.mat@um.ac.id">jamailatul.badriyah.mat@um.ac.id</a>	Universitas Negeri Malang	6
49.	Siti Rahayu Binti Mohd Hashim	<a href="mailto:rahayu@ums.edu.my">rahayu@ums.edu.my</a>	UMS: Universiti Malaysia Sabah	7
50.	Mohd Ismail Abd Aziz	<a href="mailto:mismail@utm.my">mismail@utm.my</a>	MYHIMS Solutions	8
51.	Fadhilah Yusof	<a href="mailto:fadhilahy@utm.my">fadhilahy@utm.my</a>	MYHIMS Solutions	8
52.	Zainal Abdul Aziz	<a href="mailto:zainalaz@utm.my">zainalaz@utm.my</a>	MYHIMS Solutions	8
53.	Aimi Athirah Ahmad	<a href="mailto:aimiathirah@mardi.gov.my">aimiathirah@mardi.gov.my</a>	MYHIMS Solutions	8
54.	Tagami, Daisuke	<a href="mailto:tagami@imi.kyushu-u.ac.jp">tagami@imi.kyushu-u.ac.jp</a>	Kyushu University	9
55.	Shota Shigetomi	<a href="mailto:s-shigetomi@imi.kyushu-u.ac.jp">s-shigetomi@imi.kyushu-u.ac.jp</a>	Kyushu University	9
56.	Putri Aidila Sofia Abu Bakar	<a href="mailto:aidila@ifactors.com.my">aidila@ifactors.com.my</a>	Ifactors	10

<b>NO</b>	<b>NAME</b>	<b>EMAIL</b>	<b>AFFILIATION</b>	<b>AFFILIATION CODE</b>
57.	Kamarudin Ismail	<u><a href="mailto:kamarudin@ifactors.com.my">kamarudin@ifactors.com.my</a></u>	Ifactors	10
58.	Muhammad Hanis Bin Kamaruddin	<u><a href="mailto:muhammadhanis@graduate.utm.my">muhammadhanis@graduate.utm.my</a></u>	Ifactors	10
59.	Norazlina Ismail	<u><a href="mailto:i-norazlina@utm.my">i-norazlina@utm.my</a></u>	Ranhill SAJ	11
60.	Aidah Natasah Sulaiman	<u><a href="mailto:aidah.natasah@ranhill.com.my">aidah.natasah@ranhill.com.my</a></u>	Ranhill SAJ	11
61.	Nur Nabilah Jamal	<u><a href="mailto:nabilah.jamal@gmail.com">nabilah.jamal@gmail.com</a></u>	Ranhill SAJ	11
62.	Raja Dzulfetrie Sa'ad	<u><a href="mailto:dzulfetrie@tls.com.my">dzulfetrie@tls.com.my</a></u>	TLS	12
63.	Zainal Azman Bin Zawawi	<u><a href="mailto:zainal@tls.com.my">zainal@tls.com.my</a></u>	TLS	12
64.	Hanita Daud	<u><a href="mailto:hanita_daud@utp.edu.my">hanita_daud@utp.edu.my</a></u>	UTP: Universiti Teknologi Petronas	13

**EVENT PHOTOS**



MMISG2023 group photo following the opening ceremony, at Dewan Seminar Menara Razak, UTM Kuala Lumpur.



Industry representatives presenting their industrial problems to the participants of MMISG2023.



Intense discussion among industrial representatives, domain advisors and contributors of respective industrial problems



The dedicated organizing team of MMISG2023 comprising of staff from UTM-CIAM, UTM Department of Mathematical Sciences, Faculty of Science and UTM- Malaysia-Japan International Institute of Technology

## *Transient Modeling of Subsea Cable Laying*

### **Industrial Representative:**

Kamarudin Ismail<sup>10</sup>, Putri Aidila Sofia Abu Bakar<sup>10</sup>

### **Contributors:**

Zainal Abd Aziz<sup>8</sup>, Sharidan Shafie<sup>1</sup>, Ahmad Razin Zainal Abidin<sup>1</sup>,  
Shaymaa M. H. Darwish<sup>1</sup>, Mohd Hazmil Syahidy Abdol Azis<sup>1</sup>, Nik  
Zetti Amani Nik Faudzi<sup>1</sup>, Noorehan Yaacob<sup>1</sup>, Dzuliana Fatin Jamil<sup>1</sup>,  
Daisuke Tagami<sup>9</sup>, Auni Aslah Bin Mat Daud<sup>4</sup>, Norazaliza Mohd  
Jamil<sup>5</sup>

The installation of subsea cables, involving the deployment of cables on the ocean floor, is significantly influenced by environmental factors such as ocean currents and seabed characteristics. Modeling this process is crucial during both planning and operational phases, as it enables accurate predictions and control over cable placement, thereby minimizing risks and ensuring the effectiveness, safety, and environmental sustainability of subsea installations. The challenge in such modeling lies in the dynamic nature of the ocean environment, which includes fluctuating currents, waves, and winds, coupled with the complexity of varying seabed terrains, requiring the consideration of transient effect. This report proposes the development of a dynamic model for cable laying that accounts for wave motion and the irregularities of the seafloor, merging theoretical research with practical applications and experience, creating relevant and applicable models for real-world operations. The model development is structured into three phases. The first phase involves a steady-state model focused on a rough seabed, omitting the impact of waves. This model is based on the Euler–Bernoulli equation that aims to predict the cable layout at a specific time, considering initial tension, cable properties, and fluid dynamics. The complexity is reduced by introducing a non-dimensional set of equations, which scales down all engineering parameters to two key factors: fluid hydrodynamic drag and cable bending stiffness. Applied across various sea depths and using MATLAB for numerical solutions, the finding suggests that cable elevation increases with depth. The second phase tackles a time-dependent issue, factoring in significant wave motion on a hypothetically flat seabed, thus leading to a highly nonlinear formulation that requires the inclusion of a transient model. In the final phase, the report integrates both models to represent water depth as a function of time and arc length for more comprehensive insights. Expected results from this integration are anticipated to enhance the accuracy and practicality of the developed model in the real cable installation operation.



### ***3D Shape Reconstruction of Charcoal Chamber Monument***

#### **Industrial Representative:**

Rasanubari Asmah Rahmah Abd Hamid<sup>14</sup>

#### **Contributors:**

Taufiq Khairi Ahmad Khairuddin<sup>1</sup>, Zulkepli Majid<sup>1</sup>, Mohd Ali  
Khameini Ahmad<sup>1</sup>, Abd Manan Samad<sup>3</sup>, Ismail Ma'arof<sup>3</sup>, Shota  
Shigetomi<sup>9</sup>

Langkawi Island is a world-class tourism destination as it contains various historical assets and because of this, Langkawi Island has been recognized as one of the world-class Geopark sites by UNESCO. As a world-class Geopark area and site, Langkawi Island provides 38 Geosites for tourists to visit. One of the tourism assets found in the Geosite area is the charcoal chamber monument in Kubang Badak, Bukit Menora. According to historians, there were originally 12 charcoal chamber monuments but, as time has passed, only three of these structures have endured, and they too have weathered the years, with only partial sections of their original construction remain. The agency Langkawi Development Authority (LADA) then has been entrusted to preserve and conserve these valuable relics for tourism activities and local economy development. The main purpose of this study is to redevelop the complete charcoal chamber monument by using the combination of three-dimensional (3D) modelling in geoinformation and also mathematical modelling. Specifically, the objective of this research is to develop a 3D model of the remaining historic charcoal chamber using Geospatial technology before simulating the partial data from the model with the appropriate mathematical formulation, in order to generate the complete 3D model of the monument. Besides, geometric modeling involving common surfaces such as elliptic paraboloids and hemispheres will be used in developing and predicting the actual dimensions of the charcoal chamber. Apart from that, Mathematica and Matlab software will be used to display the 3D model of the charcoal chamber. Based on the latest information during the discussion session held, three 3D models of the charcoal chamber have been proposed at the end of this MMISG 2023 workshop.

## *Predictive Modeling of Pipe Burst Towards Sustainable Non-Revenue Water*

### **Industrial Representative:**

Aida Natasah Sulaiman<sup>11</sup>, Nur Nabilah Jamal<sup>11</sup>, Norazlina Ismail<sup>11</sup>

### **Contributors:**

Norhaiza Ahmad<sup>1</sup>, Zainol Mustafa<sup>2</sup>, Arifah Bahar<sup>1</sup>, Zaiton Mat Isa<sup>1</sup>, Ista Fahrurazi Nursyirwan<sup>1</sup>, Mohamad S.J. Darwish<sup>1</sup>, Tan Lit Ken<sup>1</sup>, Hafizah Farhah Saipan @ Saipol<sup>1</sup>, Aniza Akaram<sup>1</sup>,  
Ramhya Kathirayson<sup>2</sup>

Pipe burst is one of the major contributors to water loss in water supply systems that significantly increase the Non-Revenue Water (NRW) level. The water authority has set a target to reduce NRW to 25.5% by 2024. Although the NRW level is currently close to the target at approximately 25.40% or 457 million liters per day (MLD) as of September 2023, there is a need for ongoing monitoring to prevent any potential increase in NRW if water losses are not effectively controlled. The key challenge identified is the timely detection and prediction of pipe bursts, as this is crucial for the organization to make informed decisions in monitoring water losses and minimizing the time taken to address and rectify pipe bursts. In response to this challenge, two approaches are suggested with the primary focus on the statistical approach, alongside with the Artificial Neural Network (ANN) model. For the statistical approach, the Exponentially Weighted Moving Average (EWMA) Control Charts is used to identify transient signals related to pipe bursts. Data preprocessing has been conducted, and the control charts have been applied to detect anomalies associated with pipe bursts. Feature-based data also been implemented to further enhance the detection capabilities. The study concludes that a combination of dynamic thresholding based on weekly patterns, targeted analysis of reliable Flow data, and adaptive parameter settings in control charts, particularly with a focus on shorter time series, enhance the effectiveness of pipe burst detection. The findings recommend a pragmatic approach to address the challenges posed by variations and trends in water monitoring data, providing valuable insights for proactive water system management and minimizing the impact of false alarms in anomaly detection. Additionally, utilizing pressure, flow, and CPP pressure data as inputs, an Artificial Neural Network (ANN) model is trained to predict pipe bursts. By learning from historical data where instances of bursts are correlated with specific patterns in these parameters, the ANN can quickly analyze current data upon receiving a complaint call and predict the likelihood of a forthcoming burst.

## **Tackling Carbon Emissions: Strategies for Medium and Heavy-Duty Trucks**

### **Industrial Representative:**

*Raja Dzulfetrie Sa 'ad*<sup>1,2</sup>  
*Zainal Azman Zawawi*<sup>1,2</sup>

### **Contributors:**

Nur Arina Bazilah Aziz<sup>1</sup>, Adibah Shuib<sup>3</sup>, Zaitul Marlizawati Zainuddin<sup>1</sup>, Zulkifli Mohd Nopiah<sup>2</sup>, Zulhasni Abdul Rahim<sup>1</sup>, Zulkarnain Abdul Latiff<sup>1</sup>, Zaharah Mohd Yusoff<sup>3</sup>, Jamaliatul Badriyah<sup>6</sup>, Syarifah Zyurina Nordin<sup>1</sup>, Wan Rohaizad Wan Ibrahim<sup>1</sup>, Shukur Hassan<sup>1</sup>, Khalid Solaman Almadani<sup>1</sup>

The escalating carbon emissions from transportation, particularly from medium-duty and heavy-duty trucks, pose significant challenges to the automotive supply chain logistics sector. Notably, the transport sector accounts for a substantial 28.8% of total fossil fuel combustion emissions, exceeding the global average. In response, Malaysia has committed to ambitious targets, aiming for net-zero emissions by 2050 and a 45% reduction in CO<sub>2</sub> intensity relative to GDP by 2030. In accordance with this, industries, including Total Logistic Services (M) Sdn. Bhd. (TLS) are mandated to comply with regulations to mitigate carbon emissions. As part of the Toyota Tsusho Group, TLS is engaged in a three-year strategy focusing on route optimization, eco-driving training, vehicle maintenance, and transitioning to electric trucks to tackle this challenge. In addition, TLS is also exploring avenues to further reduce the carbon emissions from their medium-duty and heavy-duty trucks. The discussion begins by examining the formula used to calculate carbon emissions, analyzing the parameters influencing carbon emissions, and proposing initiatives associated with these parameters. Additionally, the discussion also delves into tools used to measure carbon emissions. In conclusion, it is asserted that the formula for calculating carbon emissions is adequate for estimating the emissions from trucks without the need for specific tools. The controllable factor identified is fuel efficiency, which is closely linked to driving style. Consequently, initiatives aimed at improving drivers' driving style are recommended.

*Price Forecasting Model for Main Vegetables in  
Malaysia*

**Industrial Representative:**

Aimi Athirah Ahmad<sup>8</sup>

**Contributors:**

Shariffah Suhaila Syed Jamaludin<sup>1</sup>, Fadhilah Yusof<sup>8</sup>,  
Roslinazairimah Zakaria<sup>5</sup>, Mohd Mahayaudin Mansor<sup>3</sup>,  
Nor Hamizah Miswan<sup>2</sup>, Siti Rahayu Mohd Hashim<sup>7</sup>,  
Siti Mariam Norrulashikin<sup>1</sup>, Siti Rohani Mohd Nor<sup>1</sup>,  
Hanita Daud<sup>13</sup>, Razik Ridzuan Mohd Tajuddin<sup>2</sup>,  
Syahrizal Salleh<sup>5</sup>, Ruzaini Zulhusni Puslan<sup>1</sup>

A substantial portion of household income in Malaysia is allocated to food expenditures, and chili is a staple ingredient in Malaysian cuisine. Fluctuations in chili prices directly affect the cost of living for individuals and families, impacting their purchasing power and overall well-being. Forecasting chili prices helps in effective supply chain management. Producers, distributors, and retailers can plan and adjust their operations based on anticipated price trends. This, in turn, contributes to the country's efficiency and stability of the chili supply chain. This study emphasizes the importance of comparing various forecasting models to identify the most accurate predictors of chili prices. The goal is to develop a model that can contribute to more informed decision-making in crop production and market interventions, ultimately promoting stability in the chili industry and ensuring sustainable practices. Statistical models and time series forecasting models, which include multiple linear regression (MLR), AutoRegressive Integrated Moving Average with exogenous inputs (ARIMAX), and machine learning algorithms that consist of Support Vector Regression (SVR), Random Forest Regression (RFR), Artificial Neural Network (ANN) and Long Short Term Memory (LSTM) were tested and compared. SVR and RF under machine learning algorithms performed best as the forecasted model followed by ARIMAX. ARIMAX models, extension of the ARIMA model, effectively capture and predict patterns by incorporating significant exogenous variables. Overall, the results show that the price of fertilizers, Movement Control Order (PKP) season, and chili production significantly affect the prices of chilies.

*Transient Modeling of Subsea Cable Laying*

- Industry Representatives : Kamarudin Ismail<sup>10</sup>, Putri Aidila Sofia Abu Bakar<sup>10</sup>  
(Ifactors Sdn. Bhd.)
- Study Group Contributors : Zainal Abd Aziz<sup>8</sup>, Sharidan Shafie<sup>1</sup>, Ahmad Razin Zainal  
Abidin<sup>1</sup>, Shaymaa M. H. Darwish<sup>1</sup>, Mohd Hazmil  
Syahidy Abdol Azis<sup>1</sup>, Nik Zetti Amani Nik Faudzi<sup>1</sup>,  
Noorehan Yaacob<sup>1</sup>, Dzuliana Fatin Jamil<sup>1</sup>, Daisuke  
Tagami<sup>9</sup>, Auni Aslah Bin Mat Daud<sup>4</sup>, Norazaliza Mohd  
Jamil<sup>5</sup>

**1.1 Introduction**

Subsea cable laying, essential in the development of global communication and power networks, involves deploying cables on the ocean floor, a process influenced by a range of environmental factors, including ocean currents and seabed characteristics. Cable laying modeling is vital in planning and operation as it enables precise prediction and control of cable placement, minimizing risks and ensuring efficient, safe, and environmentally responsible subsea installations.

Ifactors is a subsea cable installer that provides services to Telco operators and oil and gas companies that need to install subsea cable for their IT or DATA network infrastructure. The types of cable installed are mainly fibre optics and composite. Ifactors is the only local installer that has experience in laying deep water (>2000m) and also the only Malaysian company that carries the ISO 9001:2008 certification. Among the projects handled by Ifactors were, Deep Water repair (>2500m) in Indonesia, Deep Water lay from Bali to Jawa Island, Indonesia and also Petronas platform interconnection with shore in Turkmenistan and Peninsular. With over a decade of experience, including cable laying in challenging locations like the deep waters, Ifactors has emerged as a leading service provider in the cable laying sector in the Asia Pacific Region. This study focuses on the cable laying challenges encountered by Ifactors.

Installing subsea cables is a routine responsibility for engineers, involving the placement of cables and pipelines beneath the ocean floor. The laying process is a critical and perilous phase for the cable, demanding meticulous control to prevent any damage while

optimizing the speed of installation. During cable installation, a common challenge is the occurrence of false slack. Submarine cables are usually deployed by lowering them from a

laying vessel into seawater until they reach the seafloor. Throughout this process, the cables are subjected to various forces, requiring careful consideration in cable design. While the conventional approach involves analyzing cables during installation with the assumption of a horizontally flat seafloor, the real seafloor is marked by roughness. Bathymetric maps of the seafloor reveal faults, folds, and on-bottom channel systems. These irregularities may lead to the development of false slack in certain areas or cause cable hanging in others, ultimately resulting in cable failure. Despite engineering methods that can partially mitigate seafloor roughness, it is essential to consider the actual seafloor conditions during the cable-laying process.

The laying of undersea communication cables spans nearly all of the Earth's oceans. The establishment of this global communication infrastructure is becoming more commercially competitive, where technical considerations like the speed and precision of cable laying can yield substantial commercial advantages. In this environment, the viability of high-speed cable laying is crucial, as is a comprehension of the temporary dynamics involved in the cable laying process when the cable ship adjusts its speed. Forecasting the transient behavior of the cable during installation necessitates a nonlinear time-domain analysis. Once this analysis is conducted, its verification presents a challenging problem.

Effective cable laying operations demand the prevention of elevated dynamic tensions, as they can lead to adverse consequences. While numerous researchers have addressed the static and dynamic facets of the cable laying process, only a limited number have delved into comprehensive cable dynamics due to challenges associated with the interaction between the cable and the ship in waves.

Hence, to initiate the subsea cable installation, Ifactors company must ascertain the optimal quantity of cable necessary for the successful completion of the laying process in challenging seabed conditions. This determination is contingent on establishing the suitable hydraulic brake speed and manually regulating the residual tension of the cable. The objective of this study is to develop a mathematical model and conduct a numerical simulation capable of offering a reliable prediction for the transient behaviour of cables laid in non-flat seabed environments. This includes considering the impact of wave excitation, cable/ship interaction, and cable elasticity.

In the initial phases, the study employs a steady-state model across different water depths to replicate the seabed shape and wave heights. Following this, the research advances to develop a dynamic model designed to enable real-time control of the cable laying operation in challenging sea conditions. The dynamic model aims to address the impact of wave excitation, cable/ship interaction, irregular shape of seafloor and cable elasticity.

## 1.2 Problem Statement

The process of subsea cable installation faces challenges, such as the occurrence of false slack, where irregularities in the rough seafloor can lead to cable failure. Submarine cables, typically deployed from laying vessels, are subject to various forces that necessitate meticulous cable design. The conventional approach assumes a flat seafloor; however, the actual seabed is often marked by roughness. This fact underscores the importance of considering the real conditions of the seafloor during cable laying. Another primary problem in optimizing cable laying operations is the prevention of heightened dynamic tensions, which can lead to serious adverse consequences. This issue becomes more pronounced in adverse weather conditions.

High-speed cable laying requires a comprehensive understanding of the dynamic changes that occur when adjusting the speed of the cable-laying ship. Accurately predicting the cable's transient behavior under these conditions involves complex nonlinear time-domain analysis, posing significant challenges in verification. To tackle these issues, incorporating transient modeling phase-by-phase is crucial, particularly focusing on dynamic loading conditions and the movements of the laying vessel. Despite the extensive exploration of static and dynamic aspects of cable laying in many research studies, there exists a noticeable research gap in the in-depth study of the intricate interactions between the cable and ship, particularly in wave-influenced environments. This gap is a major challenge to developing precise and reliable models for subsea cable installation, crucial for real-world operations.

## 1.3 Methodology

Our methodology comprises three primary phases: The initial phase involves modelling cable laying on a rough seafloor without considering the wave effect, and this model operates in a steady state. The second phase focuses on developing a transient cable laying model that incorporates the wave effect but assumes a flat seabed. The third phase involves the integration of both models.

### 1.3.1 First phase: Modelling cable laying in irregular seafloor

The increasing use of cables in deep-ocean engineering highlights the significance of determining cable configurations as crucial parameters in the design process. This study focuses on creating a model for the cable laying process from a vessel, employing a steady-state model depicted in Figure 1. This model, extensively discussed by Howison (2005), utilizes the Euler–Bernoulli model for the displacement of a slender nearly straight beam.

The primary goal is to ascertain the cable's shape from the point it passes through a 'tensioner' at the vessel to the moment it reaches the seabed. The cable experiences an initial tension  $T_0$  applied by the vessel and buoyancy forces as it descends to the seabed. The arc-length ( $s$ ) is defined as 0 at the vessel and  $-L$  at the seabed, where  $L$  represents the cable's actual length between the two points. The sea depth is denoted as  $h(s)$ , and  $\theta(s)$  represents the angle between the curve and the  $x$ -axis.

$$\frac{dx}{ds} = \cos \theta, \quad \frac{dy}{ds} = \sin \theta, \quad \frac{d\theta}{ds} = \kappa, \quad (1)$$

(with  $\kappa$  is the curvature)

Take into account a small segment of length  $\delta s$  on the beam, as depicted in Figure 2. The forces exerted on the element's boundaries consist solely of the internal elastic forces at its ends, along with a body force characterized by components  $f_x$  and  $f_y$  per unit length. In a state of equilibrium, the forces' disparity must be nullified. Consequently, the equilibrium equations can be expressed as:

$$\frac{dF_x}{ds} = f_x, \quad \frac{dF_y}{ds} = f_y, \quad (2)$$

$$\frac{dM}{ds} - F_x \sin \theta + F_y \cos \theta = 0$$

The body force  $f_x$  and  $f_y$  can be expressed through terms of a drag force,  $f_d$  and a buoyancy force,  $f_b$ , represented by the following equations:

$$f_d = C_d A \rho_w U^2 \quad (3)$$

$$f_b = \Delta \rho g A$$

where

$\rho_w$  is sea water density.

$U$  represents the velocity of the object in relation to the fluid,

$A$  denotes the cross-sectional area of the cable,

$C_d$  is the drag coefficient, and

$g$  stands for gravitational acceleration.

Finally, by taking into account the constitutive equation given as



$$\frac{dM}{ds} = EI \frac{d\theta}{ds} \quad (4)$$

with  $EI$  represents the cable bending stiffness, the governing equation for this particular problem can be written as

$$EI \frac{d^2\theta}{ds^2} - F_x \sin \theta + F_y \cos \theta = 0 \quad (5a)$$

$$\frac{dF_x}{ds} = C_d A \rho_w U^2 \sin \theta \quad (5b)$$

$$\frac{dF_y}{ds} = \Delta \rho g A \quad (5c)$$

$$\frac{dX}{ds} = \cos \theta \quad (5d)$$

$$\frac{dY}{ds} = \sin \theta \quad (5e)$$

Here, the unknown parameters are  $\theta$ ,  $F_x$ ,  $F_y$ ,  $X$  and  $Y$ , and also there is one second-order equation. Therefore, the required boundary conditions are

$$\text{at } s = 0; \theta = \theta_0, Y = 1, X = 0, T = T_0, \text{ at } s = -L; \theta = 0, \frac{d\theta}{ds} = 0, Y = 0 \quad (6)$$

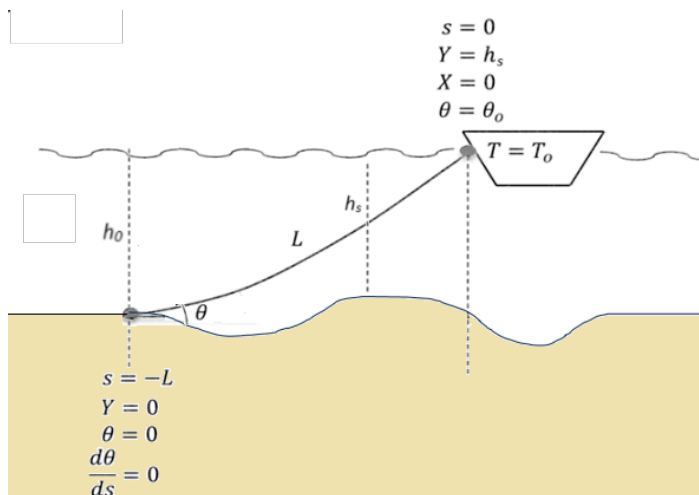


**Figure 1:** Layout of the cable

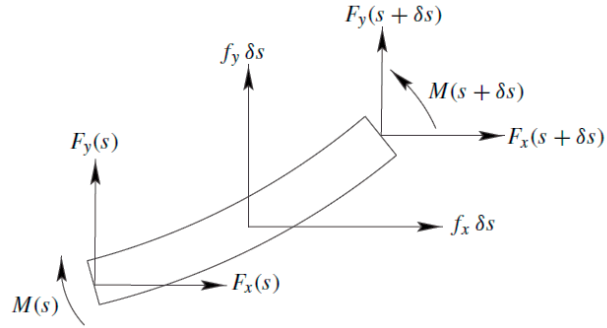


**Figure 2:** Forces and moments on an element of a beam (Howison, 2005)

Before directly addressing the governing equation, a crucial step involves transforming the system of equations into a scaled or non-dimensionalized format. This allows the grouping of all engineering parameters, facilitating the simplification of any necessary assumptions beforehand. For example, consider Equation (5c), having a scale of  $F_y \sim f_o \widehat{F}_y$  and  $s \sim s_o \widehat{s}$  (where  $\widehat{F}_y$  and  $\widehat{s}$  are the non-dimensional variables, while  $f_o$  and  $s_o$  are the scaling factor) so that:

$$\frac{dF_y}{ds} = \Delta \rho g A \frac{f_o}{s_o} \frac{d\widehat{F}_y}{d\widehat{s}} = \Delta \rho g A \frac{1}{s_o} \frac{d\widehat{F}_y}{d\widehat{s}} = \frac{\Delta \rho g A}{f_o} \quad (7)$$

If  $f_o$  is taken as  $\Delta g A h(s)$  and  $s_o$  as  $L h(s)$ , the equation becomes:

$$\frac{1}{L} \frac{dF_y}{ds} = 1 \quad (8)$$

(for simplicity, the upper mark ( $\widehat{\quad}$ ) for dimensionless variable is ignored).

Therefore, this equation, in fact all Equations (5a–e), can be converted into dimensionless equations by scaling the force variables ( $F_x$  and  $F_y$ ) by  $\Delta g A h$ , the space variables ( $X$  and  $Y$ ) by  $h$  and the arc length ( $s$ ) by  $Lh$ . The final non-dimensional governing equation can be written as:

20-22 November, 2023, UTM KUALA LUMPUR, Malaysia

$$\frac{1}{L^2} h(s)^3 \beta \theta_{,ss} - F_x \sin \sin \theta + F_y \cos \cos \theta = 0$$

$$\frac{1}{L} F_{x,s} = \alpha \sin \sin \theta$$

$$\frac{1}{L} F_{y,s} = 1 \quad (9)$$

$$\frac{1}{L} X_{,s} = \cos \cos \theta$$

$$\frac{1}{L} Y_{,s} = \sin \theta$$

in which  $\alpha$  and  $\beta$  are coefficients of:

$$\alpha = \frac{C_d A \rho_w U^2}{\Delta \rho g A} \text{ (hydrodynamic drag)}$$

$$\text{and} \quad (10)$$

$$\beta = \frac{EI}{\Delta \rho g A} \text{ (bending stiffness)}$$

(a subscript variable with a comma in front (,s) means a derivative with respect to the variable).

Now, the dimensionless boundary conditions become:

$$\begin{aligned} \text{at } s = 0; \theta = \theta_o, Y = 1, X = 0, T = T_o, \\ \text{at } s = -1; \theta = 0, \frac{d\theta}{ds} = 0, Y = 0 \end{aligned} \quad (11)$$

The governing Equation (9–11) is straightforward and can be solved via a numerical approach except that the second order term makes the solution rather complicated. If one considers an extra equation of:

$$\gamma = \frac{1}{L} \frac{d\theta}{ds} \Rightarrow \theta_{,s} = L\gamma, \quad (12)$$

so that the governing equation becomes:

$$\gamma_{,s} = \frac{L^2}{\beta h(s)^3} (-F_x \sin \theta + F_y \cos \theta)$$

$$F_{x,s} = L \alpha \sin \theta \quad (13)$$

$$F_{y,s} = L$$

$$X_{,s} = L \cos \theta$$

$$Y_{,s} = L \sin \theta$$

This set of equations was solved numerically using MATLAB software as shown in **APPENDIX A**. The results of the solution are discussed later in Section 1.4.

### 1.3.2. Second phase: Transient model of cable laying under wave effect on flat seabed

It is noted that the cable laying problem demands an analysis beyond the steady-state model as it involves many variables that often makes the real operation of cable laying unpredictable. For such concern, wave motion effect should be introduced, which leads to a variable sea depth depending on time,  $h(t)$ .

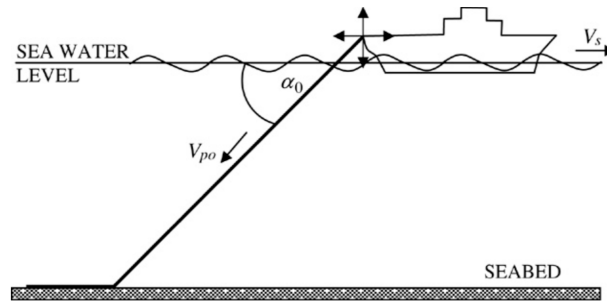


**Figure 3:** Time-dependent problem for cable laying (source: Prpić-Oršić and Nabergoj, 2005)

As the contact points (one at the sea bed and another is at the tensioner of the vessel) changes due to the wave motion, most of the variables are also depending on time, for example  $X(t)$ ,  $Y(t)$  and  $L(t)$ . Moreover, additional variables of boat speed ( $U$ ) and the cable motor speed ( $V$ ) need to be considered.

In this phase we will follow a model developed by Prpić-Oršić and Nabergoj (2005). Figure 4 illustrated the three Cartesian reference systems:  $OXY$  (an inertial system fixed to the

Earth),  $oxy$  (equilibrium axes moving with the mean velocity of the cable-laying ship), and  $o'x'y'$  (a local system attached to the cable). The transformation rule between these systems can be expressed as:

$$\begin{bmatrix} \mathbf{t} \\ \mathbf{n} \end{bmatrix} = \begin{bmatrix} \cos \theta & \sin \theta \\ -\sin \theta & \cos \theta \end{bmatrix} \begin{bmatrix} \mathbf{i} \\ \mathbf{j} \end{bmatrix} \quad (14)$$

and

$$\begin{bmatrix} \mathbf{t} \\ \mathbf{n} \end{bmatrix} = \begin{bmatrix} -\cos \theta & \sin \theta \\ \sin \theta & \cos \theta \end{bmatrix} \begin{bmatrix} \mathbf{I} \\ \mathbf{J} \end{bmatrix} \quad (15)$$

Here,  $\mathbf{t}$  and  $\mathbf{n}$  represent the tangent and normal unit vectors in the local system. The unit vectors  $\mathbf{i}$ ,  $\mathbf{j}$ , and  $\mathbf{I}$ ,  $\mathbf{J}$  correspond to the moving and inertial systems, respectively. The angle  $\theta(p, t)$  between the cable element and the horizontal axis is a function of time  $t$  and the stretched arc length along the cable  $p$ . This length, measured from the shipboard connection point, comprises the unstretched distance  $s$  and the elastic elongation. The relationship between the stretched and unstretched arc lengths is given by  $dp=ds(1+\varepsilon)$ , where  $\varepsilon$  is the uniaxial strain in the cable. Relations (14) and (15) permit expressing any point in any of the three coordinate systems.

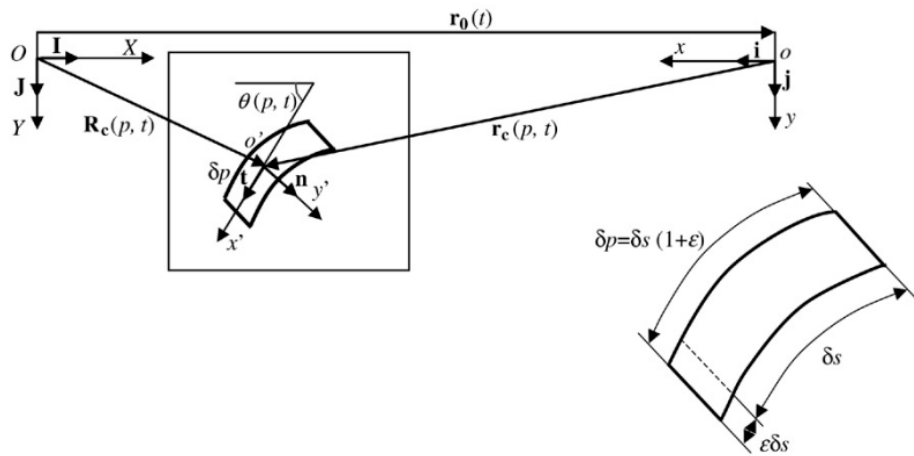


**Figure 4:** coordinate systems (source: Prpić-Oršić and Nabergoj, 2005)

From Figure 4, the following geometric compatibility relations are obtained (Prpić-Oršić and Nabergoj 2005):

$$\begin{aligned}\frac{\partial x}{\partial p} &= \frac{\partial x}{\partial s} \frac{1}{1 + \varepsilon} = \cos \theta \\ \frac{\partial y}{\partial p} &= \frac{\partial y}{\partial s} \frac{1}{1 + \varepsilon} = \sin \theta.\end{aligned}\tag{16}$$

Now the summing of the forces parallel to the tangential axes results in

$$\begin{aligned}T + dT - T + \hat{w} \sin \theta dp + \frac{1}{2} \rho C_f \pi \frac{d}{\sqrt{1 + \varepsilon}} V_t^2 dp \\ = \rho_c A_t dp \\ \frac{dT}{dp} + \hat{w} \sin \theta + \frac{1}{2} \rho C_f \pi \frac{d}{\sqrt{1 + \varepsilon}} V_t^2 = \rho_c A_t \\ \frac{dT}{ds} + w \sin \theta + \frac{1}{2} \rho C_f \pi d \sqrt{1 + \varepsilon} V_t^2 = \rho_c A_t (1 + \varepsilon)\end{aligned}\tag{17}$$

and in the direction of the normal axes,

$$\begin{aligned}T d\theta + \hat{w} \cos \theta dp - \frac{1}{2} \rho C_D \frac{d}{\sqrt{1 + \varepsilon}} V_n |V_n| dp = \bar{\rho}_c A_n dp \\ T \frac{d\theta}{dp} + \hat{w} \cos \theta - \frac{1}{2} \rho C_D \frac{d}{\sqrt{1 + \varepsilon}} V_n |V_n| = \bar{\rho}_c A_n \\ T \frac{d\theta}{ds} + w \cos \theta - \frac{1}{2} \rho C_D d \sqrt{1 + \varepsilon} V_n |V_n| \\ = \bar{\rho}_c A_n (1 + \varepsilon).\end{aligned}\tag{18}$$

The details of derivations and definitions of parameters in dynamic equilibrium condition, Eqs. (17) and (18) can be found in (Prpić-Oršić and Nabergoj 2005).

Note that, the work done by Prpić-Oršić is actually an extension to the earlier works by Vaz, M. A., & Patel, M. H. (1995) and Patel, M. H., & Vaz, M. A. (1995), considering a towed cable and a laid cable, respectively, with the assumptions of continuous, inextensible and flexible (negligible bending stiffness) conditions. These works will be the progressing steps of our modelling effort to complete the final nonlinear dynamics model by Prpić-Oršić and Nabergoj (2005) to include the complete behaviour of stretched cable being laid, accounting for the effects of transient, wave excitation, cable/ship interaction and cable elasticity.

### 1.3.3. Third phase: Transient model of cable laying under wave effect on rough seabed

In this phase Equations (9) and (10) will be combined with equations (17), (16) and (18) where the depth  $h(s, t)$  will be a function of time  $t$  and the stretched arc length  $s$ . Possibility to include the numerical model developed by Trapper, P. A. (2022) will also be considered. Trapper proposed a simple numerical technique, particularly adopting finite difference

discretization, for calculating the internal force envelope diagram as shown in Figure 5. The capability of the proposed model to consider several scenarios of a pipe-lay across different types of seafloor irregularity can be utilised.

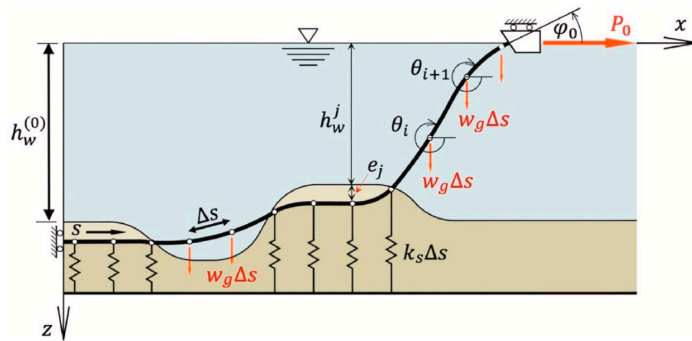


**Figure 5:** Numerical model of pipeline by finite difference approach (source: Trapper, P. A., 2022)

## 1.4 Results and discussions

### 1.4.1 First phase results

Numerical solution for Equation (12–13) gives  $\theta$ ,  $F_x$ ,  $F_y$ ,  $X$ ,  $Y$  and also  $L$ . For calculation purposes, the two parameters  $\alpha$  and  $\beta$  were given a presumed value (without comparing to any engineering parameters) so as to ease the analysis. The main objective is to get the general idea of the cable behaviour as the defining parameters change.

Figure 6 plots the shape of laying cables in a 2D plane with different water depth, starting from the point  $(0,1)$  as the cable passes through the tensioner of a vessel, to the point  $(-X,0)$  as the cable touches the sea bed. In this case, both  $\alpha$  and  $\beta$  are taken as 1, and the initial

angle between the cable and the horizontal surface ( $\theta_0$ ) is 1 radian. The value of the water depth  $h(s)$  is set to vary from 0 to 1 in order to observe the effect on the cable shape. The depth is calculated from seafloor where  $h(s)=0$  to sea surface. It can be seen that increasing the depth reduced the amount of cable being laid, indicating higher elevation in the seafloor in that particular area.

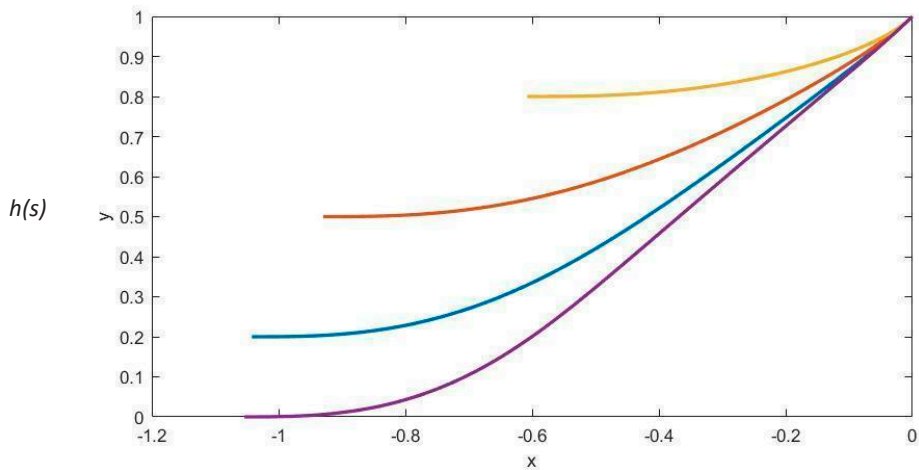


**Figure 6:** Shape of cables in different water depths

#### 1.4.2 Second phase results

At present, the first model, as outlined in Vaz, M. A., & Patel, M. H. (1995), is under development, as detailed in APPENDIX B. This model treats a towed cable as continuous, inextensible, and flexible, without considering bending stiffness.

Basically, the implemented algorithm in Vaz's model involves dividing the total cable length into  $n$  straight elements, connected by pin-nodes, to approximate the solution to the governing equation. This process transforms the integral operations in the cable configuration equations into summations over  $n$  terms, leading to a set of nonlinear ordinary differential equations that require iterative solutions. This method simplifies the problem by converting the original partial differential equations into a connected series of ordinary differential equations. Using a large number of elements effectively transforms the model into a chain assembly.



20-22 November, 2023, UTM KUALA LUMPUR, Malaysia

While the final running codes provided in APPENDIX B still require improvements and updates, the current progress of the codes has successfully plotted the initial configuration of the cable (before acceleration), as shown in Figure 7. Next, the iterative part of the nonlinear analysis will be updated, and validation will be conducted using the results available in Vaz, M. A., & Patel, M. H. (1995). This will be followed by an update on the model from Patel, M. H., & Vaz, M. A. (1995), which considers a cable being laid. Finally, the model by Prpić-Oršić and Nabergoj (2005), which takes into account the stretching effect of the cable, will be incorporated.

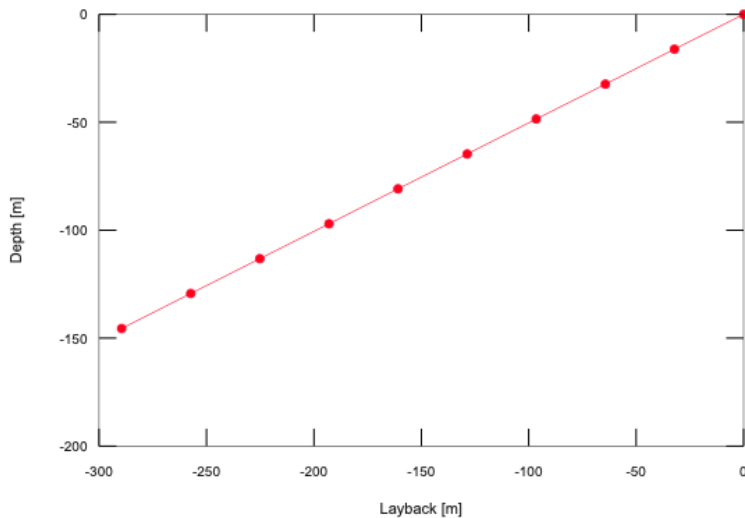


**Figure 7:** Initial cable configuration by Vaz's model

### 1.4.3 Third phase results

As highlighted earlier, this phase will involve developing a transient model of cable laying under the coupling influence of wave effects and a rough seabed. As of now, this phase has not been conducted but is planned for future works.

## 1.5 Conclusion and Recommendations

A mathematical model for cable laying was created, incorporating the impact of a non-flat seafloor and wave motion. The derivation of the model unfolds in three phases. The first

20-22 November, 2023, UTM KUALA LUMPUR, Malaysia

phase involves a steady-state model of a rough seafloor, neglecting wave effects. The formulation is based on the Euler–Bernoulli equation derived by Sam Howison, predicting the cable layout at a specific time with known initial prescribed tension, cable properties, and fluid behaviour. To simplify the formulation, a non-dimensional set of equations is derived by scaling all engineering parameters, resulting in two defining parameters related to fluid hydrodynamic drag and cable bending stiffness. The model is applied with varying sea depths, and numerical solutions are obtained using MATLAB. Results reveal a higher cable location with increased depth. In the second phase, the model addresses a time-dependent problem, incorporating significant wave motion while assuming a flat seafloor. This entails a highly nonlinear formulation requiring resolution. In the third phase, both

models are integrated, introducing a time-dependent water depth  $h$  as a function of time  $t$  and arc length  $s$ .

## 1.6 Acknowledgements

This work was supported by the Institute of Mathematics for Industry, Joint Usage/Research Center in Kyushu University. (FY2023 Workshop (I) “MMISG2023” (2023b003).)

## REFERENCES

- Howison, S. (2005). *Practical Applied Mathematics: Modelling, Analysis, Approximation*. Cambridge University Press.
- Prpić-Oršić, J., & Nabergoj, R. (2005). Nonlinear dynamics of an elastic cable during laying operations in rough sea. *Applied Ocean Research*, 27(6), 255-264.
- Vaz, M. A., & Patel, M. H. (1995). Transient behaviour of towed marine cables in two dimensions. *Applied ocean research*, 17(3), 143-153.
- Patel, M. H., & Vaz, M. A. (1995). The transient behaviour of marine cables being laid—the two-dimensional problem. *Applied Ocean Research*, 17(4), 245-258.
- Trapper, P. A. (2022). A numerical model for geometrically nonlinear analysis of a pipe-lay on a rough seafloor. *Ocean Engineering*, 252, 111146.

## APPENDIX A

```

function [l,Xn] = cable2a()
% Full cable solution
% 8 April 2015

fn = 'cableIFactor';

% PARAMETERS
alf = 1;      % hydrodynamic drag
bet = 0.01;   % bending stiffness
T0 = 1;      % tension
kap = -0;     % curvature at boat
thetastar = 1; % angle at boat (alternative bc)
h = 1;       % water depth

% INITIAL GUESS FOR SOLUTION
x_guess = linspace(0,1,100);
y_guess = [0; 0; 0; 0; 0; 0];
l_guess = 1;
solinit = bvpinit(x_guess,y_guess,l_guess);
solinit.y(1,:) = atan(solinit.x+1); % approximate solution
solinit.y(2,:) = (1+(solinit.x+1).^2).^(-1);
sol = solinit;

% SOLVE
options=bvpset('Vectorized','on','FJacobian',@fjac2,'NMax',10000);
sol = bvp4c(@geq2,@gbc2,sol,options);

l = sol.parameters;
s = sol.parameters*sol.x;
theta = sol.y(1,:);
Fx = sol.y(3,:);
Fy = sol.y(4,:);
X = sol.y(5,:);
Y = sol.y(6,:);

% PLOT
figure(1); clf;
plot(s,theta,s,Fx,s,Fy);
plot(s,theta);
xlabel('x'); ylabel('y');
l0 = (2*T0-1).^(1/2);
hold on; plot(s,atan((s-s(1))./(T0.^2-10.^2).^(1/2)), 'k--');
% asymptotic solution for alpha = 0
figure(2); clf;
plot(X,Y);

save(fn);

% PLOT
figure(2); clf;
set(gcf,'Paperpositionmode','auto','units','centimeters','position',[2 2 20 10]);
plot(sol.y(5,:),sol.y(6,),'linewidth',2);
xlabel('x'); ylabel('y');
ylim([0 1]);
shg;

% print(gcf,'-depsc2',fn,'-loose');

```

```

%% SUBFUNCTIONS %%

% BOUNDARY CONDITIONS
function res = gbc2(ya,yb,l)
    res(1,:) = ya(1,:);
    res(2,:) = ya(2,:);
%     res(3,:) = yb(2, :)-kap;
    res(3,:) = yb(1, :)-thetastar; % ( alternative bc )
%     res(4,:) = yb(3, :).*cos(yb(1, :))+yb(4, :).*sin(yb(1, :))-T0;
    res(4,:) = yb(3, :)-T0; % (alternative bc )
    res(5,:) = ya(6, :);
    res(6,:) = yb(6, :)-h;
    res(7,:) = yb(5, :);
end

% JACOBIAN OF ODE SYSTEM
function [dfdy,dfdp] = fjac2(x,y,l)
    theta = y(1, :);
    psi = y(2, :);
    Fx = y(3, :);
    Fy = y(4, :);
    X = y(5, :);
    Y = y(6, :);

    dfdy = [0 1 0 0 0 0;
            1./bet.*( Fx.*cos(theta) + Fy.*sin(theta) ) 0 1./bet.*
            ( sin(theta) ) 1./bet.*( -cos(theta) ) 0 0;
            1.*alf.*cos(theta) 0 0 0 0 0 ;
            0 0 0 0 0 0 ;
            -1.*sin(theta) 0 0 0 0 0 ;
            1.*cos(theta) 0 0 0 0 0];
    dfdp = [psi;
            1/bet.*( Fx.*sin(theta) - Fy.*cos(theta) );
            alf*sin(theta);
            1;
            cos(theta);
            sin(theta)];
end

% ODE SYSTEM
function dydx = geq2(x,y,l)
    theta = y(1, :);
    psi = y(2, :);
    Fx = y(3, :);
    Fy = y(4, :);
    X = y(5, :);
    Y = y(6, :);

    dydx(1, :) = 1.*psi;
    dydx(2, :) = 1./bet.*( Fx.*sin(theta) - Fy.*cos(theta) );
    dydx(3, :) = 1.*alf*sin(theta);
    dydx(4, :) = 1.*1;
    dydx(5, :) = 1.*cos(theta);
    dydx(6, :) = 1.*sin(theta);
end
end

```

## APPENDIX B

```

% THIS PROGRAM IS STILL UNDER DEVELOPMENT AND PROGRESSING.
% VALIDATION OF THE RESULTS IS YET TO BE MADE IN COMPARISON
% WITH THE RESPECTIVE JOURNAL ARTICLES (VAZ, PATEL, 1995)
% DATE: 15/12/2023

clear, clc

% USER INPUT
g = 9.81;
V_0_x = 0.463; % initial ship speed
V_0_y = 0;
diameter = 0.0264;
L_total = 360;
n = 3;
rho = 1;
CdUser = 2.054;
CfUser = 0.01;
cable_weighth_per_length = 10.59;
hydrodynamic_constant = 0.6173; % Hopland at LH

% ALLOCATE VARIABLES
N = zeros(n, 1);
theta_0 = zeros(n,1);
theta = zeros(n,1);
theta_dt = zeros(n,1);
theta_dtdt = zeros(n,1);
T_ds = zeros(n, 1);
T_0 = zeros(n, 1);
H = zeros(n, 1);
H_0 = zeros(n, 1);
V_0 = zeros(n, 1);
C_f = zeros(n, 1);
C_d = zeros(n, 1);
vt = zeros(n, 1); % normal midpoint velocities
vn = zeros(n, 1); % tangential midpoint velocities
w = zeros(n, 1); % cable's weight in sea water per unit length
rho_bar = zeros(n, 1);

L = ones(n, 1)*L_total/n;
d = ones(n, 1)*diameter;

% Coordinates
x = zeros(n, 1);
y = zeros(n, 1);

% Apply local properties
C_f = C_f + CfUser;
C_d = C_d + CdUser;
w = w + cable_weighth_per_length;

% Initial conditions
V_0 = V_0 + V_0_x;
x_dt_0 = -V_0_x; % [Eq2a]

% theta Eq(13a)
for i = 1:n
    theta_0(i) = acos( ...
        sqrt( 1 + 1/4 * ( hydrodynamic_constant / V_0(i) )^4 ) - 1/2 * (
        hydrodynamic_constant / V_0(i) )^2
    )
end
theta = theta_0;

```

20-22 November, 2023, UTM KUALA LUMPUR, Malaysia

```

% theta_dt Eq(13b)
for i = 1:n
    theta_dt_0(i) = 0;
end

% vt Eq(10a)
for i = 1:n
    sumTerm = 0;
    for j = 1:n-1
        sumTerm = sumTerm + theta_dt(j) * L(j) * sin( theta(i) - theta(j) );
    end
    vt(i) = - x_dt_0 * cos( theta(i) ) + sumTerm;
end

% vn Eq(10b)
for i = 1:n
    sumTerm = 0;
    for j = 1:n-1
        sumTerm = sumTerm + theta_dt(j) * L(j) * cos( theta(i) - theta(j) ) ...
            + theta_dt(i) * L(i) / 2;
    end
    vn(i) = x_dt_0 * sin( theta(i) ) + sumTerm
end

% x0_dtdt (assumed)
x0_dtdt = 0;

% TIME MARCHING START HERE

% Eq(11a)
for i = 1:n
    H(i) = - 1/2 * rho * C_f(i) * pi * d(i) * vt(i)^2 - w(i) * sin( theta(i) );
    T_ds(i) = H(i);
end

% Guess value of N
for i = 2:n
    N(i-1) = T_0(i) * sin( theta(i) - theta(i-1) ) ...
        - N(i) * cos( theta(i) - theta(i-1) )
end
disp('try!!')

% Eq(12)
for i = 1:n
    sumTerm = 0;

    for j = 1:i-1
        sumTerm = sumTerm + L(j) * ( ...
            theta_dt(j)^2 * sin( theta(i) - theta(j) ) ...
            + theta_dtdt(j) * cos( theta(i) - theta(j) )
        );
    end

    theta_dtdt(i) = ...
        2 / L(i) * ( ...
            - 1 / ( 2 * rho_bar(i) ) * rho * C_d(i) * d(i) * vn(i) * abs ( vn(i) ) ...
            + w(i) / rho_bar(i) * cos( theta(i) ) ...
            - x0_dtdt * sin( theta(i) ) ...
            + 2 * N(i) / rho_bar(i) / L(i) ...
            - sumTerm
        );
end

% Calculate x & y

% assume initial location

```

**20-22 November, 2023, UTM KUALA LUMPUR, Malaysia**

```
x(1) = 0;  
y(1) = 0;  
  
for i = 2:n  
    x(i) = x(i-1) - L(i)*sin(theta(i-1));  
    y(i) = y(i-1) - L(i)*cos(theta(i-1));  
end  
x,y  
  
plot(x,y,'r.-')
```

## INDUSTRY PRESENTATION SLIDES



### OBJECTIVES



1. To work with MYHIMS to develop a software to assist the lay of submarine cable from end to end
2. The goal of this workshop is to build upon the existing static modeling techniques established in 2015 by adding transient modeling to subsea cable laying, with a specific focus on dynamic loading conditions and vessel motions. This enhancement aims to facilitate more accurate predictions of cable behavior in the critical TDZ and to enable more precise control of cable laying operations, particularly during bad weather. The workshop attempts to merge theoretical research with practical applications and experience, creating relevant and applicable models for real-world operations. The effort is set to propel the local subsea cable laying industry forward, promoting more effective, secure, and environmentally friendly practices, with an enhanced focus on mitigating risks in the TDZ and confidently handling challenging weather conditions. In addition to facilitate operational decision making, more precise modelling can also facilitate route planning, risk assessments, and operational strategies in challenging environments.



## INTRODUCTION



- IFACTORS Sdn Bhd is a company specialized in the field of submarine cable infrastructure for power and telecommunication
- A Malaysian company, 100% owned by Bumiputra established in the year 1998 in Kota Kinabalu, Sabah
- More than 15 years experience in the field of submarine cable infrastructure in particular telecommunication and power industries
- Providing a full turnkey in house solution including:
  - Design of long haul telecommunication network
  - Design of telecommunication infrastructure in particular submarine system
  - Marine survey for submarine cable infrastructure
  - Implementation and commissioning of submarine telecommunication cable system
  - Maintenance of submarine cable system

## INTRODUCTION



- IFACTORS is an ISO Certified company and a Petronas registered vendor



ISO 9001: 2008  
Cert No: 6794



ISO 14001: 2004  
Cert No: 8397



OHSAS 18001: 2007  
Cert No: 8398

## THE TEAM



### Track Record



- Experienced team lead by a technical management team of more than 20 years in the Industry
- Associated with international company of more than 100 years experience in the industry
- Long term maintenance of more than 7 years contract with leading telcos in Indonesia
  - Attending to more than 25 operation of submarine cable cut repair including deep water repair operation in Bali
- Design and laying of 200km of submarine cable in deep water Java sea between Bali to Java Island at max water depth of 2800m
- Laying of 80km of submarine cable between Kinyali to MCRA platforms in Caspian sea on behalf of Technip for Petronas.
- Laying of 200km submarine cable between Kerteh to ANGSI platform for Petronas
- Relocate of submarine cable in Takbai Bay Thailand and rebury to the burial depth of 4m for Time.
- Design and lay of 220km of fibre optic cable for SKO-PETRONAS from BCOT to E11RC and NC3-CPP
- Design and lay of 100km of fibre optic cable for Telekom Malaysia
- Design and build fibre optic cable link from Labuan to Mainland Sabah for Sabah Electricity Sdn Bhd
- Design and build fibre optic cable link from Labuan to Mainland Sabah for Sabah

## INTRODUCTION



- IFACTORS Sdn Bhd Partners



MODUS UK

## INTRODUCTION



- IFACTORS Sdn Bhd Customers



## Certification



## Submarine Telecommunication Network Implementation Project



- Network Design
- Submarine Cable System Design
- Desktop Study and Marine Survey
- Engineering Design
- Cable and Equipment Production
- Network Infrastructure Implementation
- Commissioning
- Maintenance



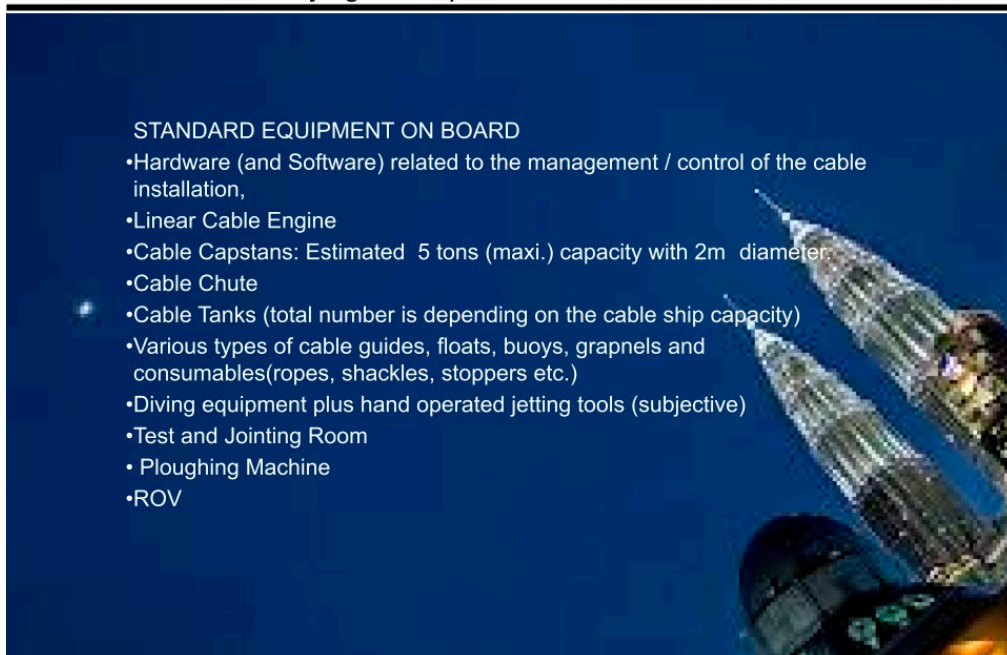
### Cable Laying Concept

A night-time photograph of the Petronas Towers in Kuala Lumpur, Malaysia, illuminated against a dark blue sky. The towers are the central focus of the image, with their spires reaching towards the top of the frame.

- MODULAR EQUIPMENT AND MACHINERIES
- INDEPENDENT OF CABLE LAYING VESSEL
- CERTIFIED JOINTERS ON BOARD



### Cable Laying Concept

A night-time photograph of the Petronas Towers in Kuala Lumpur, Malaysia, illuminated against a dark blue sky. The towers are the central focus of the image, with their spires reaching towards the top of the frame.

STANDARD EQUIPMENT ON BOARD

- Hardware (and Software) related to the management / control of the cable installation,
- Linear Cable Engine
- Cable Capstans: Estimated 5 tons (maxi.) capacity with 2m diameter.
- Cable Chute
- Cable Tanks (total number is depending on the cable ship capacity)
- Various types of cable guides, floats, buoys, grapnels and consumables(ropes, shackles, stoppers etc.)
- Diving equipment plus hand operated jetting tools (subjective)
- Test and Jointing Room
- Ploughing Machine
- ROV

## Cable Laying Equipment



## Modular Cable Tank



# MLN1



## INSTALLATION METHODOLOGY



### SHORE END PROTECTION

1. ARTICULATED PIPES  
- Rocks and Thin Layer of Sand
2. POST LAY BURIAL WITH TRENCHER
3. ENHANCED CABLE ARMOR



## INSTALLATION METHODOLOGY



### SHORE END PROTECTION

5. SHORE END TRENCH
6. PVC PIPES OR ARTICULATED PIPES IN TRENCH



## INSTALLATION METHODOLOGY



### SHORE ENDS



1. Pilot line from ship to beach
2. Cable is paid out with buoys to beach
3. Cable is anchored & tested in beach manhole
4. Plough is floated to the beach
5. Submarine cable is inserted into plough
6. Ship begins pulling plough
7. Divers cut off buoys



INSTALLATION METHODOLOGY



### MAIN LAY / BURIAL

**Burial Method:**  
Two options (subject to survey report)

1. Plough
2. Jetting

1. Check Surveyor laying computer
  - DGPS satellite navigation system
  - DP dynamic positioning system
2. Final test of plough functions in control container
3. Plough deployment –
4. Ship begins pulling plough



NSW – Fibre Optic Cable Type

**WINISUB™ DA 36 – 3 – 32 mm** NSW

**EXCELLENCIO™**

**Mechanical characteristics**

Characteristic	Value
Outer diameter	32 mm
Weight	48.0 kg/100m
Strength in tension	1000 kN
Modulus of elasticity	110 GPa
Temperature range	-40 to +70 °C
Storage temperature range	-20 to +50 °C

**Double Armored**

**WINISUB™ SA 36 – 3 – 27 mm** NSW

**EXCELLENCIO™**

**Mechanical characteristics**

Characteristic	Value
Outer diameter	27 mm
Weight	48.0 kg/100m
Strength in tension	1000 kN
Modulus of elasticity	110 GPa
Temperature range	-40 to +70 °C
Storage temperature range	-20 to +50 °C

**Single Armored**

**WINISUB™ LW 36 – 3 – 15 mm** NSW

**EXCELLENCIO™**

**Mechanical characteristics**

Characteristic	Value
Outer diameter	15 mm
Weight	18.0 kg/100m
Strength in tension	1000 kN
Modulus of elasticity	110 GPa
Temperature range	-40 to +70 °C
Storage temperature range	-20 to +50 °C

**Light Weight**

## SUMMARY



- IFACTORS is a proven company in providing full turnkey for the implementation of submarine cable network
- IFACTORS offers the alternative solution with better cost effectiveness without tolerating quality



**THANK YOU**

## OUTPUT PRESENTATION SLIDES



The slide features a dark blue background with white and green text. On the left, there is a white box with the 'iFACTORS' logo. The main title 'Transient Modeling of Subsea Cable Laying' is in white. Below it, the 'INDUSTRY :' section lists Kamarudin Ismail and Putri Aidila Sofia Abu Bakar. The 'MMISG TEAM:' section lists Zainal Abd Aziz, Sharidan Shafie, Ahmad Razin Zainal Abidin, Shaymaa M. H. Darwish, Mohd Hazmil, Syahidy Abdol Azis, Nik Zetti Amani Nik Faudzi, Noorehan Yaacob, Dzuliana Fatin Jamil, Auni Aslah Bin Mat Daud, Norazaliza Mohd Jamil, and Daisuke Tagami. On the right, the UTM logo is at the top, followed by 'MMISG2023' in large green and white letters, '4<sup>th</sup> Malaysia Mathematics in Industry Study Group' in green, and the dates '20 – 22 November 2023' and 'Universiti Teknologi Malaysia Kuala Lumpur' in white.

**iFACTORS**

**Transient Modeling of Subsea Cable Laying**

**INDUSTRY :**  
Kamarudin Ismail  
Putri Aidila Sofia Abu Bakar

**MMISG TEAM:**  
Zainal Abd Aziz, Sharidan Shafie, Ahmad Razin Zainal Abidin, Shaymaa M. H. Darwish, Mohd Hazmil  
Syahidy Abdol Azis, Nik Zetti Amani Nik Faudzi, Noorehan Yaacob, Dzuliana Fatin Jamil, Auni Aslah Bin Mat Daud, Norazaliza Mohd Jamil, Daisuke Tagami

**UTM**  
UNIVERSITI TEKNOLOGI MALAYSIA

**MMISG2023**  
4<sup>th</sup> Malaysia Mathematics in Industry Study Group

**20 – 22 November 2023**  
**Universiti Teknologi Malaysia**  
**Kuala Lumpur**

## Problem Statement

- Another primary problem in optimizing cable laying operations is the prevention of heightened dynamic tensions, which can lead to serious adverse consequences. This issue becomes more pronounced in adverse weather conditions.
- High-speed cable laying requires a comprehensive understanding of the dynamic changes that occur when adjusting the speed of the cable-laying ship.
- Accurately predicting the cable's transient behavior under these conditions involves complex nonlinear time-domain analysis, posing significant challenges in verification.
- To tackle these issues, incorporating transient modeling phase-by-phase is crucial, particularly focusing on dynamic loading conditions and the movements of the laying vessel.

## Methodology

### First phase:

Modelling cable laying in irregular seafloor

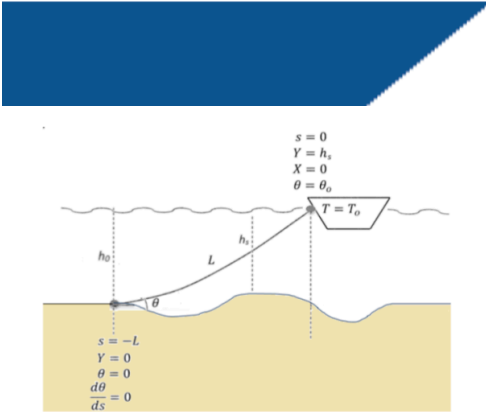


Figure 1: Layout of the cable

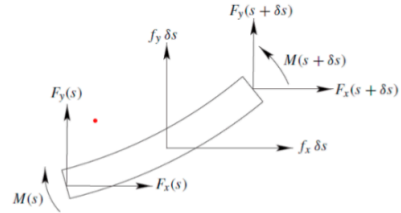


Figure 2: Forces and moments on an element of a beam (Howison, 2005)

## Methodology

### Second phase:

Transient model of cable laying under wave effect on flat seabed

It is noted that the cable laying problem demands an analysis beyond the steady-state model as it involves many variables that often makes the real operation of cable laying unpredictable. For such concern, wave motion effect should be introduced, which leads to a variable sea depth depending on time,  $h(t)$ .

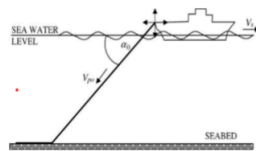


Figure 3: Time-dependent problem for cable laying (source: Papić-Orišić and Nabergoj, 2005)

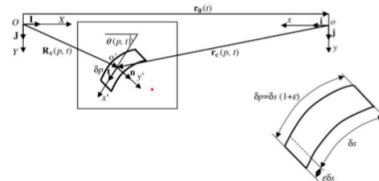


Figure 4: coordinate systems (source: Papić-Orišić and Nabergoj, 2005)

**Methodology**  
**Second phase:**

Transient model of cable laying under wave effect on flat seabed

From Figure 4, the following geometric compatibility relations are obtained (Prpić-Oršić and Nabergoj 2005):

$$\frac{\partial x}{\partial p} = \frac{\partial x}{\partial s} \frac{1}{1 + \varepsilon} = \cos \theta$$

$$\frac{\partial y}{\partial p} = \frac{\partial y}{\partial s} \frac{1}{1 + \varepsilon} = \sin \theta.$$

$$T + dT - T + \hat{w} \sin \theta dp + \frac{1}{2} \rho C_f \pi \frac{d}{\sqrt{1 + \varepsilon}} V_i^2 dp = \rho_c A_f dp$$

$$\frac{dT}{dp} + \hat{w} \sin \theta + \frac{1}{2} \rho C_f \pi \frac{d}{\sqrt{1 + \varepsilon}} V_i^2 = \rho_c A_f$$

$$\frac{dT}{ds} + w \sin \theta + \frac{1}{2} \rho C_f \pi d \sqrt{1 + \varepsilon} V_i^2 = \rho_c A_f (1 + \varepsilon)$$

$$T d\theta + \hat{w} \cos \theta dp - \frac{1}{2} \rho C_D \frac{d}{\sqrt{1 + \varepsilon}} V_n |V_n| dp = \bar{\rho}_c A_n dp$$

$$T \frac{d\theta}{dp} + \hat{w} \cos \theta - \frac{1}{2} \rho C_D \frac{d}{\sqrt{1 + \varepsilon}} V_n |V_n| = \bar{\rho}_c A_n$$

$$T \frac{d\theta}{ds} + w \cos \theta - \frac{1}{2} \rho C_D d \sqrt{1 + \varepsilon} V_n |V_n| = \bar{\rho}_c A_n (1 + \varepsilon).$$

**Remark**

Meanwhile, for the third phase, the combination between the first and second phases is working on. This phase will develop a transient model of cable laying under the coupling influence of wave effects and a rough seabed. As of now, this phase has not been conducted but is planned for future work.

## Results and Discussion

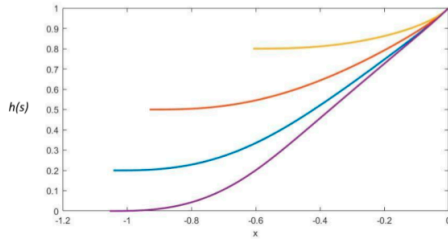


Figure 6: Shape of cables in different water depths

Figure 6 plots the shape of laying cables in a 2D plane with different water depth, starting from the point  $(0,1)$  as the cable passes through the tensioner of a vessel, to the point  $(-X,0)$  as the cable touches the sea bed. It can be seen that increasing the depth reduced the amount of cable being laid, indicating higher elevation in the seafloor in that particular area.

## Results and Discussion

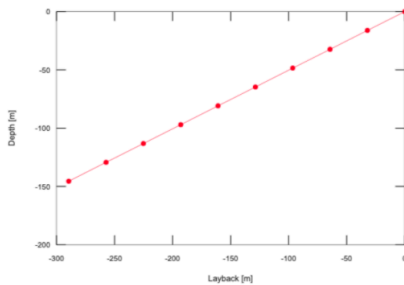


Figure 7: Initial cable configuration by Vaz's model

The current progress of the codes has successfully plotted the initial configuration of the cable (before acceleration), as shown in Figure 7.

Next, the iterative part of the nonlinear analysis will be updated, and validation will be conducted using the results available in Vaz, M. A., & Patel, M. H. (1995). This will be followed by an update on the model from Patel, M. H., & Vaz, M. A. (1995), which considers a cable being laid. Finally, the model by Prpić-Oršić and Nabergoj (2005), which takes into account the stretching effect of the cable, will be incorporated.

## Conclusion

- A mathematical model for cable laying was created, incorporating the impact of a non-flat seafloor and wave motion.
- The derivation of the model unfolds in three phases.
  - ❖ **The first phase** involves a steady-state model of a rough seafloor, neglecting wave effects. The formulation is based on the Euler–Bernoulli equation derived by Sam Howison, predicting the cable layout at a specific time with known initial prescribed tension, cable properties, and fluid behaviour. To simplify the formulation, a non-dimensional set of equations is derived by scaling all engineering parameters, resulting in two defining parameters related to fluid hydrodynamic drag and cable bending stiffness. The model is applied with varying sea depths, and numerical solutions are obtained using MATLAB. Results reveal a higher cable location with increased depth.
  - ❖ **In the second phase**, the model addresses a time-dependent problem, incorporating significant wave motion while assuming a flat seafloor. This entails a highly nonlinear formulation requiring resolution.
  - ❖ **In the third phase**, both models are integrated, introducing a time-dependent water depth  $h$  as a function of time  $t$  and arc length  $s$ .

### *3D Shape Reconstruction of Charcoal Chamber Monument*

- Industry Representatives : Rasanubari Asmah Rahmah Abd Hamid<sup>14</sup>  
(Langkawi Development Authority (LADA))
- Study Group Contributors : Taufiq Khairi Ahmad Khairuddin<sup>1</sup>, Zulkepli Majid<sup>1</sup>,  
Mohd Ali Khameini Ahmad<sup>1</sup>, Abd Manan Samad<sup>3</sup>,  
Ismail Ma'arof<sup>3</sup>, Shota Shigetomi<sup>9</sup>

#### **1.1 Introduction**

Langkawi Island boasts a distinctive tourism asset known as the Charcoal Chamber Monument in Kubang Badak, Bukit Menora. This historical site has a rich legacy dating back more than 150 years and was utilized for the production of coal, primarily from mangrove wood. According to historians, there were originally 12 charcoal chamber monuments in existence [1]. However, as time has passed, only three of these structures have endured, and they, too, have weathered the years, with only partial sections of their original construction remaining.

In light of this historical significance, it falls upon the Langkawi Development Authority (LADA) to undertake the responsibility of preserving these relics. They serve as tangible evidence of the presence of a Siamese village on Langkawi Island, dating back to approximately 1841. By safeguarding and conserving these charcoal chambers, LADA not only ensures the preservation of this invaluable historical heritage but also contributes significantly to the tourism potential of Langkawi. These chambers stand as a testament to the island's rich past and have the potential to be a compelling attraction for visitors seeking a deeper connection to Langkawi's history and culture.



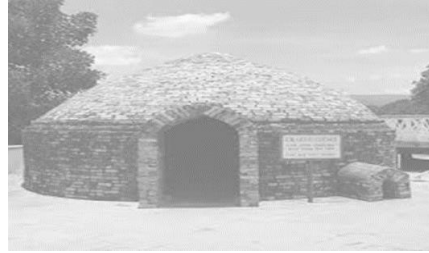


**Figure 1.** One of the remaining charcoal chamber monument (Left) in Kubang Badak, Bukit Menora versus the complete replica of the charcoal chamber monument (Right) found in Sungai Petani, Kedah.

Preserving the historic Charcoal Chamber Monument necessitates a comprehensive approach that begins with accurately documenting its dimensions and shape. To achieve this, the use of advanced techniques, such as the creation of a three-dimensional model and the application of mathematical model, has been proposed. Creating a three-dimensional model involves using modern technology, such as laser scanning or photogrammetry, to capture precise measurements and detailed images of the monument from various angles. By generating a digital 3D representation, preservationists and historians can gain a better understanding of the monument's structure, which serves as a vital reference for restoration and conservation efforts. The application of mathematical model is a scientific and analytical approach that can aid in reconstructing the monument's original form and dimensions. This model can provide insights into the monument's historical proportions and shape, helping experts determine how it might have appeared when first built.

## 1.2 Charcoal Chamber Shape Determination

In this study, the complete structure of a charcoal chamber monument will be determined based on two methods. The first method is to geometrically model the remaining charcoal chamber using laser scanning. After that, the complete structure of the charcoal chamber will be developed based on suitable mathematical models.

### 1.2.1 Geometric Model

Laser Scanning technique in geoinformation was previously used to collect the data (size, dimension, points or locations, colours etc) of the remaining charcoal chamber monument, located in Kubang Badak, Bukit Menora, Langkawi. The data was analysed to reconstruct and geometrically model the incomplete chamber in the three-dimensional space. The complete procedures to achieve this were actually explained in [1]. The left-hand side of Figure 2 shows one of the surveying stations during the scanning. Specifically, 4 stations have been used to scan the chamber (see the right-hand side of Figure 2). Next, the left-hand side of Figure 3 presents the set of images after that scanning, that has been processed into the complete model of the remaining charcoal chamber (see the right-hand side of Figure 3). In this study, further analysis on this geometric model will be carried out, in order to determine the complete structure of the charcoal chamber.

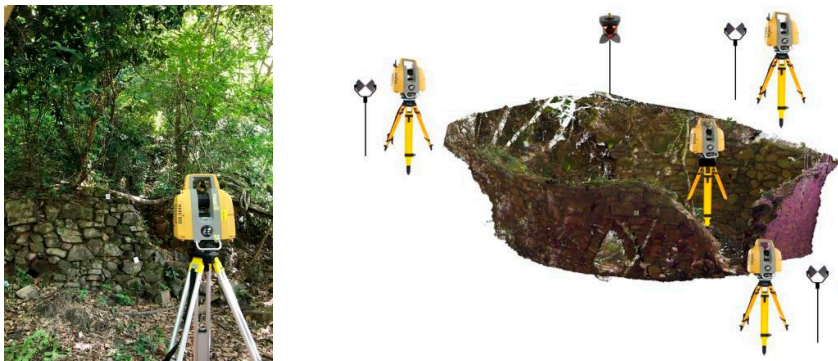


**Figure 2.** The terrestrial laser scanning is used to collect the data (size and dimension) and capture the 3D image of one of the remaining charcoal chamber monuments.

### 1.2.2 Mathematical Modelling

Based on the 3D geometric model of the partial charcoal chamber, mathematical modelling will be used to construct the complete 3D model of the charcoal chamber. Moreover, some methods in geometric modelling will be considered when constructing the 3D model based on the related mathematical formulation. These include some concepts in multivariable functions such as the common surfaces, level curves and intersection between surfaces.

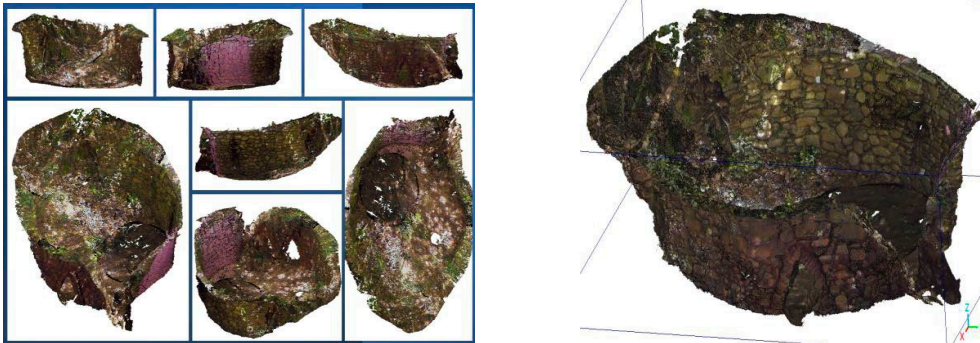


**Figure 3.** The set of images on the left are processed to produce the 3D image of the partial charcoal chamber monuments.

### 1.3 Results and Discussion

During the study group, geoinformation software called as CloudCompare was used to further visualize 3D model of the incomplete structure of the charcoal chamber. Based on the visualization, it was assumed that the remaining chamber was an open cylinder with circular base. In Figure 4, it can be seen that the partial or incomplete structure of the charcoal chamber has been further modelled as a circular cylinder.

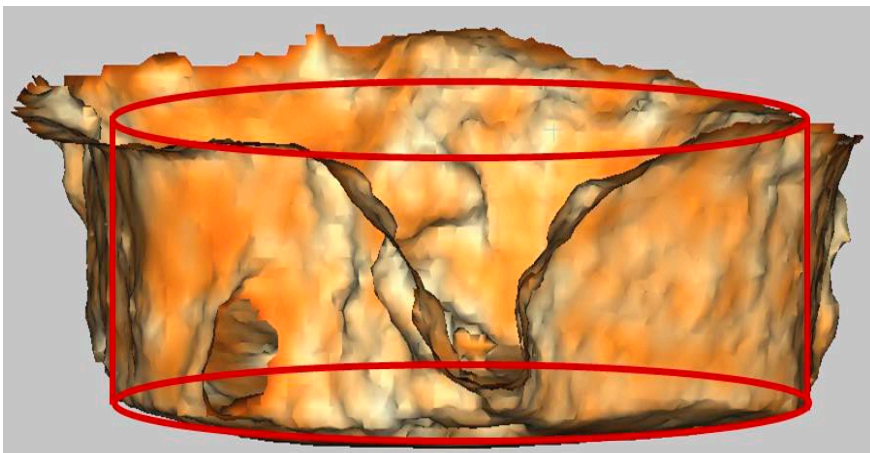


**Figure 4.** Further process and analysis of the partial charcoal chamber monument

Next, using the assumption in Figure 4 and based on historical information (such as in [1]), the complete structure of the chamber will be developed according to suitable mathematical formulations. In this case, it is further assumed that the complete charcoal chamber is built by the combination of a circular cylindrical body and also a dome, as suggested in the real replica of the chamber in Figure 1. Thus, multivariable functions of two variables have been used to construct the solid.

By following the technique presented in [3], a solid bounded by a cylinder has been firstly constructed. After that, another solid representing the dome is also constructed and attached to the top of the cylinder. However, 3 different solids have been suggested during the study, where the domes are all different, due to the lack of information about the dome. Nevertheless, each dome must be completely attached to the cylinder. Therefore, the 3 domes each is respectively constructed as a circular paraboloid, a hemisphere and a circular catenary (see Figure 5).

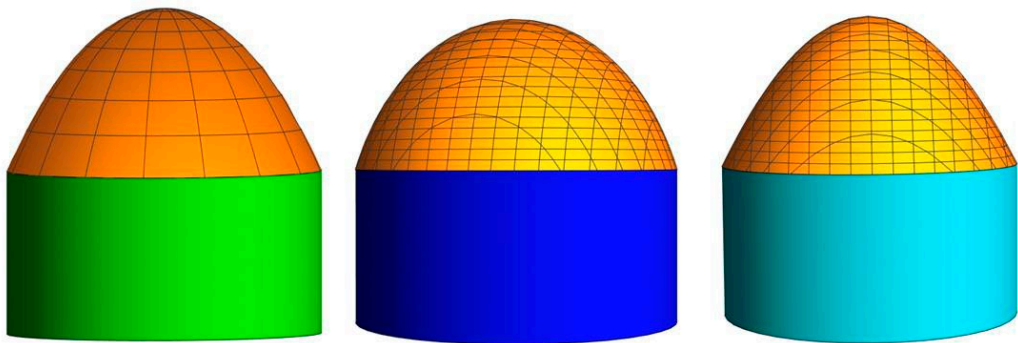


**Figure 5.** The 3 suggested complete shape of the charcoal chamber monument that has circular shape as the base and the combination of the cylinder with the dome (paraboloid (left), hemisphere (center) and catenary (right)) as the body

#### 1.4 Conclusion

The 3D complete shape of a charcoal chamber monument has been constructed based on the geoinformation technique and mathematical modelling. Specifically, three different models of the complete charcoal chamber have been suggested, where each model is built by the combination of a cylinder with different domes. In the future, the proposed models need to be further investigated to decide the actual shape of the original complete charcoal chamber.

#### 1.5 Acknowledgment

This work was supported by Institute of Mathematics for Industry, Joint Usage/Research Center in Kyushu University. (FY2023 Workshop (I) “MMISG2023” (2023b003).)

#### REFERENCES

- [1] Chen-Kim Lim, Kian-Lam Tan and Minhaz Farid Ahmed. Conservation of Culture Heritage Tourism: A Case Study in Langkawi Kubang Badak Remnant Charcoal Kilns, Sustainability 2023, 15, 6554.
- [2] Zulkepli Majid, Mohd Farid Mohd Ariff, Syamsul Hendra Mahmud, Gobi Krishna AL Sinniah, Anuar Aspuri, Azman Ariffin, Abdul Jalil Maulani and Nailul Insani. The Digital Documentations of Historical Charcoal Chamber Monument Using LiDAR Technology, Proceeding 2023 IEEE 14th Control and System Graduate Research Colloquium (ICSGRC), 5 Aug 2023, Shah Alam, Selangor, Malaysia, 163-168.
- [3] Maslan Osman dan Yusuf Yaacob (2008) Multivariable and Vector Calculus, Penerbit UTM Press, Johor Bahru, Malaysia.

MALAYSIA MATHEMATICS IN INDUSTRY STUDY GROUP  
(MMISG2023)

20-22 November, 2023, UTM KUALA LUMPUR, Malaysia

INDUSTRY PRESENTATION SLIDES



## 3D SHAPE RECONSTRUCTION OF CHARCOAL CHAMBER MONUMENT

Geoparks and Sustainably Section,  
Tourism Section,  
Langkawi Development Authority (LADA),  
Langkawi Island, Kedah, Malaysia

in cooperation with Geopark Research Satellite Lab, UTM



### Problem Background

- Langkawi Island boasts a distinctive tourism asset known as the Charcoal Chamber Monument in Kubang Badak, Bukit Menora.
- This historical site has a rich legacy dating back more than 150 years and was utilized for the production of coal, primarily from mangrove wood.
- According to historians, there were originally 12 charcoal chamber monuments in existence.
- However, as time has passed, only three of these structures have endured, and they, too, have weathered the years, with only partial sections of their original construction remaining.
- In light of this historical significance, it falls upon the Langkawi Development Authority (LADA) to undertake the responsibility of preserving these relics.
- They serve as tangible evidence of the presence of a Siamese village on Langkawi Island, dating back to approximately 1841.
- By safeguarding and conserving these charcoal chambers, LADA not only ensures the preservation of this invaluable historical heritage but also contributes significantly to the tourism potential of Langkawi.
- These chambers stand as a testament to the island's rich past and have the potential to be a compelling attraction for visitors seeking a deeper connection to Langkawi's history and culture.

MALAYSIA MATHEMATICS IN INDUSTRY STUDY GROUP  
(MMISG2023)

20-22 November, 2023, UTM KUALA LUMPUR, Malaysia



MALAYSIA MATHEMATICS IN INDUSTRY STUDY GROUP  
(MMISG2023)

20-22 November, 2023, UTM KUALA LUMPUR, Malaysia



<https://www.facebook.com/walkaboutasia/videos/775606843274664/?mibextid=zDhOQc>

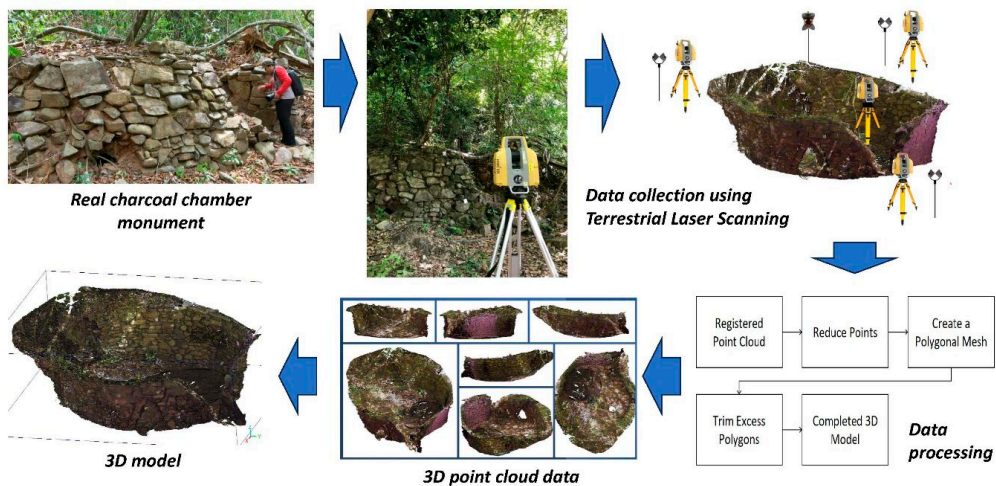
<https://youtu.be/H5mEfBuPlb4?si=9sTDE4XfxxdJQbQJ>



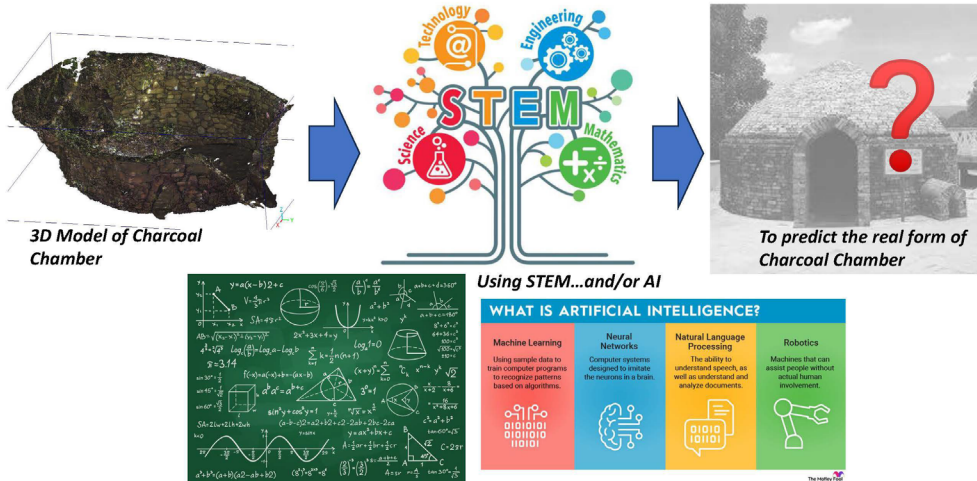
## Problem Statement

- Preserving the historic Charcoal Chamber Monument necessitates a comprehensive approach that begins with accurately documenting its dimensions and shape.
- To achieve this, the use of advanced techniques, such as the creation of a three-dimensional model and the application of mathematical model, has been proposed.
- Creating a three-dimensional model involves using modern technology, such as laser scanning or photogrammetry, to capture precise measurements and detailed images of the monument from various angles.
- By generating a digital 3D representation, preservationists and historians can gain a better understanding of the monument's structure, which serves as a vital reference for restoration and conservation efforts.
- The application of mathematical model is a scientific and analytical approach that can aid in reconstructing the monument's original form and dimensions.
- This model can provide insights into the monument's historical proportions and shape, helping experts determine how it might have appeared when first built.

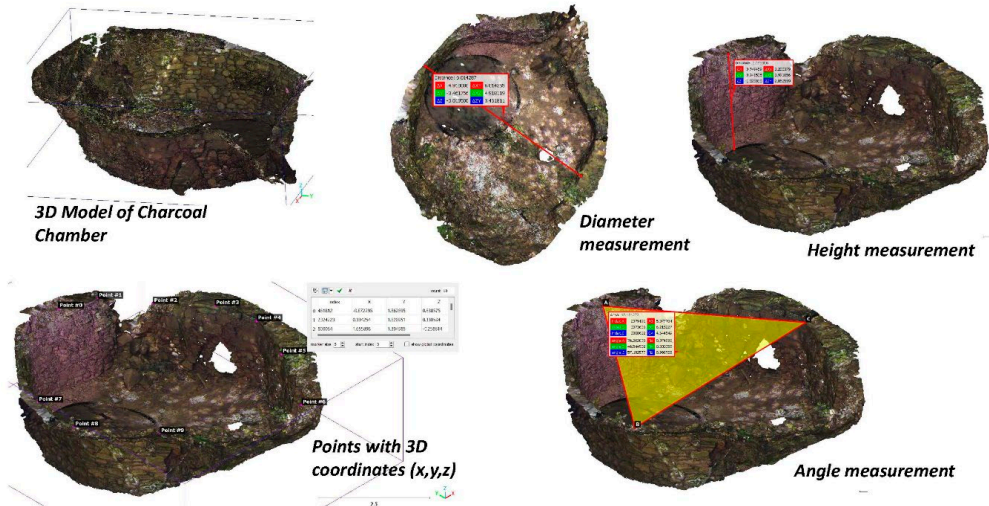
### The Process of Generating 3D Model of Charcoal Chambers using Geospatial Technology – Terrestrial Laser Scanning



## What will happen in MMISG 2023?



## Types of data that can be obtained from the 3D model of the charcoal chamber



MALAYSIA MATHEMATICS IN INDUSTRY STUDY GROUP  
(MMISG2023)

20-22 November, 2023, UTM KUALA LUMPUR, Malaysia



**Thank you...**

LANGKAWI DEVELOPMENT AUTHORITY (LADA)  
<https://www.lada.gov.my/>



## OUTPUT PRESENTATION SLIDES



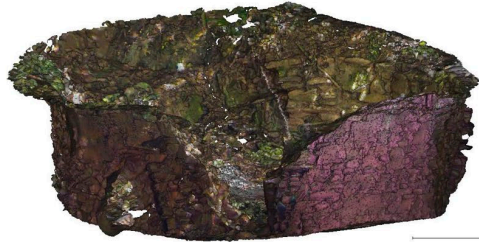
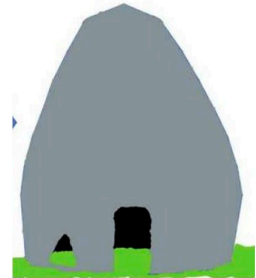
# 3D SHAPE RECONSTRUCTION OF CHARCOAL CHAMBER MONUMENT

by  
UTM-CENTRE FOR INDUSTRIAL AND  
APPLIED MATHEMATICS (UTM-CIAM)



## Problem Background

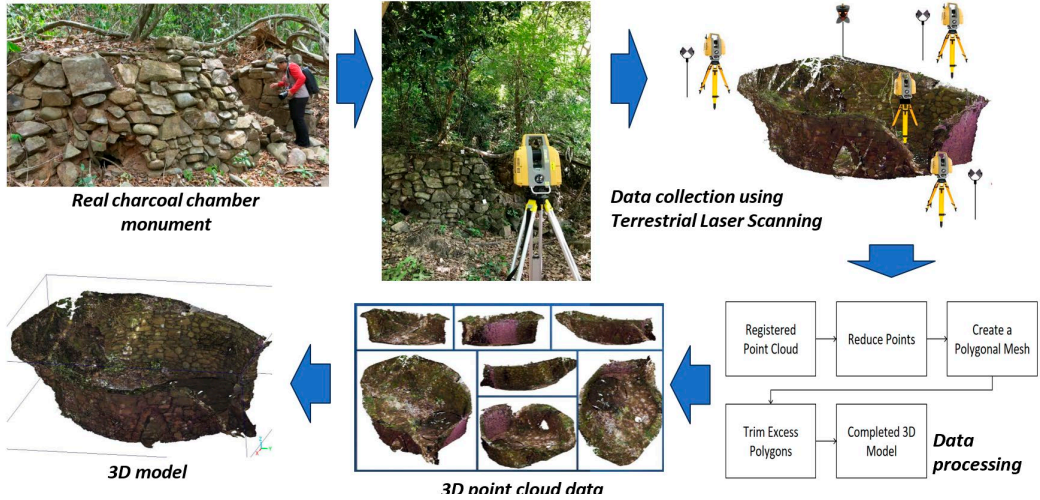
- Langkawi Island boasts a distinctive tourism asset known as the Charcoal Chamber Monument in Kubang Badak, Bukit Menora.
- This historical site has a rich legacy dating back more than 150 years and was utilized for the production of coal, primarily from mangrove wood.
- According to historians, there were originally 12 charcoal chamber monuments in existence.
- However, as time has passed, only three of these structures have endured, and they, too, have weathered the years, with only partial sections of their original construction remaining.
- In light of this historical significance, it falls upon the Langkawi Development Authority (LADA) to undertake the responsibility of preserving these relics.
- They serve as tangible evidence of the presence of a Siamese village on Langkawi Island, dating back to approximately 1841.
- By safeguarding and conserving these charcoal chambers, LADA not only ensures the preservation of this invaluable historical heritage but also contributes significantly to the tourism potential of Langkawi.
- These chambers stand as a testament to the island's rich past and have the potential to be a compelling attraction for visitors seeking a deeper connection to Langkawi's history and culture.



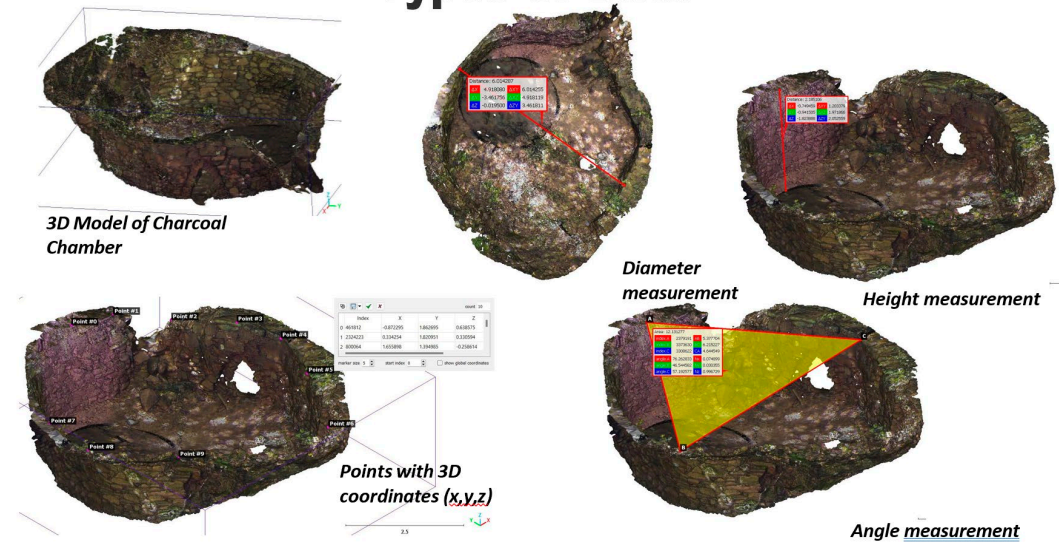
## Problem Statement

- Preserving the historic Charcoal Chamber Monument necessitates a comprehensive approach that begins with accurately documenting its dimensions and shape.
- To achieve this, the use of advanced techniques, such as the creation of a three-dimensional model and the application of mathematical model, has been proposed.
- Creating a three-dimensional model involves using modern technology, such as laser scanning or photogrammetry, to capture precise measurements and detailed images of the monument from various angles.
- By generating a digital 3D representation, preservationists and historians can gain a better understanding of the monument's structure, which serves as a vital reference for restoration and conservation efforts.
- The application of mathematical model is a scientific and analytical approach that can aid in reconstructing the monument's original form and dimensions.
- This model can provide insights into the monument's historical proportions and shape, helping experts determine how it might have appeared when first built.

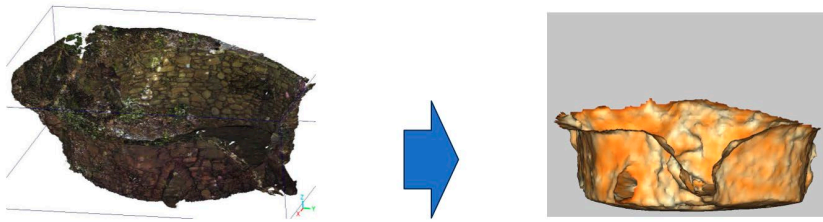
## The Process of Generating 3D Model of Charcoal Chambers using Geospatial Technology – Terrestrial Laser Scanning



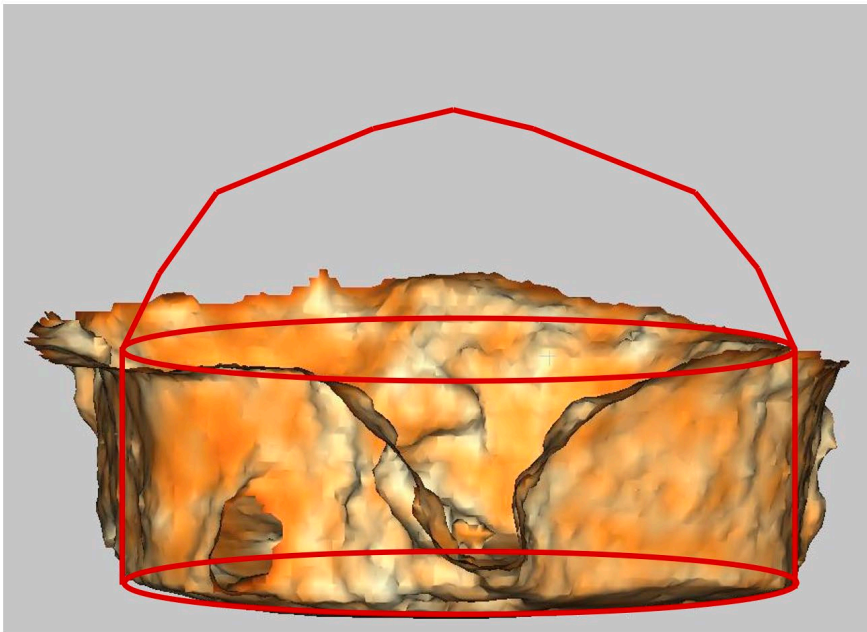
## Types of Data



## Further modelling (Geospatial and Mathematics) of the remaining charcoal chamber

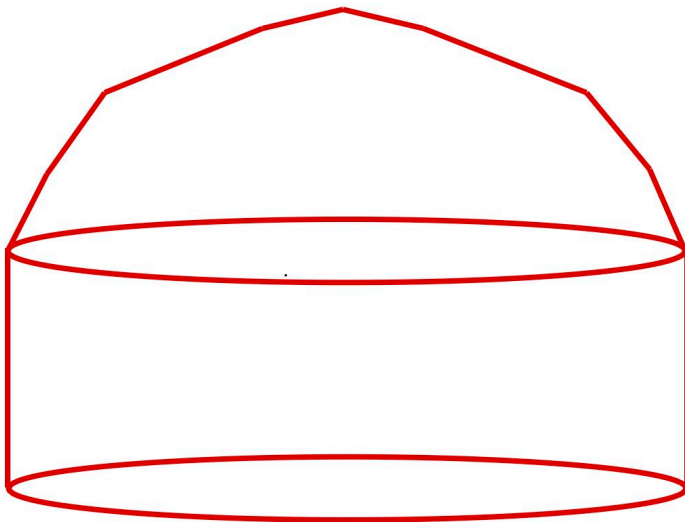
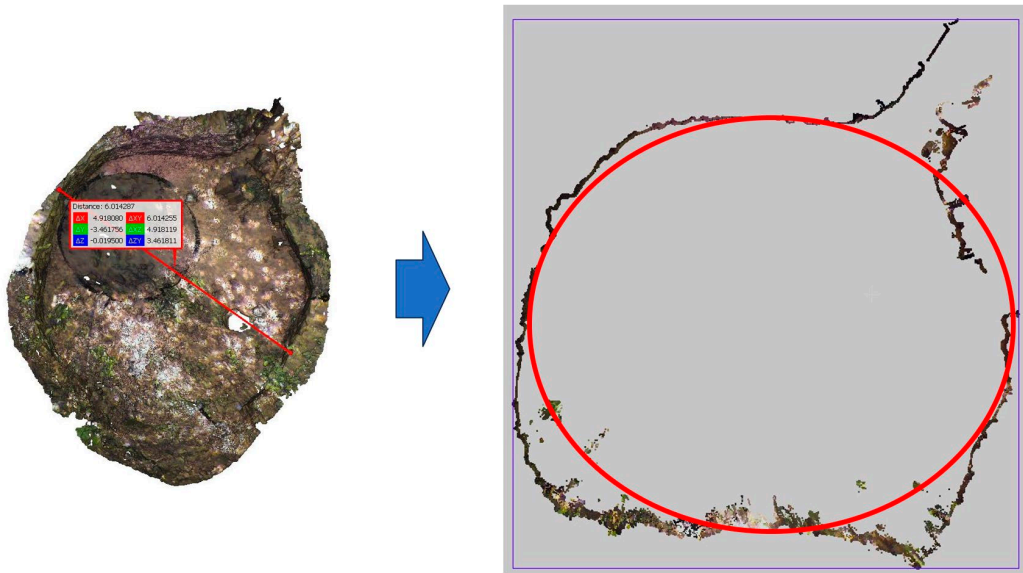


*3D Model of Charcoal Chamber*

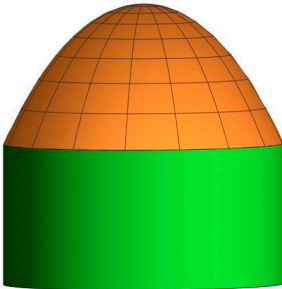


MALAYSIA MATHEMATICS IN INDUSTRY STUDY GROUP  
(MMISG2023)

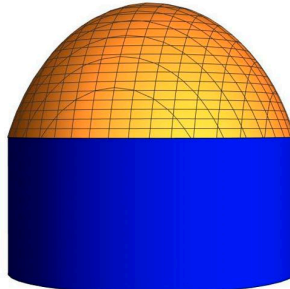
20-22 November, 2023, UTM KUALA LUMPUR, Malaysia



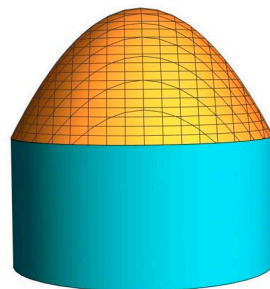




Dome: Catenary

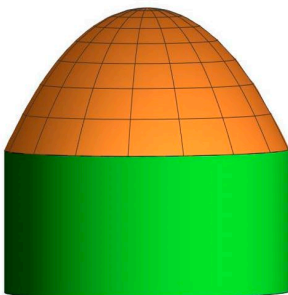


Dome: Hemisphere

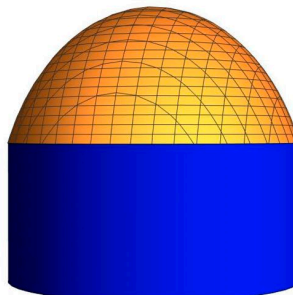


Dome: Paraboloid

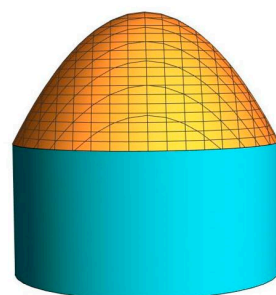
**Three possible models of a charcoal chamber are proposed**



Dome: Catenary



Dome: Hemisphere



Dome: Paraboloid



*Predictive Modeling of Pipe Burst Towards Sustainable Non-Revenue Water*

Industry Representatives : Aida Natasah Sulaiman<sup>11</sup>, Nur Nabilah Jamal<sup>11</sup>,  
Norazlina Ismail<sup>11</sup>  
(Ranhill SAJ Sdn. Bhd.)

Study Group Contributors : Norhaiza Ahmad<sup>1</sup>, Zainol Mustafa<sup>2</sup>, Arifah Bahar<sup>1</sup>,  
Zaiton Mat Isa<sup>1</sup>, Istas Fahrurazi Nursyirwan<sup>1</sup>, Mohamad  
S.J. Darwish<sup>1</sup>, Tan Lit Ken<sup>1</sup>, Hafizah Farhah Saipan @  
Saipol<sup>1</sup>, Aniza Akaram<sup>1</sup>, Ramhya Kathirayson<sup>2</sup>

**1.1 Introduction**

This report provides valuable insights into the evaluation of predictive modeling for pipe burst detection, aiming to address concerns, assess feasibility, and ensure a successful and reliable installation process. The objective is to implement a robust system that leverages on statistical approach and Artificial Neural Network Model (ANN). Concerns and constraints revolve around ensuring the accuracy of predictions, minimizing false positives, and optimizing the integration of these methodologies into existing infrastructure.

In the statistical approach, the study starts by focusing on analyzing historical data, scrutinizing the quality and patterns of the available data. The main concern lies around the data's reliability by investigating potential outliers and assessing whether the dataset, confined to a single year, is sufficient for meaningful predictive modelling. Investigation into utilizing different types of control charts specifically variations of Exponentially Weighted Moving Average Control Charts that can detect shifts in signals is considered. The study concludes that a combination of dynamic thresholding based on weekly patterns, targeted analysis of reliable flow data, and adaptive parameter settings in control charts, particularly with a focus on shorter time series, enhance the effectiveness of pipe burst detection. The adaptive parameter strategy significantly reduces the percentage of points beyond limits in the control charts (0% to 9.1%), emphasizing its effectiveness in identifying transient signals for pipe burst detection.

In ANN models, historical data serves as the foundation for training the network to recognize patterns indicative of bursts. These patterns are discerned through correlations observed within the parameters encapsulated in the historical dataset. The Levenberg-Marquardt algorithm, renowned for its efficacy in optimizing the neural network's parameters, is frequently employed for this purpose. Notably, this algorithm is conveniently accessible as a built-in function within platforms like Matlab, facilitating its seamless integration into the neural network training process. By leveraging the collective intelligence encoded in historical data and employing sophisticated optimization techniques like the Levenberg-Marquardt algorithm, ANN models can effectively discern and anticipate bursts based on underlying patterns present in the data.

## 1.2 Pipe Burst Detection With Control Chart Analysis For Water Monitoring

### 1.2.1 Introduction

Information on water distribution consists of measurements of water flow and water pressure recorded at regular time intervals are typically used for water monitoring. In statistical analysis, these data are presented in the form of continuous interval multivariate time series. In time series analysis, anomalies refer to observations or patterns in the data that deviate significantly from the expected or normal behavior. These anomalies can be indicative of unusual events, errors, or changes in the underlying processes being monitored. These deviations can manifest as sudden spikes, drops, or irregularities, signaling potential events, errors, or shifts in the underlying processes being observed.

Pipe burst events can be referred to as "anomalies" or "transients" in the time series data. A transient, in this context, denotes a brief and temporary occurrence that takes place when fluid, such as water, is rapidly and unexpectedly released due to a burst pipe. The burst initiates an uncontrolled and swift flow of fluid, leading to a transient flow condition. This transient phase is marked by an abrupt surge in both pressure and flow rate, creating a sudden and intense movement of fluid within the pipe system. In this study, we aim to detect the transient signals based on the temporal consistency in the time series based on statistical approaches.

### 1.2.2 Objectives

2.2.1 to identify the transient signals of pipe burst using a statistical approach applied to water reading measurements obtained at 15 minutes interval on a daily basis.

2.2.2 to determine an effective estimate for the control limits of statistical control charts for monitoring water distribution.

### 1.2.3 About Data

The company provides us with measurements from a logger device at a District Metered Area (DMA) meter in Skudai, Johor. In the context of water distribution systems, these devices are used to monitor and measure water flow within a specific district or zone. This technology is employed in water network management to enhance control, efficiency, and leak detection. The measurements used in the analysis are Pressure Rate (mH), Flow Rate (l/s). Other measurements are also available but they are not used since they are either aggregated or contain too many missing data.

The pressure rate (mH), and flow Rate (l/s) data provided show some distinct characteristics.

- (1) The recorded data could be affected by (1) the manner that the tap source is closed due to the pipeburst, or (2) no data transfer on the recorded device due to technical issues. These phenomena could result in spurious negative or zero values. The data needs to be treated or pre-processed prior to applying any analysis to avoid biased interpretation.

- (2) The data is recorded at every 15 minute interval. This implies that the sequence data is in the form of a continuous interval time series data. Thus, the method used for analysis needs to take into account this characteristic.

## 1.2.4 Methodology

### 1. 2.4.1 Data Pre-processing

The recorded data could be affected by: (1) the closure of the tap source due to a pipe burst and (2) the absence of data transfer on the recording device due to technical issues. These phenomena have the potential to introduce spurious negative or zero values. The company's current protocol involves either retaining zero values or substituting (imputing) negative values with zero. However, the persistence of zero values may give rise to computational challenges and could potentially lead to misleading information, particularly when consecutive data points exhibit zero values. Thus, the suggested course of action for addressing potential cases is to replace the missing values with a minimal value to reflect no flow and or to replace the missing values with the previous day's reading.

### 1. 2.4.2 Exponentially Weighted Moving Average (EWMA) Based Control Charts

Here we have applied two types of control charts suitable for autocorrelated process: a univariate Exponentially Weighted Moving Average (EWMA) control charts and its multivariate extension, the Multivariate EWMA to obtain the upper and lower bounds for the imputed Pressure and Flow dataset.

Similar to many control charts, EWMA type of charts operates on a threshold-based methodology, simplifying the process of monitoring for deviations and facilitating ease of use in quality control. The EWMA chart assigns exponentially decreasing weights to past observations, giving more emphasis to recent data (Sukparungsee et al., 2020). These charts are particularly useful for detecting small shifts in the process parameter mean.

An EWMA control chart for monitoring the mean of a process is based on the following statistic.

$$Z_i = \lambda \underline{X}_i + (1 - \lambda)Z_{i-1}, i = 1, 2, \dots \quad (\text{Eq.1})$$

where  $\lambda$  is the weighing parameter of the data with ,  $0 \leq \lambda < 1$ , and  $\underline{X}_i$  is the mean of the process at time  $i$ . At the initial value,  $Z_0 = \mu_0$ , where  $X_i (i = 1, 2, \dots)$  are independent and normally distributed observations, the statistics  $Z_i$  for sampline means  $\underline{X}_i$  is used. Then, the mean of  $Z_i$  are  $E(X)_i = \mu_0$ , and the variance of  $Z_i$  is given as follows:

$$\text{Var}(Z_i) = \sigma_{\underline{X}}^2 \left( \frac{\lambda}{2-\lambda} (1 - (1-\lambda)^{2i}) \right), i = 1, 2, \dots \quad (\text{Eq.2})$$

From this equation, as  $i \rightarrow \infty$ , then the asymptotic variance is  $Var(Z_i) = \sigma_X^2 \left( \frac{\lambda}{2-\lambda} \right)$ , leading to the control limits:

$$UCL/LCL = \mu_0 \pm H_2 \sqrt{\left( \sigma_X^2 \left( \frac{\lambda}{2-\lambda} \right) \right)} \quad (\text{Eq.3})$$

where  $H_2$  is the coefficient of the control limit of EWMA control chart and  $\mu_0$  is the mean of the process and variance is  $\sigma_X^2$ .

Multivariate Exponentially Weighted Moving Average (MEWMA) chart is a statistical control chart used in quality control to monitor the mean vector of a multivariate process. It is an extension of the univariate EWMA chart to handle multiple variables simultaneously. The MEWMA control chart is known to be sensitive to a small or gradual drift in the process for two or more numeric variables. Examining the variables in a multivariate sense can be important especially when the variables are highly correlated. This is because joint out-of-control conditions can occur without any individual variable violating its control limits when plotted separately, Niaki et al (2011).

In this chart, let  $X_i$  be a  $p \times 1$  vector of the  $i$ th process sample containing the  $p$  variate normal distribution with in-control mean,  $\mu_0 = 0$ , and covariance matrix  $\Sigma_X$ . The MEWMA control chart for monitoring the mean of a process is based on the following statistic:

$$Z_i = \lambda X_i + (1 - \lambda)Z_{i-1}, \quad i = 1, 2,$$

where  $\lambda$  is the weighing parameter of the data, with  $0 \leq \lambda < 1$ . At the initial value we set,  $Z_0 = 0$ , Note that if  $\Sigma_Z^{-1}$  is the inverse of the  $Z$  covariance matrix, then the plotted value in MEWMA chart is  $Q_i = Z_i' \Sigma_Z^{-1} Z_i$  and the MEWMA chart signals if the following is satisfied:

$$Q_i = Z_i' \Sigma_Z^{-1} Z_i > L \quad (\text{Eq.4})$$

where  $L$  and  $\lambda$  are the chart parameters to achieve a specific in-control average run length (ARL).

## 1.2.5 Results

### 1.2.5.1 Time Series Plots of Observed vs Imputed Water Monitoring Data

The time series plots presented in Figure 1 below illustrate the Pressure readings derived from imputed data.

20-22 November, 2023, UTM KUALA LUMPUR, Malaysia

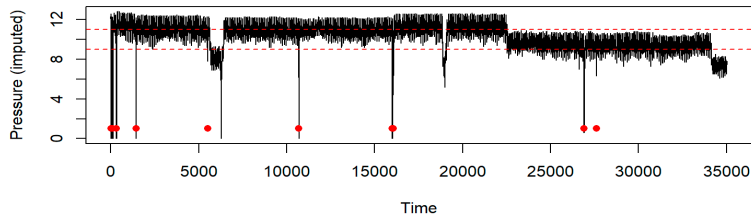


Figure 1: Annual time series plot taken at every 15 minutes interval of raw pressure of the imputed pressure data. The red horizontal lines indicate the standard measurement level and the red markers show the time of complaints received by the company.

It can be seen that following imputation, Figure 1 shows a minimum value of at least zero to reflect the actual pressure readings. The red dot markers indicate the time of the reported complaints signifying the transient phase. It is observed that all the dots align with sudden surge in flow rate, indicating an abrupt and intense fluid movement within the pipe system. The flow time series readings based on the imputed data, plotted in Figure 2.

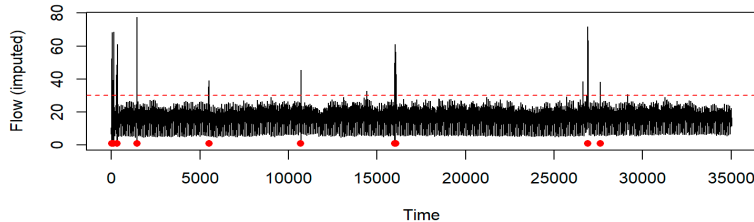


Figure 2: Annual time series plot taken at every 15 minutes interval of the imputed flow data (bottom). The red horizontal lines indicate the standard measurement level and the red markers show the time of complaint

Following imputation, the flow data reveals a minimum value of at least zero, aligning accurately with the true flow readings. Overall, the red markers consistently aligned with the reported complaints, signifying the transient phase. However, it's noteworthy that not all red markers coincide precisely with the sudden surge in flow rate, suggesting potential variations or complexities in the observed patterns.

It is essential that we opt to utilize the imputed dataset for analysis to maintain continuity in our examination and derive more meaningful observations.

### 1.2.5.2 Trends and Variations in Water Monitoring Data

We conducted additional examinations to explore potential seasonality and trends within the data. Generally, variations in statistical characteristics, such as mean and standard deviation,

can be anticipated in pipe flow and pressure. These fluctuations are attributed to the regular patterns in water usage resulting from human behavior.

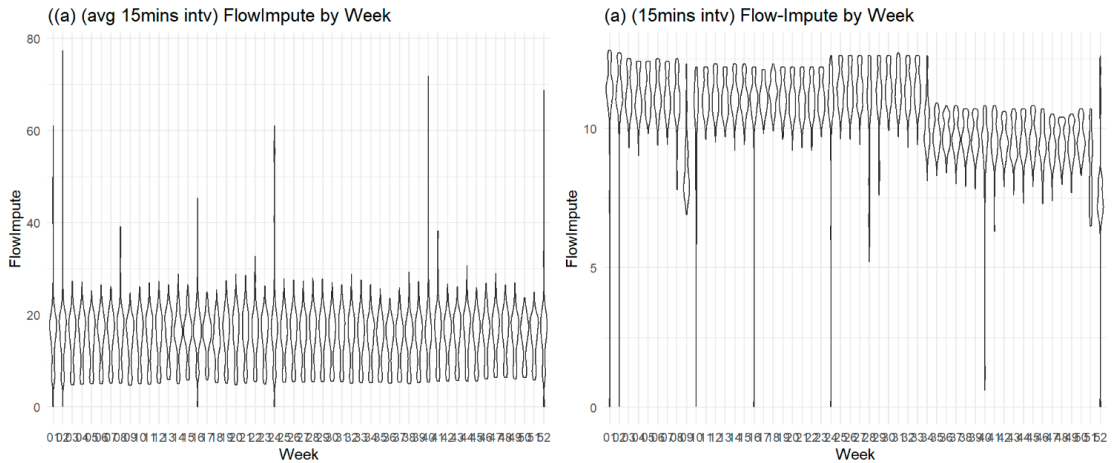


Figure 3: Violin plot for 15 mins interval weekly data within the year 2022 (a) Flow (b) Pressure

Figure 3 (a) shows the violin plot for the weekly flow across the year of data monitoring in 2022. Figure 3(b) shows the violin plot for the weekly pressure across the year of data monitoring in 2022. It could be observed that certain weeks show higher variation than the others especially for Pressure data. In contrast, flow data more or less show more stable reading except for some burst of water flow in several weeks.

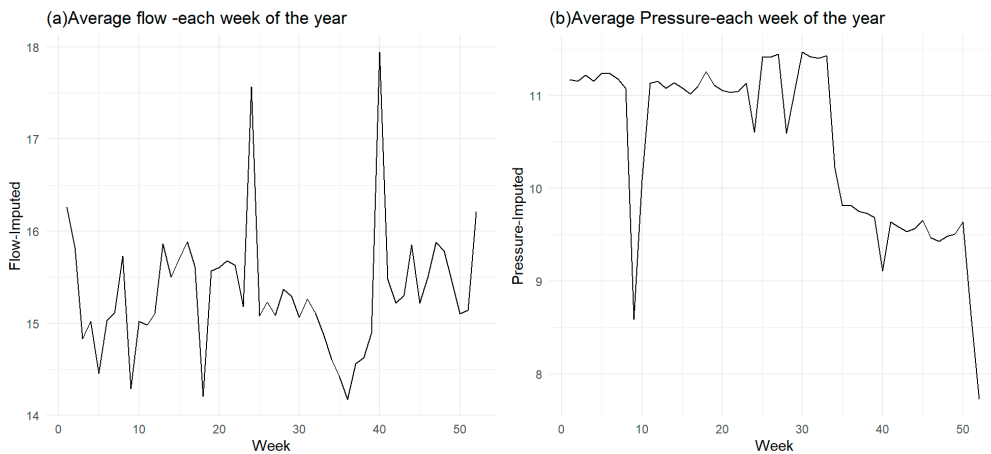


Figure 4: Average Weekly data each week within the year 2022 (a) Flow (b) Pressure

Figure 4 (a) shows the average flow for every week in 2022. Figure 4(b) shows the average pressure for every week in 2022. It could be observed that the average flow and pressure is

different from week to week especially for pressure data. Flow data also show variations but not as erratic as that of pressure data.

In summary, it can be observed that the plots presented (Figures 3 and 4) indicate variations in statistical characteristics, specifically in the mean and standard deviation of the observations. As control charts rely on these parameters to establish control limits (Eq.3, and Eq.4), the accuracy of the control chart methods may be significantly compromised if applied directly to the raw monitoring data. Thus, the weekly patterns in water consumption should be considered so that dynamic thresholds can be set according to real-time behaviour.

In addition, the noticeable shift in observations is more pronounced in the pressure data compared to the Flow data. Consequently, utilizing flow data in leakage detection analysis is deemed more reliable, as it is less prone to generating false alarms than the pressure data. In the next section, we will focus the analysis on flow data for detection of pipeburst.

### 1.2.5.3 Detection of Pipe burst using Control Charts for Water Monitoring

In this section, the results of the identification on the transient signals of the pipe burst using EWMA based Control charts are presented based on two approaches.

- a) MEWMA and EWMA Control charts on Annual Data
- b) EWMA Control charts based on data segmentation and adaptive parameter settings

#### a) MEWMA and EWMA Control charts on Annual Data

In this section, the results of detection of pipe burst using the annual water pipe records on two types of control charts: Exponentially Weighted Moving Average for multivariate data (MEWMA) and Exponentially Weighted Moving Average for univariate data (EWMA) is presented. In EWMA, pipe flow and pressure are presented in separate charts, whereas in MEWMA, the two variables are applied simultaneously.

In MEWMA, pipe flow and pressure are applied together, forming multivariate data for a single control chart. Various parameter settings are applied to MEWMA. However, the MEWMA chart (Figure 5) does not seem to show a useful representation of the data, as all the observations are still contained in the limits. This would not be helpful in detecting the transient signals as no significant points are detected to indicate the initial pipe burst event. This is likely due to the large and varying shift parameters between pressure and flow rates over the time period. When there are varying shift parameters, the chart may become overly sensitive to these changes, leading to false alarms or a decreased ability to identify genuine shifts.



20-22 November, 2023, UTM KUALA LUMPUR, Malaysia

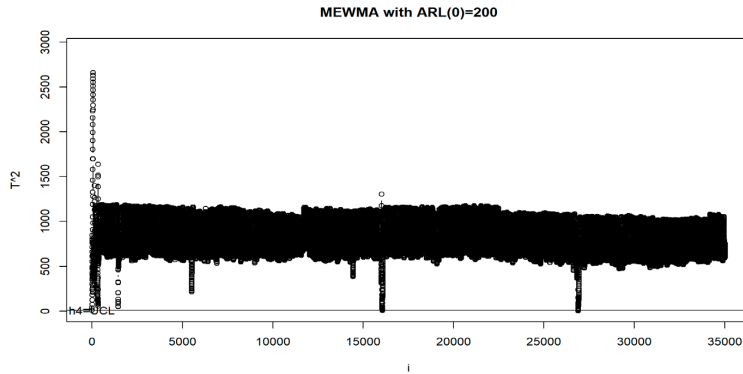


Figure 5: MEWMA control chart for both multivariate Pressure and Flow data. No detected signals beyond the control limits.

In EWMA, the parameters settings for the control charts are shown in Table 1. The control charts for the pipe flow and pressure data are presented in separate charts.

Table 1: parameter settings for EWMA control charts

MODEL	Variables	Lambda	Sigma	Points Beyond Limits (%)
EWMA	Imputed Flow	0.1	3	89%
		0.5	3	78%
		<b>0.99</b>	<b>3</b>	<b>64%</b>
	Imputed Pressure	0.5	3	88%
		0.8	3	84%
		<b>0.99</b>	<b>3</b>	<b>81%</b>

The results for EWMA with different settings are as shown in Table 1. This setting shows that a substantial number of points are contained within the limits. As shown in the last column ‘Points Beyond Limits (%)’, a subset of the observations are flagged as out of the control limits. Table 1 also shows that different settings indicate different proportions of flagged out observations. In particular the higher the value of lambda, the lower proportion of points will be flagged down. It can be seen from Table 1 that flow data gave a better reading of lowest proportion points beyond the limits at lambda 0.99 and Sigma as 3, at 64% compared to that of pressure data at 81%.

The control charts based on EWMA for flow and pressure is as shown in Figure 6 and Figure 7:

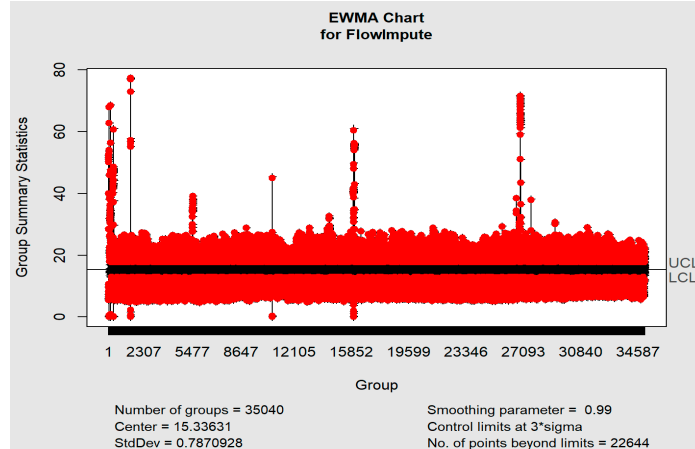


Figure 6: EWMA control chart for imputed Flow data, using the most optimal settings.

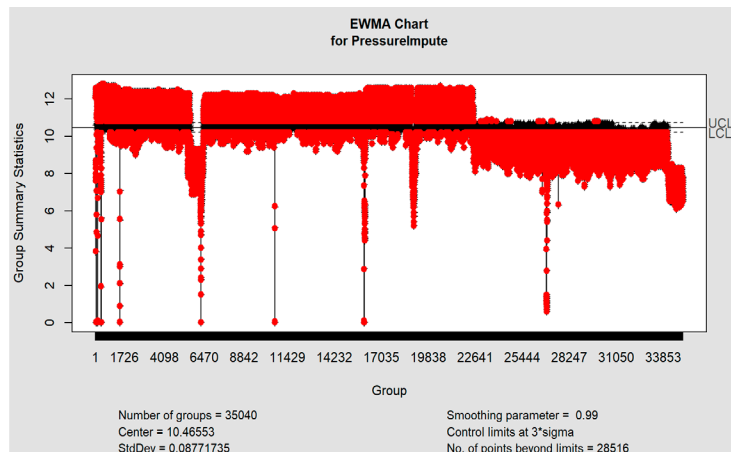


Figure 7: EWMA control chart for imputed pressure data, using the most optimal settings

Figure 6 and Figure 7, show the control charts for the most optimal settings for flow and pressure data. Due to the massive number of data, the control limits and detected points are not clear.

The EWMA chart appears to successfully detect a number of points beyond the control limits, than MEWMA chart. However, the detected points are too many, and they may likely to include false alarm detected points. Also, the detected points detected are not clearly shown in the graphs due to the massive annual data that is being analysed. In addition, the parameters used in this control chart are based on the overall parameter value for the annual data, which does not take into account of the fluctuation that occurs in phases in the data. Consequently, the detected points can be challenging to identify in the monitoring process.

In the next section, we continue to use EWMA chart and improve the detection method by using segmented data with targeted parameter settings based on the feature of the data.

### b) EWMA Control charts based on data segmentation and adaptive parameter settings

In this section, the results obtained from applying EWMA control charts to flow time series on segmented data is presented. Specifically, water monitoring is conducted on a weekly basis, employing a shorter time series data to observe transient signals on the control chart. Also, in contrast to the previous analysis in section 2.5.3(a), here the parameter settings for the control charts are adjusted to align with the weekly characteristics of the monitored data.

In section 2.5.2, it can be observed that the average flow has been found to vary overtime every week. A snapshot of the calculated weekly average flow readings, the corresponding estimated variation and coefficient variation, as well as the complaint indicator can be seen in Table 5 (for the whole list, refer to Appendix 1).

Table 2: Snapshot of the calculated weekly average flow readings, and the corresponding estimated variation and coefficient variation

Week	Mean Flow	Standard Deviation	Coefficient of Variation (%)	Complaint
1	16.3	8.5	52.1	1
2	15.8	8.3	52.5	1
...	...	...	...	-
8	15.7	6.1	38.9	1
...	...	...	...	-
16	15.9	4.9	30.8	1
...	...	...	...	-
24	17.6	10.5	59.7	2
...	...	...	...	-
40	17.9	11.8	65.9	1
...	...	...	...	-
51	15.1	4.5	29.8	-
52	16.2	8.7	53.7	2

Table 2 provides an overview of the average flow rates observed on a weekly basis, accompanied by relevant statistical measures in the year 2022. The standard deviation shows the degree of dispersion around the mean, and the coefficient of variation (CV) expressed as a percentage, provides insight into the relative variability in comparison to the mean. Higher standard deviation values implies higher variability; and higher CV implies higher relative variability. For instance in Week 1, the average flow is 16.3. The degree of variation for other observed flow values in week 1, around 16.3 is 8.5. Also, the relative variability is calculated

by the coefficient of variation is 52.1%. A higher CV may suggest increased volatility or fluctuations within the dataset. For example, a CV value of 50% is more likely to raise concerns than a CV of 29%.

It can be observed from Table 2, that the mean flow values exhibit some variation across different weeks, ranging from 14.2 to 17.9. This indicates fluctuations in the average flow rate over the monitored period. In addition, Weeks 24 and 40 stand out with relatively higher standard deviations, suggesting increased variability in flow during those periods. Also, higher CV values, such as those in weeks 24, 40, and 52, indicate greater relative variability. While the mean flow values vary, there were some consistent patterns or trends over time. Weeks 1 to 5, for instance, show a gradual decrease in mean flow, followed by a slight increase in the subsequent weeks.

Table 3 outlines the number of complaints received, corresponding statistics and the parameter settings employed. The selection of parameters in Table 3 is contingent upon the variations observed in the weekly data, with a specific focus on the coefficient of variation (CV) values. If the CV for a given week exceeds 55% (indicated by the blue row in Table 3), the sample standard deviation for that week is utilized as the variation parameter in the EWMA chart. Conversely, if the CV for the week is below 55% (highlighted by the green row in Table 3), a constant rate of 15 is applied as the variation parameter in the EWMA chart. This adaptive approach ensures a suitable adjustment of parameters based on the variability characteristics of the weekly data.

Table 3: Adaptive parameter settings for EWMA control charts (weekly)

Week	Complaint	Coefficient of Variation (%)	Standard Deviation	Adaptive Sigma	Points Beyond Limits (%)
1	1	52.1	8.5	15	7%
2	1	52.5	8.3	15	1.3%
...	-	...	...	...	...
8	1	38.9	6.1	15	3.3%
...	-	...	...	...	...
16	1	30.8	4.9	15	0.6%
...	-	...	...	...	...
24	2	59.7	10.5	10.5	9.1%
...	-	...	...	...	...
40	1	65.9	11.8	11.8	7.1%
...	-	...	...	...	...
51	-	29.8	4.5	15	0%
52	2	53.7	8.7	8.7	7.6%

It can be observed from Table 6 that this adaptive parameter setting strategy results in a much lower percentage of points beyond limits, varying from 0% to 9.1%. Notably, the data highlights

the effectiveness of adaptive control limits in identifying transient signals, with lower percentages indicating better control over the process. The data underscores the dynamic nature of the monitored system and the utility of adaptive approaches in responding to fluctuations in the observed data.

The resulting EWMA control charts from these adaptive parameters for Flow data for weeks showing different variations of data at varying CV values at Week 24 (CV 69%) as shown in Figure 13.

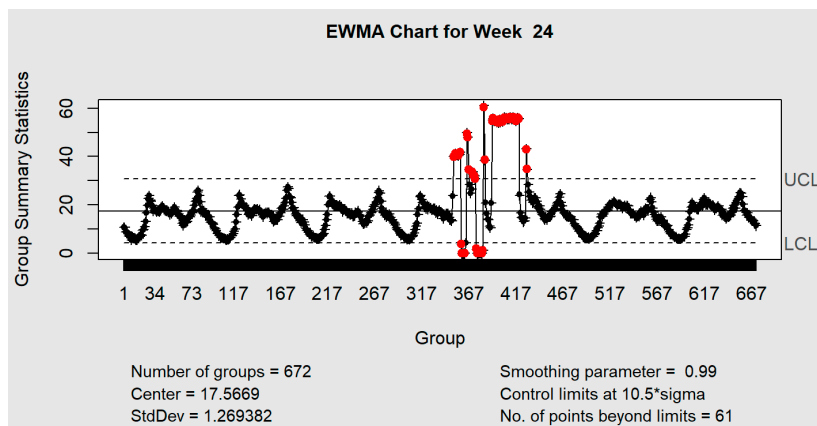


Figure 8: EWMA control chart for week 24 (CV 69%) based on adaptive variation

### 1.2.6 Conclusions and Recommendations

This report recommends a combination of dynamic thresholding based on weekly patterns, targeted analysis of reliable flow data, and adaptive parameter settings in control charts, particularly with a focus on shorter time series, enhance the effectiveness of pipe burst detection.

In this study, it can be observed that detecting gradual leakage can be challenging because it often starts with a small amplitude and a slow, incremental increase, making it harder to notice in the initial stages.

For water monitoring, data pre-processing is important to be carried out due to several factors: (1) to ensure continuity and meaningful observations (2) to identify any significant patterns or trends in the data and (3) to identify the most effective and appropriate statistical tools and parameters to use for the data. The shift in observations, particularly in Pressure data, underscores the reliability of utilizing Flow data for leakage detection due to its lower susceptibility to false alarms. The shift in observations, especially in Pressure data, suggests

that Flow data is more reliable for this purpose and has a lower susceptibility to false alarms. Therefore, Flow data is recommended over Pressure data for leakage detection.

The analysis also emphasizes the importance of considering weekly flow patterns in water monitoring for establishing dynamic thresholds in control charts. The use of EWMA control charts on segmented flow time series with fine-tuned parameters, resulting in improved control over the process. The adaptive parameter strategy significantly reduces the percentage of points beyond limits (0% to 9.1%), emphasizing its effectiveness in identifying transient signals. This underscores the dynamic nature of the system, highlighting the utility of adaptive approaches in responding to fluctuations in observed data and facilitating the easy detection of transient signals.

The analysis done in this study can be replicated to test the transient signals in future data. However, note that the adaptive parameter settings recommended in Appendix 1 assumes that the patterns in water measurements is similar from year to year. Thus, further analysis on the trends and variation of the data from several years need to be carried out to assure that this assumption is validated.

An alternative approach that can be considered to detect transient signals for water monitoring is using a form of transformation in the data called differencing in the control charts. For instance, we can transform the data by the taking the lag of 7 days to detect as an alarm to calculate the mean and variations for the control chart. By considering this weekly differencing, trend variation is expected caused by any gradual leakage events while removing the influence of the gross trend in the monitoring data that can be caused by other factors.

### **1.3 Pipe Burst Detection With Artificial Neural Network (ANN)**

#### **1.3.1 Introduction**

Utilizing pressure, flow, and critical pressure data as inputs, an Artificial Neural Network (ANN) model is trained to detect pipe bursts in water supply systems. By learning from historical data where instances of bursts are correlated with specific patterns in these parameters, the ANN can quickly analyze current data and predict the likelihood of a burst event.

#### **1.3.2 Objectives**

- (a) Develop an Artificial Neural Network (ANN) model capable of predicting pipe bursts based on input variables of pressure impute, flow impute, and critical pressure impute.
- (b) Use the generated ANN model to validate the predicted value with complaint data

### 1.3.3 Methodology

#### 1.3.3.1 Artificial Neural Network (ANN) model

An Artificial Neural Network (ANN) is a mathematical model designed to imitate the structure and functions of biological neural networks. A basic Artificial Neural Network (ANN) usually comprises three layers: input, hidden, and output layers, as illustrated in Figure 9. The initial layer is the input layer, responsible for accepting independent variables. The final layer is the output layer, responsible for generating output variables. The layers situated between the input and output layers are referred to as "hidden layers" (Zhu et al., 2022).

The fundamental component of every artificial neural network is the artificial neuron, which is a simple mathematical model or function. This model follows three basic sets of rules: multiplication, summation, and activation. At the input of the artificial neuron, the inputs undergo a process called weighting, where each input value is multiplied by its corresponding weight. In the middle section of the artificial neuron, a sum function adds up all the weighted inputs and bias. Finally, at the output of the artificial neuron, the sum of the previously weighted inputs and bias passes through an activation function, also known as a transfer function (refer Figure 10). The transfer functions usually have a sigmoid shape, but they may also take the form of other non-linear functions, piecewise linear functions, or step functions. Here, An ANN with 2 hidden layers for 3 features or inputs with Sigmoid Symmetric Transfer Function is used.

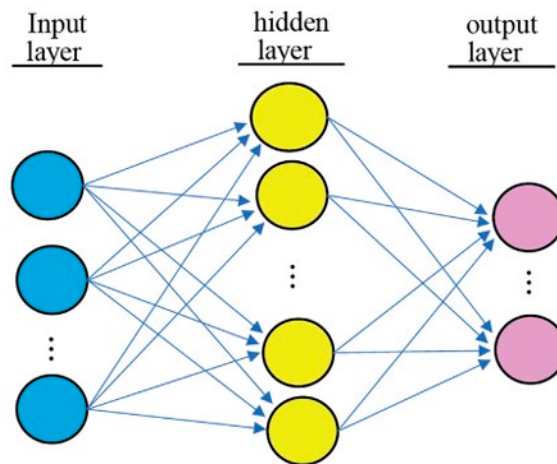


Figure 9: Illustration of a typical neural network model (Zhu et al., 2022)

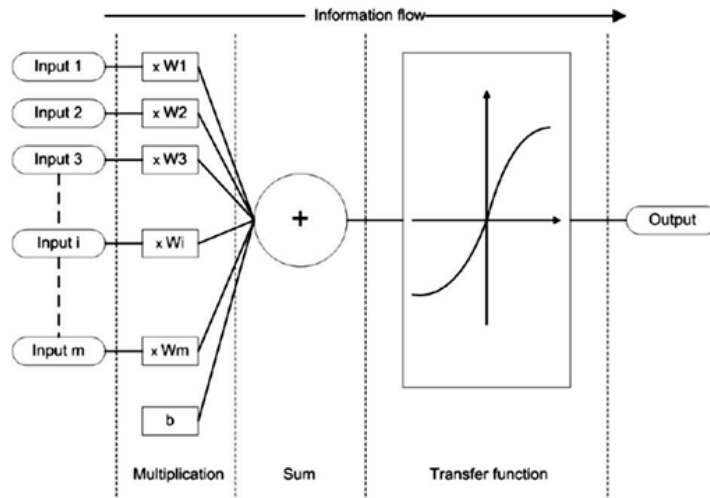


Figure 10: Illustration of a typical flow of neural network model

### 1.3.3.2 Backpropagation method Neural Network based on Levenberg-Marquardt

Although there are several various network models, the backpropagation neural network (BPNN) is particularly effective in recognizing patterns within practical applications, as highlighted by Lek & Guégan (1999). The BPNN model aims to minimize the mean square error between the predicted and expected values by adjusting the connection weights of the network (Li et al., 2012). BPNN comprises of three layers: input layer, hidden layer, and output layer. The input signal is forward-propagated from the input layer, via the hidden layer, to the output layer. The difference between the predicted output and expected output of the network is referred to as the error signal. This error signal is then backpropagated from the output layer to the input layer in a step-by-step manner across the layer. Throughout this process, the weight values of the network are adjusted based on the error feedback to make the predicted output closer to the expected one (Li et al., 2012). The Levenberg-Marquardt (LM) algorithm is essentially an evolution of the gradient descent algorithm and Newton algorithm, which significantly accelerate the convergence rate by reducing the iteration process, resulting in more accurate data. In comparison with the traditional BPNNs, such as slow convergence speed and local minimum problems, the convergence rate of the LM algorithm is the fastest of all traditional or improved networks. The improved BPNNs with the LM algorithm have demonstrated excellent results as indicated by research from Wang (2013), Hua et al. (2008), Jian et al. (2012) and Miao et al. (2011). In this study, LM will be implemented.



### 1.3.4 Results

An ANN is employed for predictive modeling, featuring two hidden layers to process three input features. The Sigmoid Symmetric Transfer Function is applied, and the Levenberg-Marquardt (LM) algorithm is utilized for optimization. The training data, depicted in Table 4, offers a glimpse into the input and output layers.

The initial three columns of Table 4 represent the input layer, comprising Pressure, Flow, and CP Pressure. The last column of Table 4 signifies the output layer, indicating the occurrence of pipeburst. The training data for the output layer adopts values ranging from 0 to 1. Zero values denote non-occurrence and the value one denotes occurrence of pipeburst events. Other values in this column are strategically designed to mirror the gradual progression of pipeburst events. Specifically, output values are set from 0.2 to 0.5 before a reported incident, escalating to 1 post-complaint. This design aims to capture and reflect the evolving nature of pipeburst occurrences in the model's training phase.

Table 5 presents the outcomes of the generated artificial neural network (ANN) model's validation process. The results demonstrate the model's performance in predicting events based on actual data. Upon validation, it was observed that out of the total 10 complaints considered, the ANN model accurately predicted the occurrence of events in 7 instances, while in 3 cases, the predictions deviated from the actual outcomes. This discrepancy underscores the necessity for further refinement and optimization of the ANN model to enhance its predictive accuracy.

Table 4: Sample training data for ANN input and output layers

PressureImpute	FlowImpute	CPPressureImpute	Pipeburst Event Occurrence
12.6	6.03	12.23	0
12.6	5.72	12.34	0
12.6	6	12.34	0
12.6	5.96	12.34	0.2
10.6	28.71	9.73	0.5
8.7	50.36	5.78	0.5
8.6	51	5.69	0.5
8.5	50.99	5.48	0.5
8.3	51.49	5.3	1
8	51.76	5.11	1

20-22 November, 2023, UTM KUALA LUMPUR, Malaysia

7.8	52.3	4.89	1
7.6	52.44	4.74	1
3.8	39.91	2.19	1
5.8	62.8	1.09	0
7.1	53.98	3.58	0
8.3	45.93	5.73	0

Table 5 ANN model's validation

Actual Pipeburst Event Occurrence	ANN LM-15		ANN LM-30	
	Probability of Pipeburst Occurrence	Predicted Pipeburst Event Occurrence	Probability of Pipeburst Occurrence	Predicted Pipeburst Event Occurrence
1	0.78	1	0.74	1
1	0.27	0	0.35	0
1	0.79	1	0.71	1
1	0.93	1	0.92	1
1	0.71	1	0.91	1
1	0.12	0	0.25	0
1	0.96	1	0.92	1
1	0.83	1	0.82	1
1	0.89	1	0.93	1
1	0.0002	0	0.0004	0

#### 1.4 Acknowledgements

This work was supported by the Institute of Mathematics for Industry, Joint Usage/Research Center in Kyushu University. (FY2023 Workshop (I) "MMISG2023" (2023b003).)

**REFERENCES**

- Hua, Z. L., Qian, W., & Gu, L. (2008). Application of improved LM-BP neural network in water quality evaluation. *Water resources protection*, 24(4), 22-25.
- Jian, X. C., Wang, L. W., & Min, F. (2012). BP neural network based on LM algorithm for the forecasting of vehicle emission. *J. Chongqing Univ. Technol*, 26, 11-16.
- Lek, S., & Guégan, J. F. (1999). Artificial neural networks as a tool in ecological modelling, an introduction. *Ecological modelling*, 120(2-3), 65-73.
- Li, J., Cheng, J. H., Shi, J. Y., & Huang, F. (2012). Brief introduction of back propagation (BP) neural network algorithm and its improvement. In *Advances in Computer Science and Information Engineering: Volume 2* (pp. 553-558). Springer Berlin Heidelberg.
- Miao, X., Chu, J., & Du, X. (2011). Application of LM-BP neural network in predicting dam deformation. *Jisuanji Gongcheng yu Yingyong(Computer Engineering and Applications)*, 47(1), 220-222.
- Niaki, S. T. A., Malaki, M., & Ershadi, M. J. (2011). A particle swarm optimization approach on economic and economic-statistical designs of MEWMA control charts. *Scientia Iranica*, 18(6), 1529-1536.
- Shuai, Y., Zhang, X., Huang, H., Feng, C., & Cheng, Y. F. (2022). Development of an empirical model to predict the burst pressure of corroded elbows of pipelines by finite element modelling. *International Journal of Pressure Vessels and Piping*, 195, 104602.
- Sukparungsee, S., Areepong, Y., & Taboran, R. (2020). Exponentially weighted moving average—Moving average charts for monitoring the process mean. *Plos one*, 15(2), e0228208.
- Wang, Z. P. (2013). Application of LM-BP neural network in lake trophic evaluation. *Environ. Sci. Surv*, 32, 98-101.
- Wei, X., Li, X., Liu, T., Luo, Y., Chen, W., & Wang, Z. (2021). Mechanism analysis of the retaining wall collapse of a foundation pit induced by water supply pipeline burst: A case study. In *IOP Conference Series: Earth and Environmental Science* (Vol. 861, No. 3, p. 032088). IOP Publishing.
- Zhu, X. K., Johnson, W. R., Sindelar, R., & Wiersma, B. (2022). Artificial neural network models of burst strength for thin-wall pipelines. *Journal of Pipeline Science and Engineering*, 2(4), 100090.

## INDUSTRY PRESENTATION SLIDES

# Prediction of Pipe Failure Modeling For Sustainable Non-Revenue Water (NRW)

### Introduction Ranhill SAJ Sdn Bhd

Ranhill SAJ Sdn Bhd, a subsidiary of Ranhill Utilities Berhad is an integrated water supply company, involved in the process of water treatment and distribution of treated water to consumers right up to billing and collection.

### Business Activities

- Collect and retain from the customers charges and fees relating to the supply of treated water for different classes of consumers.
- Distribution of treated water to domestic, commercial and institutional customers.
- Operations, maintenance and development of water treatment, reticulation and supporting systems.

### Problem Statement:

Pipe burst is one of the major contributors to water loss in water supply systems that significantly increase the Non-Revenue Water (NRW) level. Water authority aims to reduce the NRW to 25.5% in 2024. Although the NRW level, as of September 2023, has nearly met the target at approximately 25.40%, monitoring is crucial due to possibility of increasing NRW % if water losses are not controlled. An effective pipe burst detection and prediction is essential for the organization to make good decisions in monitoring water losses and minimizing the time taken to detect the pipe burst.

Therefore, one of the strategies taken by Ranhill SAJ to reduce the NRW % rate is to start with mathematical approach by proposed statistical hypothesis test for effective leakage recovery. Last but not least by using statistical analysis and mathematics it is hoped that the model will be able to help organization to made good decision in manage water losses and minimized the time taken to detect the pipe burst.

Table 1 IWA standard water balance, adopted from Lambert (2002)

	Billed Authorised Consumption	Billed Metered Consumption (including water exported)	Revenue Water
		Billed Unmetered Consumption	
Authorised Consumption	Unbilled Authorised Consumption	Unbilled Metered Consumption	
		Unbilled Unmetered Consumption	
System Input Volume	Apparent Losses	Unauthorised Consumption	Non- Revenue Water (NRW)
		Metering Inaccuracies	
Water Losses	Real Losses	Leakage on Transmission and/or Distribution Mains	
		Leakage and Overflows at Utility's Storage Tanks	
		Leakage on Service Connections up to the Measurement Point	

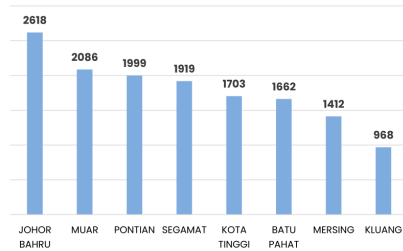
**Project Objective:**

1. To suggest the best practices for data pre processing and explain the historical pipe burst event in 2022 based on input factors of water supply in DMA GP03 by using mathematical model.
2. To determine the most effective mathematical model for DMA GP03 Taman Sri Pulai real-time pipe burst detection and prediction.
3. To verify the best practices to calculate of commercial losses & physical losses for DMA GP03.

# Project Location Selection

## Major leak cases by districts 2019 – 2022 :

DISTRICT	2019	2020	2021	2022	Total
JOHOR BAHRU	636	764	717	501	2618
MUAR	534	621	506	425	2086
PONTIAN	698	432	453	416	1999
SEGAMAT	461	517	451	490	1919
KOTA TINGGI	348	380	546	429	1703
BATU PAHAT	235	534	501	392	1662
MERSING	368	353	332	359	1412
KLUANG	233	215	258	262	968
JOHOR	3513	3816	3764	3274	



## Prioritize matrix rank :

DISTRICT	2019	2020	2021	2022	Total
JOHOR BAHRU	2	1	1	1	5
MUAR	3	2	3	4	12
SEGAMAT	4	4	6	2	16
PONTIAN	1	5	5	5	16
KOTA TINGGI	6	6	2	3	17
BATU PAHAT	7	3	4	6	20
MERSING	5	7	7	7	26
KLUANG	8	8	8	8	32

Important and urgent

Description	Likelihood key
Important and urgent	1-8
Important but not urgent	9-18
Not important but urgent	19-27
Not important and not urgent	28-36

## MALAYSIA MATHEMATICS IN INDUSTRY STUDY GROUP (MMISG2023)

20-22 November, 2023, UTM KUALA LUMPUR, Malaysia

### Top 10 Major leak cases by DMA 2019 – 2022

2019	Major leak frequency
J00 OUTSIDE JOHOR BAHRU	51
SK129 TMN MAS & TAN YOKE FONG	20
BE24 STULANG BARU	14
SK47 TMN SRI SKUDAI B	13
BW05 LARKIN DOMESTIC	12
JOZ OUTZONE JOHOR BAHRU	12
GP10 TANJUNG KUPANG	11
BW60 ABDUL SAMAD RESIDENTIAL	10
PG01A PASIR GUDANG INDUSTRI (KELULU)	10
<b>Grand Total</b>	<b>183</b>

2020	Major leak frequency
PG14 PERMAS JAYA A	47
BB06 KELAPA SAWIT	44
SK13 TMN SRI SKUDAI A	43
SK47 TMN SRI SKUDAI B	40
GP02 LIMA KEDAI	39
SK05 KULAI A	35
UT45 SG TIRAM A	34
SK22 TMN SKUDAI BARU A	33
BB03 SEDENAK LUAR	32
GP50 TAMAN NUSANTARA A	31
<b>Grand Total</b>	<b>342</b>

2021	Major leak frequency
PG14 PERMAS JAYA A	23
SK13 TMN SRI SKUDAI A	22
SK47 TMN SRI SKUDAI B	20
UT45 SG TIRAM A	20
SK05 KULAI A	15
SK22 TMN SKUDAI BARU A	14
BB06 KELAPA SAWIT	12
PG20 TMN SRI PLENTONG	11
UT01 TMN BKT TIRAM	11
<b>GP03 TMN SRI PULAI A</b>	<b>11</b>
<b>Grand Total</b>	<b>170</b>

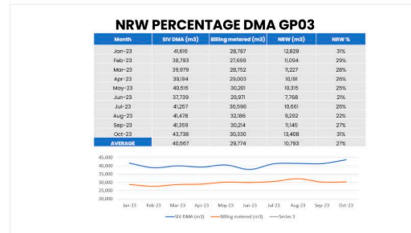
  

2022	Major leak frequency
BB06 KELAPA SAWIT	18
<b>GP03 TMN SRI PULAI A</b>	<b>14</b>
SK35 TMN TUN AMINAH E	12
SK13 TMN SRI SKUDAI A	12
SK51B TMN SELESA JAYA B	12
UT01 TMN BKT TIRAM	11
PG04 PASIR GUDANG RESIDENTIAL C	9
BB03 SEDENAK LUAR	9
GP02 LIMA KEDAI	8
SK22 TMN SKUDAI BARU A	8
<b>Grand Total</b>	<b>113</b>

GP03 : Rank 59 (2019), Rank 14 (2020), Rank 10 (2021) & Rank 2 (2022)

#### Current NRW % as September 2023 Report

DISTRICT	% SPAN Calculation (Sept 2023)	% 12 Months	% 1 Month
JOHOR BAHRU	20.96	21.16	19.29
MUAR	29.32	29.7	29.05
PONTIAN	28.07	28.7	30.81
SEGAMAT	37.01	36.99	37.44
KOTA TINGGI	23.99	24.21	21.78
BATU PAHAT	34.4	34.99	32.68
MERSING	22.75	22.78	19.75
KLUANG	29.17	29.48	26.84
<b>JOHOR</b>	<b>25.12</b>	<b>25.40</b>	<b>23.79</b>



DMA Background		
No.	Information	Details
1	Pipe Length	10,144.413 m
	AC	Total AC Length (m) : 9,719.426 m D150 – 7,922.44 m D200 – 200.148 m D250 – 1,206.900 m D300 – 389.938 m
		MS
2	Pipe Age	Date Laid : 9/12/1985 Date Capture : 18/03/2004  Age : 37 years
3	Local Authority	Majlis Perbandaran Kulai
4	Customer Info	Active Account : 1,372 Acc Average Cons monthly : 40,000 m3 Average Billing monthly : 29,649 m3  Domestic Tariff : 1,330 Acc ( 30,756 m3) Non Domestic Tariff: 41 Acc ( 1,430 m3) 3% <span style="border: 1px solid red; padding: 2px;">August 2023 BIS Data</span>

DMA Background		
No.	Information	Details
5	Water Supply Information	<ul style="list-style-type: none"> <li>Water Treatment Plant: Semanggar WTP</li> <li>Bkt 75 A &gt; Bkt Skudai 2 &gt; Sri Pulai 1 &amp; 2</li> <li>No PRV</li> </ul>
6	System reference	<ul style="list-style-type: none"> <li>Aquasmart – CP, HP, MNF , Flow</li> <li>HWM Online – Flow , Pressure</li> <li>RMS Monitoring – Res. Information , Res water level</li> <li>IJMS – Job ID LK (Mp) , NW Complaint , OP Complaint</li> </ul>



MALAYSIA MATHEMATICS IN INDUSTRY STUDY GROUP (MMISG2023)

20-22 November, 2023, UTM KUALA LUMPUR, Malaysia

**Summary Major Leak (LK) Job in 2022**

LK Date (Complaint)	Location	Pipe type & Size	Complaint Date	Job Date	On Site Date	Leave Site Date	Date Close	Total Job ID	NW	OP
01-Jan	Jalan Rotan 4	AC 150	5:05:09 AM	5:12:59 AM	5:15:00 AM	7:00:00 AM	10:16:18 AM	1	18	0
02-Jan	Jalan Pakis 3	AC 150	5:57:53 AM	6:01:30 AM	6:05:00 AM	6:10:00 AM	9:42:45 AM	1	10	0
04-Jan	Jalan Pakis 18	AC 150	7:36:33 AM	7:37:10 AM	8:00:00 AM	8:05:00 AM	10:23:39 AM	1	7	1
16-Jan	Jalan Rotan 2	AC 150	1:14:33 AM	1:15:07 AM	1:45:00 AM	2:45:00 AM	11:10:44 AM	1	2	0
27-Feb	Jalan Batai 2	AC 150	8:18:04 AM	8:29:49 AM	8:50:00 AM	8:55:00 AM	11:13:44 AM	1	0	0
22-Apr	Jalan Pakis 17	AC 150	9:05:35 AM	9:13:53 AM	10:00:00 AM	10:30:00 AM	9:31:28 AM	1	0	0
16-Jun	Jalan Pakis 10	AC 150	4:00:26 PM	4:01:22 PM	4:25:00 PM	5:30:00 PM	10:11:55 AM	2	1	0
17-Jun	Jalan Batai 11	AC 150	7:17:39 AM	8:00:54 AM	8:25:00 AM	8:30:00 AM	9:53:47 AM	1	8	1
08-Oct	Jalan Rotan 2	AC 150	8:43:05 AM	8:46:34 AM	9:55:00 AM	10:00:00 AM	9:14:29 AM	2	12	1
15-Oct	Jalan Rotan 3	AC 150	10:08:47 AM	10:09:17 AM	10:10:00 AM	10:15:00 AM	9:16:38 AM	3	2	1
<b>GP03 TMN SRI PULAI A Total</b>								14	60	4

OUTPUT PRESENTATION SLIDES

**UTM**  
UNIVERSITI TEKNOLOGI MALAYSIA

**MMISG 2023 – RANHILL SAJ SDN BHD**

**PREDICTIVE MODELLING OF PIPE BURST TOWARDS SUSTAINABLE NON-REVENUE WATER**

Date : 20-22 November 2023  
Time : 8:30 – 5:00 pm  
Venue : Dewan Seminar & Lecture Room 5

**Ranhill SAJ**

**KYUSHU UNIVERSITY** Institute of Mathematics for Industry

**MYHIMS SOLUTIONS PTE**

*Innovating Solutions*

## Presentation Outline

- 01** Problem Background & Statement
- 02** DATA PREPROCESSING
- 03** Proposed Solution
  - Statistical Approach
    - Multivariate Control Chart
    - Pattern Extraction
  - Engineering Approach
- 04** Way Forward/Future Recommendation

2

# PROBLEM BACKGROUND & STATEMENT

## PROBLEM BACKGROUND

- Water Supply System (WSS) is a complex process that is composed of multi-hydraulic elements (e.g., reservoirs and consumption nodes) which are interconnected together by links (e.g., pumps, valves, and pipes).
- The water losses in any type of distribution systems have been identified as being dependent on many factors, including specifications of the WSS pipe network and other internal and external factors such as the utility provider operational management practice, the level of proficiency and technology deployed to control the system.
- In the literature, the difficulty of controlling losses in WSS has been acknowledge as there are more than hundreds methods captured that focus on controlling different types of WSS losses.
- Although it is almost economically impossible to totally eliminate losses in WSS due to the complexity of these socio-technical systems, but research and effort should be perpetually invested in refining the understanding, planning, and execution.

## PROBLEM STATEMENT

Pipe burst is one of the major contributors to water loss in water supply systems that significantly increase the Non-Revenue Water (NRW) level. Water authority aims to reduce the NRW to 25.5% in 2024. Although the NRW level, as of September 2023, has nearly met the target at approximately 25.40% or 457 MLD, monitoring is crucial due to possibility of increasing NRW % if water losses are not controlled. An effective pipe burst detection and prediction is essential for the organization to make good decisions in monitoring water losses and minimizing the time taken to detect the pipe burst.

# ABOUT DATA

## ABOUT DATA

Two reading devices, DMA meter and Logger provides reading relate to water measurements.

These devices are located at different locations in the area of GP03. However, the readings are recorded at the same 15 minutes interval.

- DMA meter records: Pressure Rate (mH) and Flow Rate (l/s)
- Logger: Critical Pressure (Cpp) & High Pressure (Hpp) Rates

**DATA:  
CONTINUOUS INTERVAL/TIME SERIES FORM  
MORE THAN ONE VARIABLE (MULTIVARIATE)**

Note:

Other readings

-from DMA e.g. 15 m Flow m<sup>3</sup>, Hourly flow, Daily Flow- they are not included as these are aggregated data from the original Pressure Rate and Flow Rate data

-Daily Midnight night flow (MNF) located at nearby reservoir. -these data not included in the analysis due to the distance from GP03

Data Collection and Management Challenges

- 1) 15 minute interval – smaller more costly
- 2) Missing Values – replaced by 0 to indicate no water supply (tap source closed)
- 3) Sources of Missing Values – Pipe replacement, Maintenance (battery replacement, network coverage)
- 4) Data not integrated

**DMA Background**

No.	Information	Details
1	Pipe Length	10,144.413 m
	AC	Total AC Length (m) : 9,719.426 m D150 – 7,922.44 m D200 – 200.148 m D250 – 1,206.900 m D300 – 389.938 m
	MS	Total MS Length (m) : 424.987 m D380 – 373.278 m D250 – 51.709 m
2	Pipe Age	Date Laid : 9/12/1985 Date Capture : 18/03/2004 Age : 37 years

7



Method

- 1) 15 minute interval – smaller more costly
- 2) Missing Values at CPHP – replaced by 0 to indicate no water supply (tap source closed) - to be changed to 0.01
  - o Due to maintenance (battery replacement) - estimate using the next day value eg if the missing value occur at 20 April at 5:00:00 am then it will be estimated by 19 April at 5:00:00 am
  - o Negative values for pressure - as is - indicate the reverse flow
  - o Pattern of
- 3) Sources of Missing Values – Pipe replacement, Maintenance (battery replacement, network coverage) but not directly informed from the 'data logger'
- 4) Suggestion Data not integrated - Data Management/Data Science Centre





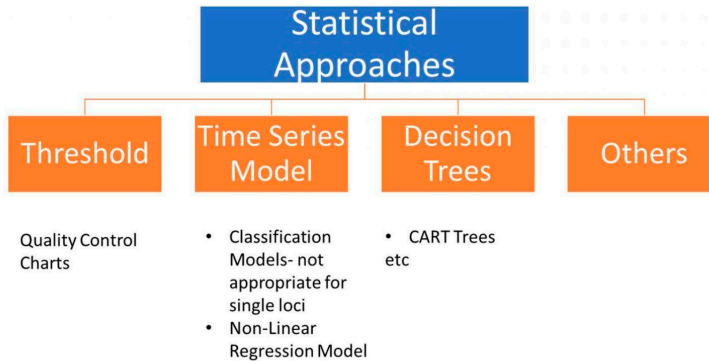
## MULTIVARIATE TIME SERIES -INTERVAL -DATASET

### METHOD DETECT ANOMALIES

- A time series is a sequence of numbers over time.
- Recorded data from DMA & Logger are in the form of continuous interval, multivariate time series.
- Anomalies in time series are values that are highly inconsistent with those expected around at those time points.
- Types of Anomalies detection for time series data:
  - retroactive anomaly detection- based on historical data
  - real-time anomaly detection.

Build approach based on historical data to form basis for real-time anomaly detection

## MULTIVARIATE TIME SERIES -INTERVAL -DATASET METHOD DETECT ANOMALIES



15



## Multivariate EWMA Control Charts

A Multivariate Exponentially Weighted Moving Average (MEWMA) chart is a statistical control chart used in quality control to monitor the mean vector of a multivariate process. It's an extension of the univariate Exponentially Weighted Moving Average (EWMA) chart to handle multiple variables simultaneously.

The EWMA control chart can be made sensitive to a small or gradual drift in the process, whereas the traditional Shewhart control chart can only react when the last data point is outside a control limit.

The EWMA statistics can be defined, in which  $\lambda$  represents the weighting factor attributed to the observations :

$$z_i = \lambda x_i + (1 - \lambda)z_{i-1}$$

The variance of  $z_i$  is given by:  $\sigma_{z_i}^2 = \sigma^2 \left( \frac{\lambda}{2 - \lambda} \right) [1 - (1 - \lambda)^{2i}]$

Once the process standard deviation is estimated, the control limits are represented by :

$$UCL = \mu_0 + L\sigma \sqrt{\frac{\lambda}{(2 - \lambda)} [1 - (1 - \lambda)^{2i}]}$$

$$CL = \mu_0$$

$$LCL = \mu_0 - L\sigma \sqrt{\frac{\lambda}{(2 - \lambda)} [1 - (1 - \lambda)^{2i}]}$$





## MULTIVARIATE EWMA

A Multivariate Exponentially Weighted Moving Average (MEWMA) chart is a statistical control chart used in quality control to monitor the mean vector of a multivariate process. It's an extension of the univariate Exponentially Weighted Moving Average (EWMA) chart to handle multiple variables simultaneously.

The EWMA control chart can be made sensitive to a small or gradual drift in the process, whereas the traditional Shewhart control chart can only react when the last data point is outside a control limit.

The EWMA statistics can be defined, in which  $\lambda$  represents the weighting factor attributed to the observations :

$$z_i = \lambda x_i + (1 - \lambda)z_{i-1}$$

The variance of  $z_i$  is given by :  $\sigma_{z_i}^2 = \sigma^2 \left( \frac{\lambda}{2 - \lambda} \right) [1 - (1 - \lambda)^{2i}]$

Once the process standard deviation is estimated, the control limits are represented by :

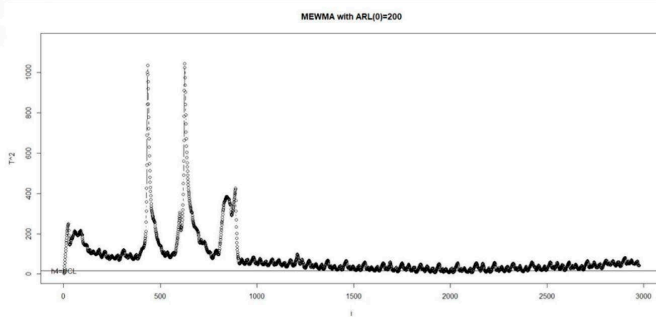
$$UCL = \mu_0 + L\sigma \sqrt{\frac{\lambda}{(2 - \lambda)}} [1 - (1 - \lambda)^{2i}]$$

$$CL = \mu_0$$

$$LCL = \mu_0 - L\sigma \sqrt{\frac{\lambda}{(2 - \lambda)}} [1 - (1 - \lambda)^{2i}]$$



## RESULTS



The multivariate chart shows that the four variables are correlated. Therefore, the univariate charts on the separate variables may not even signal.

The Multivariate EWMA procedure creates control charts for two or more numeric variables. Examining the variables in a multivariate sense is extremely important when the variables are highly correlated, since joint out-of-control conditions can occur without any individual variable violating its control limits when plotted separately.



## Granger Causality Test INTERPRETATION

The Granger Causality test is used to determine whether or not one time series is useful for forecasting another.

This test uses the following null and alternative hypotheses:

**Null Hypothesis (H<sub>0</sub>):** Time series  $x(\text{Flow})$  does not Granger-cause time series  $y(\text{Pressure})$ .

**Alternative Hypothesis (H<sub>A</sub>):** Time series  $x(\text{Flow})$  Granger-causes time series  $y$ . ( $\text{Pressure}$ )

- **Model 1:** This model attempts to predict the Flow in the previous three months and Pressure in the previous three months as predictor variables.
- **Model 2:** This model attempts to predict Flow using only Pressure in the previous three months as predictor variables.
- **P( $>F$ ):** This is the p-value that corresponds to the F test statistic. It turns out to be  $2.2 \times 10^{-16}$ .

Since the p-value is  $2.2 \times 10^{-16}$ , less than .05, we can reject the null hypothesis of the test.

19



## TIME SERIES MODEL

FEATURE BASED NON-LINEAR TS MODEL:  
WAVELET INPUTS LSSVR MODEL

Least Squares Support Vector Regression (LSSVR) is a variation of Support Vector Regression (SVR) that is based on the principles of support vector machines. SVR is a type of machine learning algorithm used for regression tasks, and it aims to find a hyperplane that best fits the data while minimizing the error.

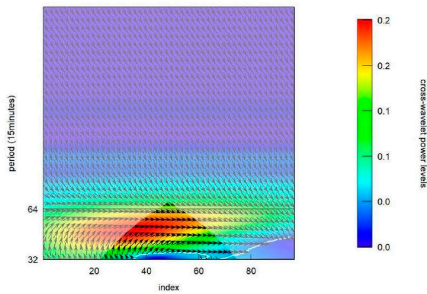
The LSSVR model, in particular, uses a least squares loss function to optimize the parameters of the regression model. In traditional SVR, the optimization problem involves minimizing the error subject to a certain margin and a penalty for points that fall outside this margin. LSSVR, on the other hand, focuses on minimizing the sum of squared errors between the predicted and actual values.

JAN 2022:Pressure Over Flow

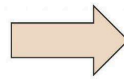


# TIME SERIES MODEL

FEATURE BASED NON-LINEAR TS MODEL:  
WAVELET INPUTS LSSVR MODEL



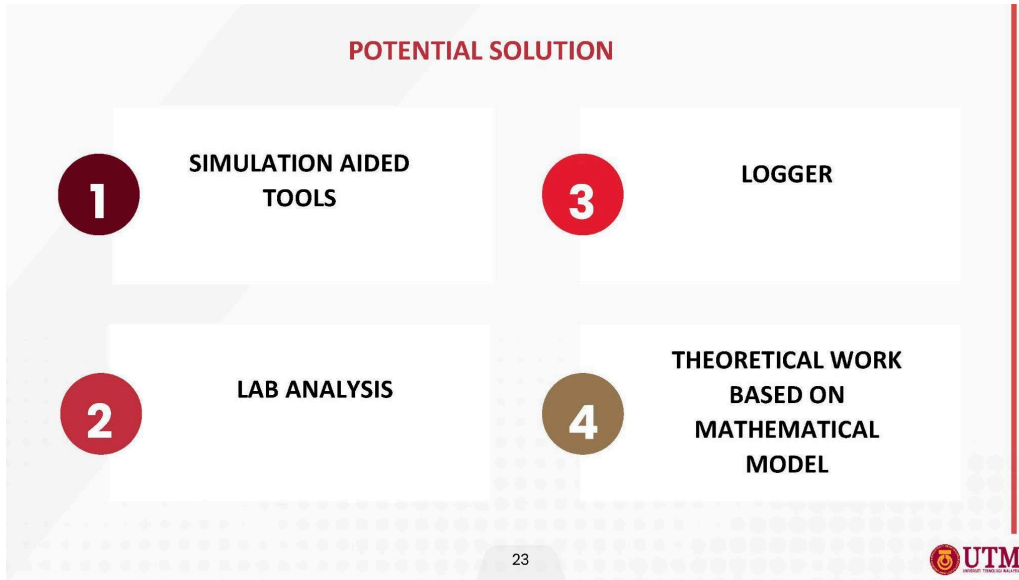
JAN 2022:Pressure Over Flow



**LEAST SQUARES  
SUPPORT  
VECTOR  
REGRESSION  
MODEL**



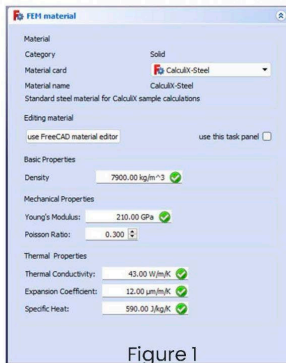
**ENGINEERING APPROACH/ APPLIED  
MATHEMATICAL MODELLING**



23

Simulation tools can be employed to analyze various performance indicators, including structural integrity, hydraulic efficiency, and stress tensor, in the context of asbestos cement/mild steel water pipes.

The preliminary simulation results, given the value of basic, mechanical, and thermal properties of steel as given in Figure 1 is generated through the utilization of FreeCAD—an open-source parametric 3D CAD (Computer-Aided Design). The output is shown in Figure 2



**1. SIMULATION AIDED TOOLS**

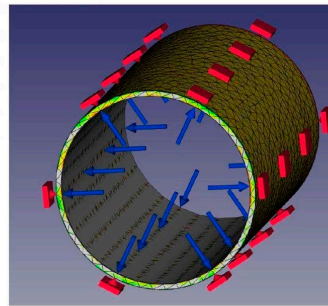


Figure 2

24



## 2: LAB ANALYSIS

### Phase 1 : Collecting Info/identify factors

- sample of materials the ruptured part

Phase 1 is to collect ruptured samples, photos of the ruptured location, soil sample, depth of the pipe, dimensions of the pipe and all other data.

### Phase 2 : Lab test/ lab analysis

- To find the structural integrity – e.g: elasticity. Using SEM
- Molecular structure - To look into the grain structure of the ruptured sample. The motivation is to identify the presence of material degradation.

### Phase 3 : Comparison

- Compare with new one
- To compare the ruptured pipe with the new pipe in terms of thickness, the presence of rust and others.

25



## 3: LOGGER

### Logger works

- The use of raspberry pie
- To get more data (every second)
- To design a low cost logger that can collect pressure, flow data in a predetermined time-step and transmit the data to the central server for processing and analysis.

### Real Time Data Analytics

- Data from various sources will be collected and fused.
- The fused data shall be displayed in a real time dashboard to see pattern and trends.
- The pattern and trend can be used to identify pipe burst.

26



4: THEORETICAL WORK BASED ON MATHEMATICAL MODEL

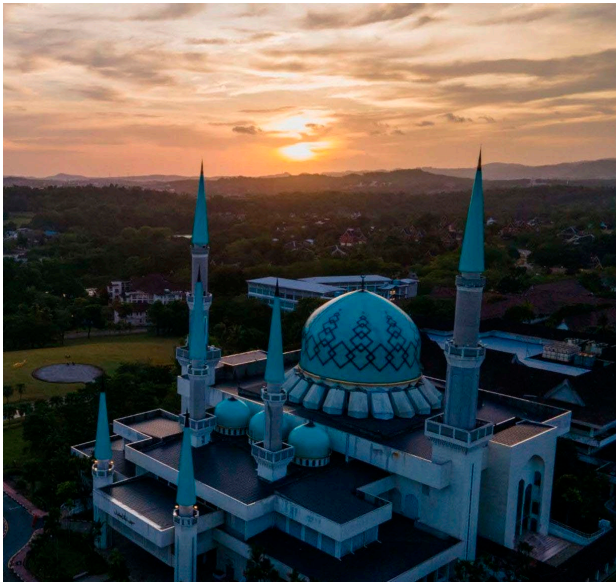
No.	References	Remarks	
1	Rajani, B., & Makar, J. (2000). A methodology to estimate remaining service life of grey cast iron water mains. <i>Canadian Journal of Civil Engineering</i> , 27(6), 1259-1272.	Life span of grey cast iron. A preferred approach to make decisions on pipe repair and replacement is to determine the expected remaining service (residual) life of each pipe segment and ensure that the necessary work is performed before failure occurs.	<p><b>Design procedures for grey cast iron water mains</b></p> <p>The design procedure for grey cast iron mains as outlined in C101.67 (AWWA 1977) considers a pipe as a rigid structural element. Rigid pipes support loads by virtue of resistance of the pipe as a ring to bending and do not rely on horizontal thrust from the soil at the sides. Experimental work done by Schlick (1940) showed that failure of a grey cast iron pipe under combined internal pressure (<math>P</math>) and an external three-edge (bearing) ring load (<math>w</math>) will not occur if</p> $[1] \quad \left(\frac{w}{W}\right)^2 + \left(\frac{P}{P_c}\right) \leq 1$ <p>where <math>W</math> is the three-edge crushing (ring) load necessary to cause failure in the absence of internal pressure, and <math>P_c</math> is the internal bursting pressure necessary to cause failure in the absence of external load. The factor of safety need not be identical for internal pressure and external three-edge load, though the design standard suggests a common value of 2.5. <math>W</math> and <math>P_c</math> are determined on the basis of hoop stress as follows:</p> $[2] \quad W = \frac{\pi h^2 \sigma_r}{3(D+h)}$ $[3] \quad P_c = \frac{2h\sigma_t}{D}$ <p>where <math>h</math> and <math>D</math> are pipe wall thickness and internal diameter, respectively, <math>\sigma_r</math> is the "rupture modulus" and <math>\sigma_t</math> is the "bursting tensile strength." The rupture modulus represents the local flexural or bending action along the ring whereas the burst tensile strength represents the hoop tension in the grey cast iron pipe.</p>

4: THEORETICAL WORK BASED ON MATHEMATICAL MODEL

No.	References	Remarks	
2	Jing, K., Zhi-Hong, Z. (2012). Time Prediction Model for Pipeline Leakage Based on Grey Relational Analysis. <i>Physica Procedia</i> , 25, 2019-2024.	Prediction of initial leakage time after the supply network comes into use. Assists to identify significant factors (pipe material, diameter, depth and age) and build a linear regression model	<p>According to the results of Grey relational analysis, we select the first four factors which has great correlation with the leakage. Take cast iron pipe as example, assuming that pipe leakage factors and the initial pipeline leakage time after the networks come into use have a linear relationship, independent variables are diameter, pressure and depth, water supply pipe leakage time multivariate linear regression model is established<sup>[10]</sup>.</p> $Y = \beta_0 + \beta_1 D + \beta_2 H + \beta_3 P \quad (5)$ <p>Where <math>D</math> is pipe diameter(mm); <math>H</math> is depth(m); <math>P</math> is pipe pressure(Mpa); <math>Y</math> is the initial leakage time after the networks come into use; <math>\beta_0, \beta_1, \beta_2, \beta_3</math> are regression coefficients.</p> <p>Take cast iron pipe as example, use the pipe data of a city in North China and establish water supply pipeline leakage time prediction model:</p> $Y = -6000.741 - 1999.02D - 17318.428H + 450.949P$ <p>Comparing the observations of pipe's safe use time and of predicted value of regression model, model's average relative error is 14.74%.</p>

**4: THEORETICAL WORK BASED ON MATHEMATICAL MODEL**




No.	References	Remarks
3	Verde, C. (2001). Multi-leak detection and isolation in fluid pipelines. <i>Control Engineering Practice</i> , 9(6), 673-682.	<p>Assuming the convective changes in velocity and compressibility to be negligible, and that the liquid density and pipe cross-sectional area are constant, the motion and continuity equations governing one dimensional transient flow are (Chaudry, 1979)</p> $\frac{\partial Q}{\partial t} + gA \frac{\partial H}{\partial z} + \mu Q Q  = 0, \quad (1)$ $b^2 \frac{\partial^2 Q}{\partial z^2} + gA \frac{\partial H}{\partial t} = 0, \quad (2)$ <p>with <math>H</math> the pressure head (m), <math>Q</math> the flow (m<sup>3</sup>/s), <math>z</math> the length co-ordinate (m), <math>t</math> the time co-ordinate (s), <math>g</math> the gravity (m/s<sup>2</sup>), <math>A</math> the section area (m<sup>2</sup>), <math>D</math> is the pipeline diameter <math>m</math> and <math>b</math> is the speed of sound (m/s). Also, <math>\mu = f/2DA</math> where <math>f</math> is the adimensional friction coefficient. A leak at point <math>z_r</math> of the pipeline with outflow</p> $Q_{z_r} = \lambda \sqrt{H} z_r \quad (3)$ <p>and <math>\lambda \geq 0</math>, produces a discontinuity in system (1) and (2) (Zhidkova, 1973). As consequence the pipeline with a</p>



**THANK YOU**

PRESENTATION DESCRIPTION

In enim a arcu imperdiet malesuada. Fusce wisi, Nullam at arcu a est sollicitudin euismod. In convallis, Nullam dapibus fermentum ipsum. Aliquam erat volutpat. Excepteur sint occaecat cupidatat non proident, sunt in culpa qui officia deserunt mollit anim id est laborum. Vestibulum fermentum tator id mi.

-  utm.my
-  univteknologimalaysia
-  utmofficial

Kerana Tuhan untuk Manusia

***Tackling Carbon Emissions: Strategies for Medium and Heavy-Duty Trucks***

- Industry Representatives : Raja Dzulfetrie Sa'ad<sup>12</sup>  
Zainal Azman bin Zawawi<sup>12</sup>  
(Total Logistic Services (M) Sdn. Bhd.)
- Study Group Contributors : Nur Arina Bazilah bt Aziz<sup>1</sup>, Adibah Shuib<sup>3</sup>, Zaitul Marlizawati Zainuddin<sup>1</sup>, Zulkifli Mohd Nopiah<sup>2</sup>, Zulhasni Bin Abdul Rahim<sup>1</sup>, Zulkarnain Bin Abdul Latiff<sup>1</sup>, Zaharah Mohd Yusoff<sup>3</sup>, Jamaliatul Badriyah<sup>6</sup>, Syarifah Zyurina Nordin<sup>1</sup>, Wan Rohaizad Wan Ibrahim<sup>1</sup>, Shukur Hassan<sup>1</sup>, Khalid Solaman Almadani<sup>1</sup>

**1.1 Introduction**

As a country experiencing rapid industrialization and economic growth, Malaysia faces significant challenges related to carbon emissions and their impact on the environment. The nation's economic development, while crucial for progress, has led to increased carbon emissions primarily from industries, transportation, and energy production. Emissions levels across all economic sectors have increased over the 2010–2017 period. CO<sub>2</sub> emissions from the transport sector represented 28.8% of total fossil fuel combustion in Malaysia, well above the global average of 24.5%. Road transport is also the largest CO<sub>2</sub> emitter among all transport subsectors (International Energy Agency- IEA, 2019).

To address this issue, Malaysia has implemented substantial efforts to address greenhouse gas (GHG) emissions by making a dedicated commitment to the global community. Under its National Determined Contribution (NDC) pledge presented during COP26 and reiterated in COP27, the Malaysian government has pledged to achieve net-zero emissions by 2050. Additionally, there is a commitment to reduce CO<sub>2</sub> intensity in relation to GDP by 45% by 2030 (MIDA, 2023).

This pledge has been incorporated into the 12<sup>th</sup> Malaysia Plan and the National Energy Policy 2022-2040 (NEP, 2022). This policy documents the way forward strategically and outlines key priorities for the energy sector in the coming years. Figure 1 below shows the action plan for the heavy vehicles segment in the National Energy Policy 2022-2040 (Ministry of Economy, 2022)



MALAYSIA MATHEMATICS IN INDUSTRY STUDY GROUP (MMISG2023)

20-22 November, 2023, UTM KUALA LUMPUR, Malaysia

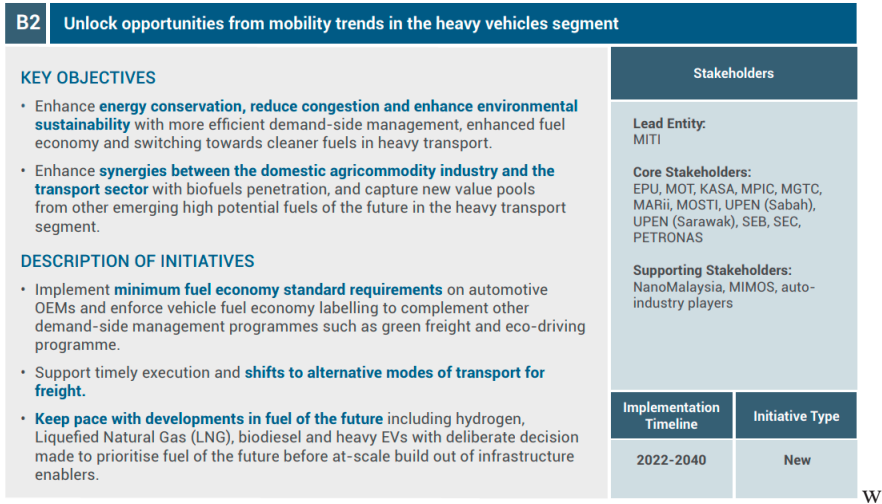


Figure 1: Action Plan for the Heavy Vehicles Segment in Malaysia National Energy Plan 2022-2040

Under the government's recent policy, industries are mandated to adhere to and follow regulations aimed at curbing carbon emissions including Total Logistic Services (M) Sdn. Bhd (TLS).

As an integral part of the Toyota Tsusho Group of companies, TLS is mandated to participate in the Company Group Wide Carbon Neutrality Challenges, which entail achieving two primary objectives as shown in Figure 2 below.

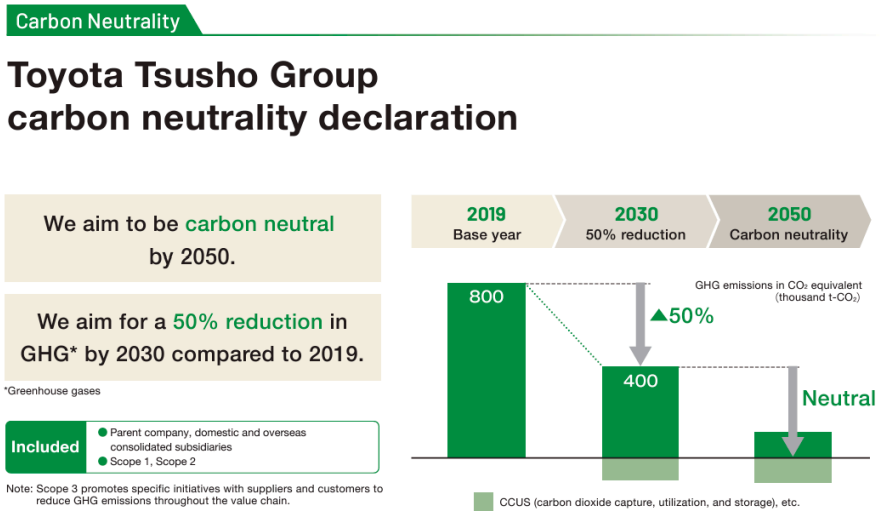


Figure 2: Toyota Tsusho Group Carbon Neutrality Declaration

At present, TLS has devised a three-year strategy to meet these challenges. This plan includes several scheduled activities such as optimizing routes, scheduled vehicle maintenance, implementing a truck aging policy limiting trucks to a maximum of 20 years in service, providing eco-driving skill training for drivers, setting a maximum idling period of 3 minutes, exploring innovative solutions using mathematical approaches or tools, and transitioning to electric trucks.

One approach involves employing innovative solutions, notably mathematical approaches, to identify the factors contributing to carbon emissions. Through this analysis, TLS aims to effectively address the carbon emission issue by gaining a deeper understanding of the involved factors.

## 1.2 Identification of Factors Contributing to Carbon Emissions

### 1.2.1 Carbon Emission Formula

To ascertain the factors contributing to carbon emissions in heavy and medium-duty vehicles, an examination of the carbon emission formula has been conducted. This formula has been obtained from the TLS calculation sheet.

$$\text{Carbon emission} = \left( \frac{\text{emission}}{\text{factor}} \right) \left( \frac{\left( \frac{\text{distance (km)}}{\text{fuel efficiency } \left( \frac{\text{km}}{\text{l}} \right)} \right) \times \left( \frac{\text{num. of}}{\text{trips}} \right)}{\text{fuel usage}} \right) \times (\text{vehicle utilization \%})$$

Within this formula, Toyota Tshusho has predefined certain parameters including distance, number of trips, and vehicle utilization. Consequently, the parameters available for investigation encompass emissions factor and fuel efficiency. The exploration of factors influencing carbon emissions will be centered around these two parameters.

### 1.2.2 Factors Contributing to the Carbon Emissions

As global concerns regarding climate change and environmental sustainability intensify, there is a growing need to understand and address the factors that contribute to carbon emissions. Carbon emissions, largely in the form of carbon dioxide (CO<sub>2</sub>), are a significant driver of anthropogenic climate change. From the carbon emission formula in Section 1.2.1, the carbon emission factors can be investigated based on the carbon emission parameter and fuel efficiency.

#### 1.2.2.1 Emission Factor

An emission factor is a fundamental concept used to quantify the rate at which a particular pollutant, such as carbon dioxide (CO<sub>2</sub>), is emitted into the atmosphere per unit of activity or fuel consumption. It provides a standardized measure of emissions associated with various industrial processes, transportation activities, energy production, and other human

20-22 November, 2023, UTM KUALA LUMPUR, Malaysia

activities. In most instances, these factors are derived from averages of available data of acceptable quality, assumed to represent long-term averages for all facilities within the source category, thus serving as population averages. The emission factor is typically calculated using empirical data obtained from laboratory experiments, field measurements, or emissions inventories. It may vary depending on the specific activity or process being analysed. The general equation for emission estimation is formulated as

$$E = A \times EF \times \left( 1 - \frac{ER}{100} \right)$$

where  $E$  represents emissions,  $A$  signifies the activity rate,  $EF$  denotes the emission factor, and  $ER$  stands for overall emission reduction efficiency, expressed as a percentage.  $ER$  is further delineated as the product of the efficiency of the control device's destruction or removal and the capture efficiency of the control system. Some factors influencing the emission factor, including fuel type, combustion technology, operating conditions, fuel quality and control technologies. Table 1 below shows the Carbon emissions factors for different types of fuel (EEA, 2023).

Table 1: Carbon emission factors for different types of fuel

Subsector units	Fuel	kg CO <sub>2</sub> per kg of fuel <sup>1</sup>
All vehicle types	Petrol	3.169
All vehicle types	Diesel	3.169
All vehicle types	LPG <sup>2</sup>	3.024
All vehicle types	CNG <sup>3</sup> (or LNG)	2.743
All vehicle types	E5 <sup>4</sup>	3.063
All vehicle types	E10 <sup>4</sup>	2.964
All vehicle types	E85 <sup>4</sup>	2.026
All vehicle types	ETBE11 <sup>5</sup>	3.094
All vehicle types	ETBE22 <sup>5</sup>	3.021

Accurate estimation of emission factors is essential for assessing the environmental impact of various human activities and for developing effective strategies to mitigate emissions and combat climate change. Based on Table 1, one way of reducing the carbon emissions is by changing the fuel type to the one with low emission factor.

### 1.2.2.2 Fuel Efficiency

The quantity of emissions generated by medium and heavy-duty vehicles in various scenarios is influenced by multiple factors such as vehicle class and weight, driving patterns, vehicle use, fuel category, engine exhaust treatment, vehicle age, and terrain conditions (Clark et al., 2002). Understanding the complex interplay of these factors is paramount for devising effective strategies to mitigate carbon emissions, transition towards sustainable practices, and fostering a more resilient and environmentally conscious global community.

Factors influencing fuel efficiency were investigated, exploring both controllable and uncontrollable factors as shown in Figure 3 below.

<b>Uncontrollable factors</b> <ol style="list-style-type: none"> <li>1. Vehicle design</li> <li>2. Maintenance practices</li> <li>3. Vehicle load</li> <li>4. Route planning</li> <li>5. Vehicle age</li> </ol>	<b>Controllable factors (short-term)</b> <ol style="list-style-type: none"> <li>1. Driving behaviour</li> <li>2. Fuel quality</li> <li>3. Alternative fuel</li> </ol>
	<b>Controllable factors (long-term)</b> <ol style="list-style-type: none"> <li>1. Engine technology</li> </ol>

Figure 3: Uncontrollable and controllable factors in carbon emissions influencing fuel efficiency

#### 1.2.2.2.1 Uncontrollable Factors

Uncontrollable factors are those that have been either addressed or are beyond the control of TLS, such as fixed elements or external conditions like weather. However, the fixed factors such as vehicle age, vehicle load and maintenance schedule could also be further studies to validate the efficacy of the specified scheme.

##### i) Vehicle Design

Vehicle design plays a pivotal role in determining the efficiency and environmental impact of automobiles. Two crucial aspects of vehicle design that significantly influence fuel efficiency are aerodynamics and weight. Aerodynamics plays a crucial role in the design of medium and heavy trucks, influencing both fuel efficiency and overall performance. Streamlined designs that minimize air resistance are essential for reducing drag forces, especially at higher speeds. For trucks, which often operate on highways and cover long distances, aerodynamic features such as sloped front ends, side fairings, and aerodynamic mirrors are implemented to enhance fuel efficiency. The objective is to reduce the energy required to overcome air resistance, thereby optimizing fuel consumption. Engineers employ wind tunnel testing and computational fluid dynamics to refine truck designs, ensuring they cut through the air with minimal resistance.

The weight of a medium or heavy truck is a critical factor affecting its fuel efficiency and operational cost. Lighter vehicles generally demand less energy to move, translating to improved fuel efficiency. Truck designers and manufacturers focus on employing materials that offer strength while minimizing weight, such as high-strength steel and aluminum alloys. Additionally, advancements in materials technology and manufacturing processes contribute to the development of lightweight components without compromising structural integrity. Payload capacity is another consideration, balancing the need for a robust structure with the ability to carry substantial loads. By optimizing the weight of truck components, manufacturers can enhance fuel efficiency, reduce emissions, and increase the overall economic viability of the vehicle.

**Recommendation:** While currently classified as an uncontrollable factor, there is potential in the future to procure more aerodynamic designs featuring optimal truck component weights to boost fuel efficiency. Additionally, TLS can consider integrating multiple vehicles with varying weights into their delivery schedule.

## ii) Maintenance Practices

Maintenance practices contribute to the longevity and efficiency in the medium and heavy-duty vehicles. These substantial machines demand meticulous care to ensure optimal performance, longevity, and fuel efficiency. Proper and timely maintenance is the cornerstone of ensuring that medium and heavy-duty vehicles operate at their peak efficiency. This is the current practices in TLS to ensure optimal engine functioning, improving fuel efficiency and reducing emissions. Regular maintenance practices include scheduled oil changes, which are essential for preserving engine health and lubrication. This prevents friction-induced wear and tear, enhancing fuel efficiency. Air filter replacements are equally crucial, as clean filters optimize air intake, facilitating efficient combustion. Engine tune-ups, involving inspections of various components and adjustments, ensure that the engine operates at its designed efficiency, promoting not only performance but also fuel economy. Regular maintenance practices, when adhered to diligently, contribute significantly to extending the operational life of these vehicles and minimizing fuel consumption. For the old engine, it is advisable to maintain the catalytic converter regularly to help reduce the carbon emissions.

Tire maintenance is not to be ignored for medium and heavy-duty vehicles. Properly inflated tires reduce rolling resistance, the force required to move a tire over a surface. By maintaining the recommended tire pressure, rolling resistance is minimized, improving fuel efficiency. Routine tire inspections for wear and alignment issues are also essential. Misaligned or improperly inflated tires not only compromise safety but can also lead to increased fuel consumption. Regular tire rotations further ensure even wear, optimizing the lifespan of the tires and contributing to sustained fuel efficiency. In essence, tire maintenance is a proactive measure that directly impacts operational costs and the overall environmental footprint of these vehicles.

**Recommendation:** TLS may explore the utilization of Operations Research (OR) techniques to optimize maintenance schedules, taking into account factors like vehicle availability, resource constraints, maintenance requirements, and operational priorities. This approach ensures that maintenance tasks are scheduled at optimal times to minimize operational disruptions while maximizing vehicle uptime. Additionally, proactive preventive maintenance planning can be conducted by analyzing historical maintenance data, vehicle usage patterns, and manufacturer recommendations. By scheduling maintenance preemptively based on anticipated failure rates or usage thresholds, the risk of costly breakdowns and unexpected downtime can be mitigated.

### iii) Vehicle Load

The concept of optimal vehicle load is a fundamental consideration in the carbon emission investigation for medium and heavy-duty vehicles. For the logistics companies, the transportation must navigate the delicate balance between payload requirements and fuel conservation. The weight a vehicle carries, specifically in terms of cargo, is a critical factor influencing fuel efficiency for medium and heavy-duty vehicles. Carrying unnecessary weights demands more energy for acceleration and maintaining speed, resulting in increased fuel consumption. Therefore, careful consideration of cargo weight is vital. Understanding the payload requirements for a given journey and loading only what is essential not only conserves fuel but also ensures compliance with safety regulations and enhances the overall efficiency of the transportation process. One of the proactive measures for enhancing fuel efficiency is the periodic removal of excess cargo. Regular assessments of payload requirements and ensuring that vehicles only carry what is necessary contribute to sustained fuel savings. Moreover, this practice aligns with safety standards and ensures that vehicles operate within their designed capacities, promoting both efficiency and longevity. In TLS, the vehicle load is already determined according to their demand and delivery schedule. Therefore, this is not a controllable factor in this study. However, it is known that heavier loads increase fuel consumption and emissions, necessitating more energy to transport goods.

**Recommendation:** By utilizing OR techniques to optimize vehicle loading based on delivery schedules and demand patterns, it can efficiently load vehicles with the right mix of deliveries hence reduce the number of trips needed and maximize vehicle utilization, thereby minimizing carbon emissions per delivery.

### iv) Route Planning

The efficiency of route planning is essential for medium and heavy-duty vehicles. The strategic selection of routes is crucial not only for timely deliveries but also for the optimization of fuel efficiency. Optimal routes consider factors such as traffic patterns, road conditions, and potential delays. Leveraging advanced mapping technologies and real-time traffic data, route planners can identify the most efficient paths for vehicles to navigate. Route planning that strategically circumvents congested areas helps vehicles maintain a consistent speed, reducing the overall fuel consumption. This not only conserves resources but also contributes to timely deliveries, streamlining the logistics process.

**Recommendation:** TLS can consider alternative delivery strategies such as consolidation, pooling, or collaborative delivery models to reduce the number of vehicles on the road and minimize emissions. By consolidating deliveries to maximize route efficiency, TLS can lower overall carbon emissions.

**v) Vehicle Age**

The age of medium and heavy-duty vehicles significantly influences carbon emissions, with older vehicles typically emitting higher levels of pollutants compared to newer counterparts. As vehicles age, wear and tear on engine components can lead to decreased efficiency and suboptimal combustion processes, resulting in increased carbon emissions. Older engines may lack advanced technologies and emission control systems found in newer models, further exacerbating their environmental impact. Additionally, aging vehicles may experience deteriorating fuel efficiency, requiring more fuel to achieve the same level of performance, thereby contributing to higher carbon emissions. Regular maintenance and periodic upgrades or replacements of older vehicles with newer, more fuel-efficient models can help mitigate the impact of vehicle age on carbon emissions, promoting cleaner and more sustainable transportation practices.

**Recommendation:** While acquiring newer vehicles may seem like the straightforward solution, given the high cost involved, it is advisable for TLS to prioritize regular maintenance and upgrades for their older vehicles. This approach will aid in mitigating the impact of vehicle age on fuel efficiency and carbon emissions. In addition, instead of a fixed years service, strategy such as fleet replacement planning could also be utilized. Fleet replacement planning involves developing a structured approach to determine when existing vehicles or equipment should be replaced with newer models or upgraded versions. By systematically evaluating the condition and performance of fleet assets and making informed decisions about replacement timing and strategy, organizations can optimize fleet efficiency, minimize operating costs, and ensure the reliability and safety of their operations.

**1.2.2.2.2 Controllable Factors**

This discussion will focus on the controllable factors that could be administered by TLS. They are divided into short-term and long-term factors. Short-term factors here are the factors that can be adjusted relatively quickly and have an immediate impact on carbon emissions such as driving behavior, fuel quality and alternative fuel. Meanwhile, long-term factors are those that require more time and effort to adjust and have a gradual impact on carbon emissions over an extended period such as fleet replacement plan. Although it takes time to implement and yield results, they often lead to sustained reductions in carbon emissions over the long term.

**i) Driving Behaviour**

Efficient driving behavior is a pivotal factor in the quest for sustainability and fuel efficiency in the realm of medium and heavy-duty vehicles. How drivers operate these substantial machines has a profound impact on fuel consumption, emissions, and overall

operational costs. This emphasizes the significance of maintaining optimal speeds and embracing smooth driving techniques to enhance fuel efficiency.

The speed at which a medium or heavy-duty vehicle is operated is directly linked to its fuel efficiency. Maintaining optimal speeds is paramount in ensuring that the engine operates within its most efficient range. Excessive speeds not only lead to increased air resistance, demanding more energy to propel the vehicle, but they can also result in the engine operating at less efficient levels. Striking the right balance by adhering to recommended speed limits and adjusting driving speed based on road conditions contributes significantly to fuel efficiency. By doing so, drivers can achieve a harmonious blend of performance and economy. Through observation from the TLS's fleet management system, the drivers' speed is recorded and those exceeding the speed limit of 90 km/hr will be monitored further.

Smooth driving techniques, characterized by gentle acceleration and braking, are integral to fuel savings. Abrupt acceleration and harsh braking not only consume more fuel but also contribute to increased wear and tear on the vehicle's components. Gentle acceleration allows the engine to operate more efficiently, while gradual braking harnesses kinetic energy, potentially reducing the need for excessive fuel consumption. Driver training programs often emphasize the importance of smooth driving habits, recognizing that a steady and controlled approach to acceleration and braking positively influences fuel efficiency, enhances safety, and extends the lifespan of the vehicle. Minimizing stops, such as unnecessary detours or frequent breaks, optimizes fuel efficiency. Continuous motion allows the vehicle to operate within its most efficient range, contributing to overall energy conservation. Moreover, reducing the number of stops enhances the predictability of delivery schedules, improving the reliability of logistics operations.

Idling, or leaving the engine running while the vehicle is stationary, is a significant contributor to unnecessary fuel consumption. Addressing idling time is a crucial aspect of driving behavior for medium and heavy-duty vehicles. Excessive idling not only consumes fuel without contributing to forward motion but also increases emissions. Implementing strategies to minimize idling, such as turning off the engine during prolonged stops, contributes to substantial fuel savings and aligns with eco-friendly driving practices.

**Recommendation:** TLS may also consider initiating a carbon emission awareness program for drivers and providing incentives to those who exhibit exemplary driving behavior.

## ii) Fuel Quality

The type and quality of fuel a vehicle consumes plays a foundational role in its overall efficiency. Medium and heavy-duty vehicles, often equipped with robust engines, are designed to operate optimally with specific fuel types. High-quality fuels, meeting, or exceeding industry standards, ensure a cleaner and more efficient combustion process. Clean fuels, such as those with low sulfur content, contribute to reduced emissions, aligning with stringent environmental



20-22 November, 2023, UTM KUALA LUMPUR, Malaysia

regulations. Moreover, the compatibility between the fuel type and the engine design is crucial for achieving peak performance and fuel efficiency.

**Recommendation:** TLS may consider employing high-quality, cleaner fuels to improve combustion, thereby reducing carbon emissions. Regular testing can help detect any variations in fuel quality, enabling prompt corrective action to be taken.

### iii) Alternative Fuel

The utilization of alternative fuels presents a promising avenue for reducing carbon emissions from medium and heavy-duty vehicles. By transitioning away from traditional fossil fuels to cleaner alternatives such as biodiesel, ethanol, natural gas, or hydrogen, these vehicles can significantly mitigate their environmental impact. Alternative fuels offer the potential for lower carbon content, resulting in reduced greenhouse gas emissions during combustion. Additionally, some alternative fuels, such as natural gas or hydrogen, produce fewer harmful pollutants like particulate matter and nitrogen oxides, further enhancing air quality. However, the adoption of alternative fuels is not without challenges. The production and distribution infrastructure for alternative fuels are often underdeveloped and costly to implement, limiting their widespread availability and affordability. Additionally, certain alternative fuels may require modifications to vehicle engines or fuel systems, adding complexity and expense to the transition process. Moreover, the production of some alternative fuels may still generate emissions or contribute to other environmental concerns, highlighting the importance of comprehensive lifecycle assessments when evaluating their impact on carbon emissions. Another common alternative is to use fuel additives to improve combustion efficiency and reduce emissions. Certain additives can help optimize fuel performance, leading to improved engine efficiency.

**Recommendation:** Given that the adoption of alternative fuels could entail significant expenses associated with engine modifications and transitioning processes, TLS may initially explore the use of fuel additives. However, it's crucial to approach the use of fuel additives cautiously due to potential side effects such as decreased engine performance or increased emissions.

### iv) Engine Technology

For medium and heavy-duty vehicles, the convergence of advanced technology and emission control systems represents a pivotal step towards sustainability and operational efficiency. Innovative solutions such as hybrid systems, regenerative braking, and start-stop systems offer promising avenues for reducing fuel consumption and minimizing environmental impact. Hybrid technologies seamlessly integrate electric propulsion with traditional internal combustion engines, optimizing fuel efficiency and curbing emissions. Similarly, regenerative braking harnesses kinetic energy during braking, while start-stop systems mitigate unnecessary idling, further enhancing fuel savings. However, despite their transformative potential, these

20-22 November, 2023, UTM KUALA LUMPUR, Malaysia

technologies may pose challenges such as higher upfront costs and potential maintenance complexities. Additionally, the integration of advanced systems requires careful consideration of infrastructure and training to ensure optimal performance and reliability in diverse operating conditions.

**Recommendation:** TLS can opt for the new engine technology for their current vehicles in order to have the latest emission control technology. Although this solution might be costly, it is still cheaper compared to purchasing new trucks or the electric trucks.

### 1.3 Emission Analysis and Evaluation

In order to see the relationship between selected factors, a comprehensive analysis of carbon emissions, fuel efficiency, vehicle age dynamics, and optimization strategies was conducted. By exploring various analytical approaches and tools, we endeavour to offer insights into optimizing vehicle assignments and mitigating carbon emissions effectively. This section serves as a foundational exploration into understanding and addressing key challenges in TLS's quest for carbon neutrality and operational excellence.

#### 1.3.1 Data

The data obtained from TLS is shown in Table 2 as follows. This data is collected from TLS fleet management systems. There are 10 trucks varies from 6 to 20 years old. In this data, the information on the type of roads, the distance and fuel used are given. Based on these information, fuel consumption and fuel efficiency are calculated using the following formula.

$$\text{Fuel Efficiency} = \frac{\text{Total distance (km)}}{\text{Total fuel used (l)}}, \quad \text{Fuel Consumption} = \frac{\text{Total fuel used (l)}}{\text{Total distance (km)}}$$

Table 2: Data from TLS fleet management system.

Vehicle No.	Engine Age	Engine Displ.	Road Type	Km (Sept)	Litre (Sept)	Fuel Efficiency (Km/L) (Sept)	Fuel Consumption (L/Km) (Sept)	Km (Oct)	Litre (Oct)	Fuel Efficiency (Km/L) (Oct)	Fuel Consumption (L/Km) (Oct)
BPF6316	6	7961	federal	4366.5	1590	2.75	0.36	4812.4	1747.8	2.75	0.36
BPF6318	6	7961	federal	5335.6	1475.4	3.62	0.28	6074.4	1739.18	3.49	0.29
BPF6317	6	7961	highway	13772.3	2565.15	5.37	0.19	15088.9	3618.2	4.17	0.24
BPF6319	6	7961	highway	5066.4	1596.43	3.17	0.32	6140.6	1809.4	3.39	0.29
WA4314G	9	7961	federal	3368.4	1202.9	2.8	0.36	3492.8	1305.8	2.67	0.37
W5044Q	10	7961	federal	7743.2	2497.74	3.1	0.32	9822.2	3451.43	2.85	0.35
W3087A	10	7961	highway	6749.9	2790.7	2.42	0.41	7761.1	2763.4	2.81	0.36
BJV4101	16	7961	federal	2511.9	846.8	2.97	0.34	3196.1	1097.9	2.91	0.34
DEE9884	18	7961	federal	5166.9	1682.74	3.07	0.33	5683.1	1518.7	3.74	0.27
NBK9957	20	7961	federal	7677.3	2510.31	3.06	0.33	7518.9	2324.2	3.24	0.31

### 1.3.2 Carbon Emissions Calculation

Using the data in Section 1.3.1 and carbon emission formula in Section 1.2.1, the carbon emissions for September and October have been calculated and shown in Table 3 and Table 4, respectively.

Table 3: Carbon emissions in September 2023

Veh. No.	Engine Age	Engine Displacement	Road Type	Distance Sept (km)	Fuel Sept (L)	Fuel Efficiency Sept (km/L)	Fuel Consumption Sept (L/km)	Carbon Emission (kg)
BPF6316	6	7961	federal	4366.5	1590	2.75	0.3636	4255.35
BPF6318	6	7961	federal	5335.6	1475.4	3.62	0.2762	3950.11
BPF6317	6	7961	highway	13772.3	2565.15	5.37	0.1862	6873.33
BPF6319	6	7961	highway	5066.4	1596.43	3.17	0.3155	4283.27
WA4314G	9	7961	federal	3368.4	1202.9	2.8	0.3571	3224.04
W5044Q	10	7961	federal	7743.2	2497.74	3.1	0.3226	6694.12
W3087A	10	7961	highway	6749.9	2790.7	2.42	0.4132	7475.10
BJV4101	16	7961	federal	2511.9	846.8	2.97	0.3367	2266.63
DEE9884	18	7961	federal	5166.9	1682.74	3.07	0.3257	4510.52
NBK9957	20	7961	federal	7677.3	2510.31	3.06	0.3268	6723.91

Table 4: Carbon emission in October 2023

Veh. No.	Engine Age	Engine Displacement	Road Type	Distance Oct (km)	Fuel Oct (L)	Fuel Efficiency Oct (km/L)	Fuel Consumption Oct (L/km)	Carbon Emission (kg)
BPF6316	6	7961	federal	4812.4	1747.8	2.75	0.3636	4689.90
BPF6318	6	7961	federal	6074.4	1739.18	3.49	0.2865	4664.58
BPF6317	6	7961	highway	15088.9	3618.2	4.17	0.2398	9697.42
BPF6319	6	7961	highway	6140.6	1809.4	3.39	0.2950	4854.52
WA4314G	9	7961	federal	3492.8	1305.8	2.67	0.3745	3505.88
W5044Q	10	7961	federal	9822.2	3451.43	2.85	0.3509	9236.31
W3087A	10	7961	highway	7761.1	2763.4	2.81	0.3559	7402.05
BJV4101	16	7961	federal	3196.1	1097.9	2.91	0.3436	2943.49
DEE9884	18	7961	federal	5683.1	1518.7	3.74	0.2674	4072.38
NBK9957	20	7961	federal	7518.9	2324.2	3.24	0.3086	6219.34

The analysis of the data above reveals several key insights into the factors influencing fuel efficiency and carbon emissions. Engine age appears to correlate with fuel efficiency, with older vehicles generally exhibiting lower efficiency. Road type significantly affects fuel consumption and carbon emissions, with vehicles traveling on highways demonstrating higher efficiency and lower emissions compared to those on federal roads. Variation in fuel efficiency among vehicles suggests the influence of factors such as driving behavior and maintenance practices.

### 1.3.3 Fuel Efficiency and Vehicle Age Analysis

Figure 4 illustrates the fuel efficiency comparison among vehicles during September and October. The plot also incorporates engine age to examine the correlation between fuel efficiency and engine age. The data reveals that while newer vehicles generally exhibit higher fuel efficiency, there are instances where older vehicles, such as NBK9957 (20 years old), outperform newer counterparts like BPF6316 (6 years old) in terms of fuel efficiency.

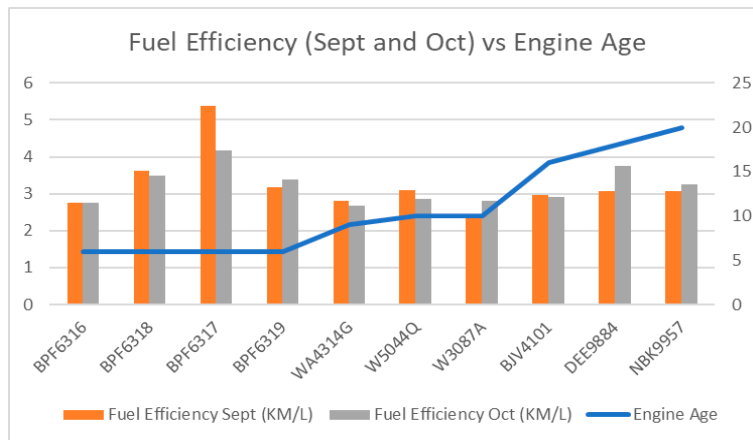


Figure 4: Fuel efficiency for September and October compared with the vehicle age.

This is further proved through correlation test as shown in Figure 5.

```
In [42]: cor(data$engine_age, data$fuel_efficiency_oct)
-0.0402794006529332

In [43]: cor(data$engine_age, data$fuel_efficiency_sep)
-0.290728092224943
```

Figure 5: Correlation test between fuel efficiency in September and October with the vehicle age.

The negative correlation coefficient values for both results suggest a very weak negative correlation between engine age and fuel efficiency. In other words, there appears to be a slight tendency for fuel efficiency to decrease slightly as the engine age increases, but the relationship is extremely weak. This means that engine age alone may not be a significant predictor of fuel efficiency for the medium and heavy-duty vehicles being studied. Other factors, such as maintenance practices, driving conditions, and vehicle technology, likely have a more substantial influence on fuel efficiency than engine age alone. Therefore, while there may be a minor trend indicating decreased fuel efficiency with older engines, it is not a strong enough relationship to draw definitive conclusions about the impact of engine age on fuel efficiency in

this context. Additionally, given the relatively small sample size, the results may lack accuracy and robustness.

### 1.3.4 Carbon Emissions and Fuel Efficiency Analysis

Fuel efficiency refers to the amount of energy extracted from a fuel source relative to the amount of fuel consumed during operation. Vehicles with higher fuel efficiency can travel longer distances using the same amount of fuel, resulting in reduced fuel consumption per unit of distance or work done. On the other hand, carbon emission refers to the release of carbon dioxide (CO<sub>2</sub>) and other greenhouse gases into the atmosphere as a byproduct of fuel combustion.

In theory, there exists a direct relationship between fuel efficiency and carbon emission where higher fuel efficiency typically leads to lower carbon emission. This is because vehicles that can extract more energy from a given amount of fuel produce fewer emissions per unit of distance travelled. However, the relationship is not always straightforward. Various factors can influence carbon emission independently of fuel efficiency, such as engine technology, fuel type, vehicle weight, driving conditions, and maintenance practices. Additionally, improvements in fuel efficiency alone may not necessarily result in proportional reductions in carbon emission if other factors influencing emissions remain unchanged.

Figure 6a) and 6b) show the relationship between carbon emissions and fuel efficiency for September and October 2023 in TLS.

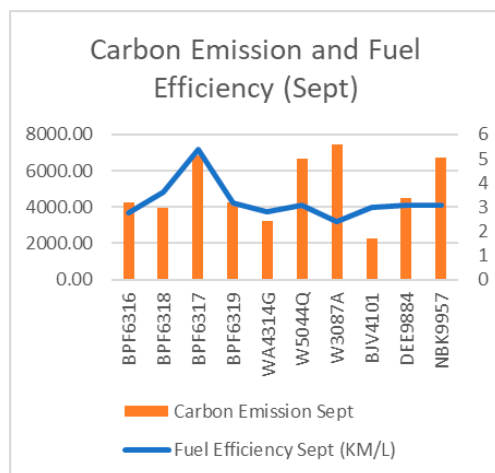


Figure 6a): Carbon emission and fuel efficiency in September 2023

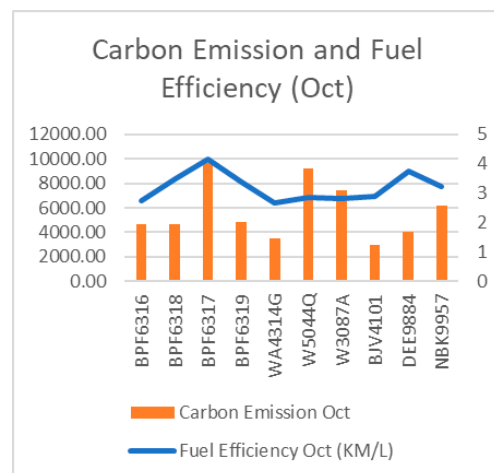


Figure 6b): Carbon emission and fuel efficiency in October 2023

It is observed in Figure 6 that there is variability in both fuel efficiency and carbon emission values across the sampled vehicles. Upon examining the relationship between fuel efficiency and carbon emission, no clear linear trend emerges. While some vehicles with higher

20-22 November, 2023, UTM KUALA LUMPUR, Malaysia

fuel efficiency exhibit lower carbon emissions, this pattern is not consistent across all vehicles. This suggests that factors beyond fuel efficiency alone play a role in determining carbon emission levels, such as vehicle technology, driving conditions, and maintenance practices. Further analysis may be necessary to fully understand the complex relationship between fuel efficiency and carbon emission in medium and heavy-duty vehicles.

In practice, achieving significant reductions in carbon emission often requires a multifaceted approach that includes improving fuel efficiency, adopting cleaner fuel sources, implementing emission control technologies, optimizing vehicle design, and promoting sustainable driving practices. By addressing these factors holistically, it is possible to maximize fuel efficiency while minimizing carbon emission, leading to more environmentally friendly and sustainable transportation systems.

### 1.3.5 Vehicle Assignments Analysis

Presently, TLS has devised a three-year strategy to meet the carbon emission challenges. This plan includes pre-determined vehicle load, routing, delivery schedule and staff assignment. However, based on the sample vehicle data from TLS as shown in Table 5 and Table 7 below, high fuel efficiency vehicle is assigned to the shorter distance. Therefore, alternative measures must be explored to address the impact of these pre-determined parameters on fuel consumption and emissions. One potential strategy involves optimizing vehicle assignments. It is anticipated that by reassigning fuel efficient vehicles to the longer routes, can help reduce fuel consumption and emissions associated with transporting goods.

Table 5: Data from TLS in September 2023

SEPTEMBER	Distance (km)	Fuel (Litre)	Fuel Consumption (Litre/km)	Fuel Efficiency (km/Litre)	Total Carbon Emission (kg)
<b>BPF6316</b>	4366.50	1590.00	0.364	2.75	4261.20
<b>WA4314G</b>	3368.40	1202.90	0.357	2.80	3223.77
<b>WYR2942</b>	7433.40	2790.70	0.375	2.66	7479.08
<b>NBK9957</b>	7677.30	2510.31	0.327	3.06	6727.63
<b>BJV4101</b>	2511.90	846.80	0.337	2.97	2269.42
<b>BPF6318</b>	5335.60	1475.40	0.277	3.62	3954.07
<b>W5044Q</b>	7743.20	2497.74	0.323	3.10	6693.94
<b>BPF6317</b>	13772.30	2565.15	0.186	5.37	6874.60
<b>BPF6319</b>	5066.40	1596.43	0.315	3.17	4278.43
<b>W3087A</b>	6749.90	2790.70	0.413	2.42	7479.08
<b>DEE9884</b>	5166.90	1682.74	0.326	3.07	4509.74
<b>Total Carbon Emitted</b>					<b>57750.97</b>

20-22 November, 2023, UTM KUALA LUMPUR, Malaysia

By prioritizing the assignment of the most fuel-efficient vehicles to cover longer distances, potential gains in operational efficiency and environmental sustainability could be achieved. Table 6 presents the proposed vehicle reassignment plan, organized from the most fuel-efficient vehicles to the least. Through this reassignment strategy, a notable reduction in total carbon emissions of 2.96% was attained, decreasing from 57,750.97 kg to 56,039.83 kg. This outcome underscores the efficacy of proactive measures such as vehicle reassignment in mitigating environmental impact while enhancing operational performance within the logistics framework.

Table 6: Vehicle reassignment in September 2023

SEPTEMBER	Distance (km)	Fuel Consumption (Litre/km)	Fuel Efficiency (km/Litre)	Total Carbon Emission (kg)
<b>BPF6317</b>	13772.30	0.186	5.37	6874.60
<b>BPF6318</b>	7743.20	0.277	3.62	5738.28
<b>BPF6319</b>	7677.30	0.315	3.17	6483.26
<b>W5044Q</b>	7433.40	0.323	3.10	6426.12
<b>DEE9884</b>	6749.90	0.326	3.07	5891.41
<b>NBK9957</b>	5335.60	0.327	3.06	4675.60
<b>BJV4101</b>	5166.90	0.337	2.97	4668.13
<b>WA4314G</b>	5066.40	0.357	2.80	4848.87
<b>BPF6316</b>	4366.50	0.364	2.75	4261.20
<b>WYR2942</b>	3368.40	0.375	2.66	3389.10
<b>W3087A</b>	2511.90	0.413	2.42	2783.25
<b>Total Carbon Emitted</b>				<b>56039.83</b>
<b>Carbon Reduction</b>				<b>1711.15</b>

Table 7: Data from TLS in October 2023

OCTOBER	Distance (km)	Fuel (Litre)	Fuel Efficiency (km/Litre)	Fuel Consumption (Litre/km)	Total Carbon Emission (kg)
<b>BPF6316</b>	4812.40	1747.80	2.75	0.363	4684.10
<b>WA4314G</b>	3492.80	1305.80	2.67	0.374	3499.54
<b>WYR2942</b>	6710.20	1590.64	4.22	0.237	4262.92
<b>NBK9957</b>	7518.90	2324.2	3.24	0.309	6228.86
<b>BJV4101</b>	3196.10	1097.90	2.91	0.344	2942.37
<b>BPF6318</b>	6074.40	1739.18	3.49	0.286	4661.00
<b>W5044Q</b>	9822.20	3451.43	2.85	0.351	9249.83
<b>BPF6317</b>	15088.90	3618.2	4.17	0.240	9696.78
<b>BPF6319</b>	6140.60	1809.4	3.39	0.295	4849.19
<b>W3087A</b>	7761.10	2763.40	2.81	0.356	7405.91
<b>DEE9884</b>	5683.10	1518.7	3.74	0.267	4070.12
<b>Total Carbon Emitted</b>					<b>61550.62</b>

In a parallel investigation conducted using data from October as shown in Table 7, the total carbon emissions were computed to be 61,550.62 kg. Following the implementation of vehicle reassignments, aimed at optimizing efficiency and reducing emissions, the new total carbon emissions were significantly decreased to 59,749.96 kg, representing a notable reduction of approximately 2.93%. This data is presented in Table 8, showcasing the effectiveness of strategic vehicle reallocation in achieving environmental sustainability goals within the logistics operation. Through such initiatives, not only can carbon emissions be curtailed, but operational efficiency can also be enhanced, exemplifying the potential benefits of proactive measures in the pursuit of a greener and more efficient transportation landscape.

Table 8: Vehicle reassignment in October 2023

OCTOBER	Fuel Efficiency (km/Litre)	Fuel Consumption (Litre/km)	Distance (km)	Total Carbon Emission (kg)
WYR2942	4.22	0.237	15088.90	9585.81
BPF6317	4.17	0.240	9822.20	6312.17
DEE9884	3.74	0.267	7761.10	5558.34
BPF6318	3.49	0.286	7518.90	5769.39
BPF6319	3.39	0.295	6710.20	5299.00
NBK9957	3.24	0.309	6140.60	5087.04
BJV4101	2.91	0.344	6074.40	5592.17
W5044Q	2.85	0.351	5683.10	5351.93
W3087A	2.81	0.356	4812.40	4592.16
BPF6316	2.75	0.363	3492.80	3399.68
WA4314G	2.67	0.374	3196.10	3202.27
<b>Total Carbon Emitted</b>				<b>59749.96</b>
<b>Carbon Reduction</b>				<b>1800.66</b>

#### 1.4 Tools for Measuring the Amount of Carbon Emitted

A discussion was also held regarding the methodology for quantifying carbon emissions from medium and heavy-duty vehicles. It was observed that there are currently no available tools specifically designed for this purpose. Instead, the carbon emission formula was deemed adequate for measurement.

Additionally, there is a contention regarding the existence of a tool aimed at reducing carbon emissions. However, it has only undergone testing with small vehicles, and there is no evidence supporting its effectiveness for medium and heavy-duty vehicles.



## 1.5 Conclusion and Recommendations

In conclusion, our investigation into carbon emissions and fuel efficiency in medium and heavy-duty vehicles has provided valuable insights into strategies for reducing environmental impact while enhancing operational efficiency within the logistics sector. Analysis of the data revealed a correlation between fuel efficiency and vehicle age, albeit with a weak negative correlation, indicating that newer vehicles tend to exhibit slightly higher fuel efficiency. Additionally, while no clear linear relationship was observed between carbon emissions and fuel efficiency, it was evident that factors beyond fuel efficiency alone influence emissions levels.

Our findings show the importance of proactive measures such as vehicle reassignment, route optimization, and the adoption of cleaner fuels to mitigate carbon emissions. By prioritizing the assignment of the most fuel-efficient vehicles to cover longer distances, significant reductions in carbon emissions were achieved, highlighting the potential impact of strategic planning on environmental sustainability.

Furthermore, driving behaviour emerged as a critical factor influencing fuel efficiency and carbon emissions. Gentle acceleration, smooth driving, and maintaining optimal speeds were found to contribute to fuel savings and reduced emissions. As such, investing in driver training programs and promoting eco-driving behaviours can play a pivotal role in achieving emission reduction targets while optimizing fuel efficiency. Providing incentives based on efficient driving style could also serve as a method to instill this value among drivers.

Considering these findings, we recommend the implementation of comprehensive mitigation strategies that encompass vehicle reassignment, route optimization, adoption of cleaner fuels, and driver training initiatives. By adopting a multifaceted approach to address the complex interplay between fuel efficiency, carbon emissions, and driving behaviour, logistics companies such as TLS can achieve significant reductions in their carbon footprint while simultaneously enhancing operational efficiency and sustainability.

## 1.6 Acknowledgements

This work was supported by Institute of Mathematics for Industry, Joint Usage/Research Center in Kyushu University. (FY2023 Workshop (I) “MMISG2023” (2023b003).)

## REFERENCES

- Clark, N. N., Kern, J. M., Atkinson, C. M. & Nine, R. D. 2002. Factors Affecting Heavy-Duty Diesel Vehicle Emissions. *Journal of the Air & Waste Management Association*, 52, 84 - 94.
- EEA 2023. The European Handbook of Emission Factor for Road Transportation. *In: Agency, E. E. (ed.). International Energy Agency- lea, P. 2019. CO2 Emissions From Fuel Combustion 2019 Edition.*
- MIDA, M. I. D. A. 2023. *Carbon Pricing: Path Towards Carbon Neutral Growth In Malaysia* [Online]. Available: <https://www.mida.gov.my/carbon-pricing-path-towards-carbon-neutral-growth-in-malaysia/> [Accessed 18/12/2023 2023].
- Ministry of Economy. 2022. *National Energy Policy 2022-2040* [Online]. Available: [https://www.ekonomi.gov.my/sites/default/files/2022-09/National\\_Energy\\_Policy\\_2022-2040.pdf](https://www.ekonomi.gov.my/sites/default/files/2022-09/National_Energy_Policy_2022-2040.pdf) [Accessed].
- NEP 2022. National Energy Policy 2022-2040. *In: Economic, M. O. (ed.).*

INDUSTRY PRESENTATION SLIDES



**TOTAL LOGISTIC SERVICES (M) SDN BHD**

▶▶

# MALAYSIA MATHEMATICS INDUSTRY STUDY GROUP (MMISG) 2023



**TOTAL LOGISTIC SERVICES (M) SDN BHD** Value Logistic Provider



## INDEX

- 1 • About Us
- 2 • Mission & Vision
- 3 • Management Structure
- 4 • History & Milestone
- 5 • Branches & Location
- 6 • Scope of Services
- 7 • ISO Certification
- 8 • Problem Study

## 2.0 OUR MISSION & VISION



### OUR VISION

To be a **premier world-class logistic provider** with excellent customer service and prompt delivery. Offering the fullest range of services, freight forwarding, warehousing, distribution, consultations and transportation for domestic and international customers.

## 2.0 OUR MISSION & VISION

### MISSION

To achieve this, we always **emphasize on constant and systematic training programs** for our staff and workers conducted both locally and overseas. This is to provide a better service to our customer from time to time and fulfils the company mission & vision

**VALUE ADDED SERVICE**



**CONTINUOUS IMPROVEMENT**



**3<sup>rd</sup> PARTY LOGISTIC LEADER**



**ONGOING DEVELOPMENT OF THE LOGISTIC TEAM**



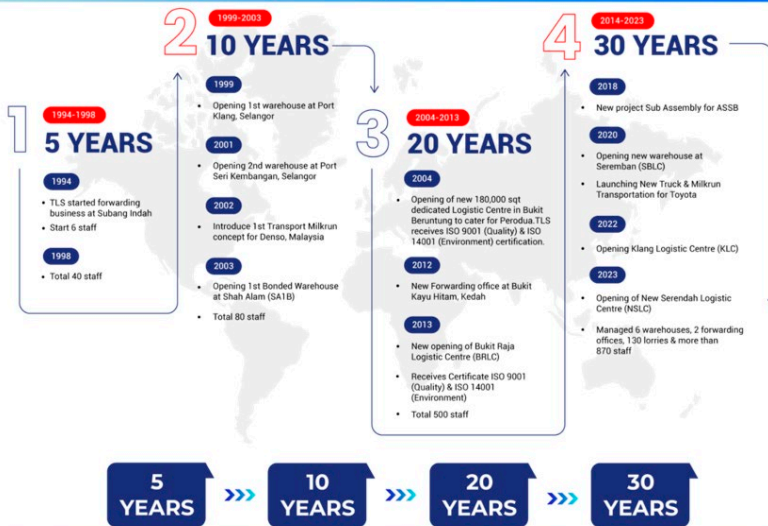
**QUALITY DRIVEN SERVICES**



# 3.0 MANAGEMENT STRUCTURE



# 4.0 HISTORY & MILESTONES



## 5.0 BRANCHES & LOCATION

### HEADQUARTERS



No.1-Gate 4, Jalan Keluli 2/KU2,  
Kawasan Perindustrian Bukit Raja, 41050  
Klang, Selangor Darul Ehsan.  
Tel : 03-3361 3333  
Fax : 03-3361 3334

### BUKIT RAJA LOGISTICS CENTER (BRLC)

#### OPERATION IN BRLC

- OFFICE
- WAREHOUSE
- TRANSPORTATION
- SUB ASSEMBLY

#### BRLC WAREHOUSE

- 290,970 sqft

## 5.0 BRANCHES & LOCATION



## 6.0 SCOPE OF SERVICES

FORWARDING	WAREHOUSING	TRANSPORTATION	SUB ASSEMBLY
 <ul style="list-style-type: none"> <li>• Import &amp; Export Transportation</li> <li>• Custom Clearance</li> <li>• Large Cargo Transportation</li> </ul>  	 <ul style="list-style-type: none"> <li>• CKD Warehouse</li> <li>• Bonded Warehouse</li> <li>• Export &amp; Import Warehouse</li> </ul>  	 <ul style="list-style-type: none"> <li>• HAULAGE (Port to Warehouse)</li> <li>• Milkrun (Auto Parts)</li> </ul>  	 <ul style="list-style-type: none"> <li>• Assembly</li> <li>• Processing</li> <li>• Inspection</li> </ul>  

## 6.1 FORWARDING

TLS is a member of the Selangor Freight Forwarders & Logistics Association (SFFLA)



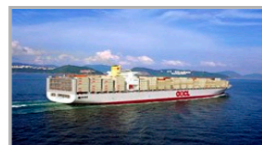
### IMPORT & EXPORT BUSINESS

- Customs Clearance
- CBU, CKD and Part by Part
- NVOCC Business
- Door to Door / Project Deliveries
- Heavy Machinery Transportation and installation Service
- Specialist in RO-RO Car Carrier Service to East Malaysia and Muara Ports
- Regular RO-RO Car Carrier Service From Japan to Far East Ports
- Load Loader carrier



### TLS FORWARDING OFFICE

1. Bukit Tinggi, Klang, Selangor
2. Bukit Kayu Hitam, Kedah



## 6.2 WAREHOUSING

### LIST OF WAREHOUSE :

WH	ADDRESS
Shah Alam 1B Warehouse (BONDED)	Lot 10, Jalan Pahat 16/8A, Seksyen 16, Shah Alam
Serendah Logistics Center (SLC)	Lot 4240, Jalan Kesidang 5, Jalan Mohd Taib, Kaw. Industri Sg.Choh, Selangor
BANGI	Block D1&D2, Lot 3, Jalan P/10, Kaw. Perusahaan Seksyen 10, Bandar Baru Bangi.
Klang Logistic Center (KLC)	No.7, Jalan Permata 8A/KS 09, Taman Perindustrian Air Hitam, Klang
Seremban Logistic Center (SBLC)	No.23, Jalan Industri Galla 3, Taman Perindustrian Galla, Seremban.
Bukit Raja Logistics Center (BRLC-HQ)	No.1-Gate 4, Jalan Keluli 2/KU2, Kawasan Perindustrian Bukit Raja, Klang




## 6.3 TRANSPORTATION

TLS MILK RUN	
1)MILK RUN P2	Logistic Dept, Perodua Mfg. Center, Sg.Choh, Locked Bag 226, Rawang
2)MILK RUN DENSO	Lot 2,Jalan P/1, Seksyen 13, Bandar Baru Bangi
3)MILK RUN TOYOTA	No.1-Gate 4, Jalan Keluli 2/KU2,Kawasan Perindustrian Bukit Raja, 41050 Klang, Selangor Darul Ehsan.






## 6.4 SUB ASSEMBLY



**“Beyond Logistics”**



MISSION & VISION

1

OBJECTIVES

- To be a part of Automotive Industry in Malaysia in producing high quality vehicles with increased automation
- To value add process by sub assembly and provide timely parts supply to plant

3

OBJECTIVES

- To contribute for Automotive Industry :-
  - i) Sub-assembly with continuous KAIZEN
  - ii) Outsourcing internal and external logistic for new plant

STRATEGY

2

STRATEGY


**S (Safety) : '0' Accident**  
**E (Environment) : Environmental care (CO<sup>2</sup> emission & potential waste)**

**P (Productivity) : CKD Sub Assembly (To Be No.1 sub assy assembler in Malaysia)**


**Q (Quality) : External check + Build in quality**

**C (Cost) : Cost reduction and continuous KAIZEN**

**D (Delivery) : Timely delivery and '0' downtime**



**TOTAL LOGISTIC SERVICES (M) SDN BHD**



Value Logistic Provider

14

## 7.0 ISO CERTIFICATION

LRQA CERTIFIED

ISO 9001

LRQA CERTIFIED

ISO 14001

LRQA CERTIFIED

ISO 45001

ISO 9001:2015 (QMS) CERTIFICATION

Total Logistic Services (M) Sdn. Bhd. has been certified by Llyods Quality Assurance to the following Quality Management System Standards :

ISO 9001 : 2015  
 EN ISO 9001 :2015  
 BS EN ISO 9001:2015  
 MS ISO 9001 : 2015

The Quality Management System is applicable to :  
 Provisions of warehousing, freight forwarding and transportation services.

ISO 14001:2015 (EMS) CERTIFICATION

Total Logistic Services (M) Sdn. Bhd. has been approved by Llyods Quality Assurance to the following Environmental Management System Standards :

ISO 14001 : 2015  
 MS ISO 14001 : 2015


The Environmental Management System is applicable to :  
 Provisions of warehousing, freight forwarding and transportation services.

ISO 45001:2018 (OHSMS) CERTIFICATION


Total Logistic Services (M) Sdn. Bhd. has been approved by Llyods Quality Assurance to the following Occupational Health & Safety Management System :

ISO 45001 : 2018

The Occupational Health & Safety Management System is applicable to :  
 Provisions of warehousing and transportation services.



**TOTAL LOGISTIC SERVICES (M) SDN BHD**



Value Logistic Provider

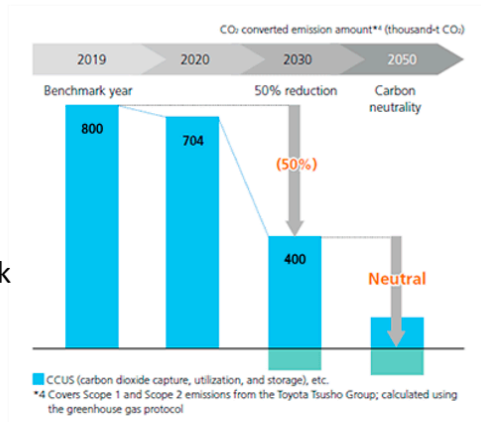
15

## 8.0 Problem Study

### Problem Background

#### Company Group Wide Carbon Neutrality Challenges

- Carbon Neutrality by 2050
- Reduction in greenhouse gas emissions by 50% (benchmark 2019 data)

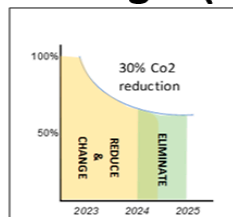


## 8.0 Problem Study

### Problem Background

#### TLS Plan Towards Challenges (3 years plan)

- 1 Reduce
- 2 Change
- 3 Eliminate



#### Activities

- Utilize Routing
- Truck Aging Policy > *Max truck age = 20 years*
- Eco Driving Training > *Internal & External*
- Truck Idling Monitoring > *Policy : Max 3 mins idling*
- Co2 Emission Study
- Carbon Reduction Innovations > *i.e Exhaust Catalyst, Alternative Fuel*
- EV Trucks

## 8.0 Problem Study

---

### Problem Statement

- Truck Aging vs Co2
  - Efficient truck life time
  - Impact of age on carbon emission



***THANK YOU***

**TOTAL LOGISTIC SERVICES (M) SDN. BHD.**

OUTPUT PRESENTATION SLIDES



TOTAL LOGISTIC SERVICES (M) SDN BHD  
Value Logistic Provider



## Malaysia Mathematics in Industry Study Group 2023 (MMISG2023)



### The Influence of Vehicle Age in Mitigating Carbon Emissions from Medium-Duty and Heavy-Duty Trucks

20<sup>th</sup> – 22<sup>nd</sup> November, 2023  
Universiti Teknologi Malaysia (UTM), Kuala Lumpur.



**MMISG2023 is a collaborative problem solving workshop where academia and researchers (known as Contributor) tackle real life problems shared by the industries**

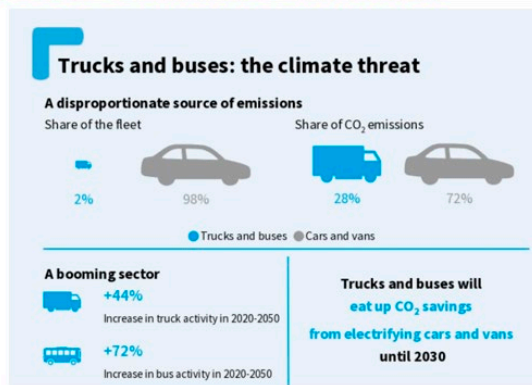
2

## TLS's Objective

- To achieve 50% CO<sub>2</sub> reduction by 2030
- To find way to measure accurate CO<sub>2</sub> emission – through mathematical formulation or tools.



## Trucks and buses pose a threat to the EU's climate ambition



Addressing the heavy-duty climate problem  
[https://www.transportenvironment.org/wpcontent/uploads/2022/09/2022\\_09\\_Addressing\\_heavy-duty\\_climate\\_problem\\_final.pdf](https://www.transportenvironment.org/wpcontent/uploads/2022/09/2022_09_Addressing_heavy-duty_climate_problem_final.pdf)



## TRANSPORT SECTOR OF MALAYSIA

- Transportation in Malaysia accounted for 8% of real gross domestic product (GDP) and 4% of employment in 2018. It has experienced an average annual growth rate of 3% over the last decade.
- The transport sector contributes to 36.4% of the total final energy demand (23,555 ktoe) in 2018, which is the largest energy user in Malaysia. Carbon dioxide is responsible for 96% of greenhouse gas (GHG) emissions in this sector.
- The transport sector is the second biggest driver to CO<sub>2</sub> emissions in Malaysia after electricity and heat production, while the industrial sector is the third-largest contributor (International Energy Agency-IEA, 2019).
- Emissions levels across all economic sectors have increased over the 2010–2017 period. CO<sub>2</sub> emissions from the transport sector represented 28.8% of total fossil fuel combustion in Malaysia, well above the global average of 24.5% (International Energy Agency-IEA, 2019). Road transport is also the largest CO<sub>2</sub> emitter among all transport subsectors (International Energy Agency-IEA, 2019).

CO<sub>2</sub> Emissions and The Transport Sector in Malaysia  
<https://www.frontiersin.org/articles/10.3389/fenvs.2021.774164/full>

7



## ISSUES

### Vehicle Age

- The age structure of the vehicle stock is particularly relevant in developing regions of the world, where a significant portion of the vehicle fleet consists of imported second-hand (vehicles from developed countries)– and often poorly maintained.
- The main concern is on the impacts of aging heavy vehicle fleets and the measure that could be used to manage this challenge.

### Carbon Emission

- Emissions from motor vehicles and their fuels contribute to ambient levels of ozone, fine particulate matter, Nitrogen Dioxide (NO<sub>2</sub>), Sulfur Dioxide (SO<sub>2</sub>), and Carbon Monoxide (CO). These pollutants are linked with adverse health impacts

### Policy Implementation

- Policymakers have added a range of regulatory measures over time to help ensure that emissions remain low as the vehicles age, including useful life durability requirements, emissions in-use verification and confirmatory testing, and requirements for on-board diagnostics of emissions control systems

8



## DEFINING AGE HEAVY VEHICLES

- The old heavy vehicles impact the community in several ways, including air pollution, noise, and health
- Defining aged heavy vehicles by their emissions standard provides the clearest definition and will likely result in the greatest positive impact of any targeted actions (Richard Delplace, Austroads Transport Network Operations Program Manager).
- The heavy vehicle was defined as being above 4.5 tonnes GVM, used in freight transport and manufactured before 2008. Three sub-classes of categorization are based on the vehicle's compliance with exhaust emission standards in the Australian Design Rules.
- the nature and structure of the national fleet and freight sector means that the aged truck problem is difficult to overcome with equitable and effective measures

**Notes:**

1. Austroads is the association of the Australian and New Zealand transport agencies.
2. Gross vehicle mass (GVM) - The GVM is the maximum loaded weight of a rigid vehicle while driving on the road.

<https://austroads.com.au/latest-news/options-for-managing-the-impacts-of-aged-heavy-vehicles>

9



## HEAVY VEHICLES & AGE

- In Malaysia, heavy vehicle or a commercial transportation is one that has a Gross Vehicle Mass (GVM) over 4,500 kilograms. (4.5 tonnes).
- Regulatory measures have helped to keep in-use emissions low as vehicles age, but they are subject to significant limitations. The durability requirements only apply to properly used and maintained vehicles, and manufacturers are not responsible for emission control system malfunctions.
- The useful life requirements are also limited. For example, the latest Tier 3 light-duty useful life requirements cover 15 years or 150,000 miles (whichever is sooner), up from 10 years or 120,000 miles for the light-duty Tier 2 standards. For heavy-duty diesel engines, the useful life is 10 years or 435,000 miles.
- However, most vehicles are driven for longer periods of time, and although the oldest contribute a relatively small share of the miles driven, their emissions can continue to deteriorate as they age. Also, malfunctions increase as vehicles age and are less likely to be repaired.
- Consequently, while the oldest vehicles constitute a relatively small share of the in-use vehicle fleet, they contribute disproportionately to total fleet emissions.

[https://cammer18.weebly.com/uploads/1/1/6/6/116631271/paper\\_id\\_-\\_35.pdf](https://cammer18.weebly.com/uploads/1/1/6/6/116631271/paper_id_-_35.pdf)  
<https://theicct.org/sites/default/files/publications/US.TRUE-emissions-distribution-oct2020.pdf>

10



## How to calculate your fleet's carbon footprint

### 1) Mathematical estimate / Truck Emissions Calculator:

Step 1: Work out how many litres of fuel you use.

Step 2: Calculate how many kilograms of CO<sub>2</sub> this creates

<https://8billiontrees.com/carbon-offsets-credits/carbon-ecological-footprint-calculators/truck-co2-emissions-per-km-calculator/>

### 2) Accurate measurement with fleet management services and solutions – varying technologies.

<https://connectedfleet.michelin.com/blog/calculate-co2-emissions/>

11



## CARBON EMISSION FORMULA

$$f = \left( \text{Carbon emission parameter} \right) \left( \frac{\text{distance (km)}}{\text{fuel efficiency } \left( \frac{\text{km}}{\text{l}} \right)} \times \text{(num. of trips)} \right) \times \text{(vehicle utilization \%)}$$

Fixed value  
by Toyota

Values to be  
investigated

12





## FACTORS AFFECTING EMISSIONS

The parameters that most heavily affect the emissions from compression ignition engine-powered vehicles include:

### Uncontrollable factors

1. Vehicle class and weight
2. Vehicle vocation (work purpose)
3. Weather conditions
4. Vehicle age
5. Route conditions (federal roads, highway, state road, hilly, flat road)
6. Load
7. Maintenance schedule

### Controllable factors short time

1. Driving style
2. Route/truck assignment – truck efficiency, distance
3. Fuel type
4. Optimal speed

### Controllable factors long term

1. Engine technology

**Note:** An after treatment system is a method or device for reducing harmful exhaust emissions from internal-combustion engines. In other words, it is a device that cleans exhaust gases to ensure the engines meet emission regulations

Factors Affecting HeavyDuty Diesel Vehicle Emissions  
<https://www.tandfonline.com/doi/pdf/10.1080/10473289.2002.10470755>

13



## DATA

In [36]: data

A data.frame: 11 × 11

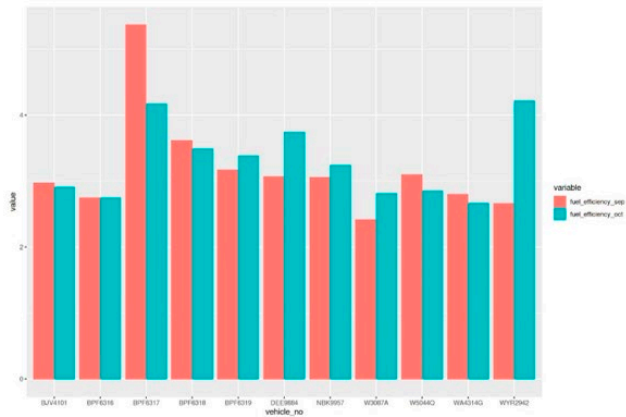
vehicle_no	km_sep	litre_sep	fuel_efficiency_sep	km_oct	litre_oct	fuel_efficiency_oct	engine_displ	engine_age	co2_sep	co2_oct
<chr>	<dbl>	<dbl>	<dbl>	<dbl>	<dbl>	<dbl>	<dbl>	<int>	<int>	<dbl>
BPF6316	4366.5	1590.00	2.75	4812.4	1747.80	2.75	7961	6	4255.353	4689.903
WA4314G	3368.4	1202.90	2.80	3492.8	1305.80	2.67	7961	9	3224.040	3505.882
WYR2942	7433.4	2790.70	2.66	6710.2	1590.64	4.22	7961	10	7489.290	4261.454
NBK9957	7677.3	2510.31	3.06	7518.9	2324.20	3.24	7961	20	6723.910	6219.337
BJV4101	2511.9	846.80	2.97	3196.1	1097.90	2.91	7961	16	2266.630	2943.487
BPF6318	5335.6	1475.40	3.62	6074.4	1739.18	3.49	7961	6	3950.113	4664.582
W5044Q	7743.2	2497.74	3.10	9822.2	3451.43	2.85	7961	10	6694.121	9236.314
BPF6317	13772.3	2565.15	5.37	15088.9	3618.20	4.17	7961	6	6873.327	9697.423
BPF6319	5066.4	1596.43	3.17	6140.6	1809.40	3.39	7961	6	4283.266	4854.516
W3087A	6749.9	2790.70	2.42	7761.1	2763.40	2.81	7961	10	7475.096	7402.046
DEE9884	5166.9	1682.74	3.07	5683.1	1518.70	3.74	7961	18	4510.519	4072.382

## CORRELATION BETWEEN ENGINE AGE AND FUEL EFFICIENCY IN SEPT AND OCT

```
In [42]: cor(data$engine_age, data$fuel_efficiency_oct)  
-0.0402794006529332
```

```
In [43]: cor(data$engine_age, data$fuel_efficiency_sep)  
-0.290728092224943
```

## COMPARISON OF FUEL EFFICIENCY IN SEPT AND OCT





## ROUTE / TRUCK ASSIGNMENT

SEPT 2023

SEPTEMBER	Distance	Litre	Fuel Eff (km/l)	Fuel Cons (l/km)	Total Carb	Carb Rate
BPF6316	4366.50	1590.00	2.75	0.364	4261.20	0.98
WA4314G	3368.40	1202.90	2.80	0.357	3223.77	0.96
WYR2942	7433.40	2790.70	2.66	0.375	7479.08	1.01
NBK9957	7677.30	2510.31	3.06	0.327	6727.63	0.88
BJV4101	2511.90	846.80	2.97	0.337	2269.42	0.90
BPF6318	5335.60	1475.40	3.62	0.277	3954.07	0.74
W5044Q	7743.20	2497.74	3.10	0.323	6693.94	0.86
BPF6317	13772.30	2565.15	5.37	0.186	6874.60	0.50
BPF6319	5066.40	1596.43	3.17	0.315	4278.43	0.84
W3087A	6749.90	2790.70	2.42	0.413	7479.08	1.11
DEE9884	5166.90	1682.74	3.07	0.326	4509.74	0.87
Total Carbon Emitted					57750.97	

SEPTEMBER	Fuel Eff (km/l)	Fuel Cons (l/km)	Distance Cover	Total Carb	Carb rate
BPF6317	5.37	0.186	13772.30	6874.60	0.50
BPF6318	3.62	0.277	7743.20	5738.28	0.74
BPF6319	3.17	0.315	7677.30	6483.26	0.84
W5044Q	3.10	0.323	7433.40	6426.12	0.86
DEE9884	3.07	0.326	6749.90	5891.41	0.87
NBK9957	3.06	0.327	5335.60	4675.60	0.88
BJV4101	2.97	0.337	5166.90	4668.13	0.90
WA4314G	2.80	0.357	5066.40	4848.87	0.96
BPF6316	2.75	0.364	4366.50	4261.20	0.98
WYR2942	2.66	0.375	3368.40	3389.10	1.01
W3087A	2.42	0.413	2511.90	2783.25	1.11
Total Carbon Emitted				56039.83	
Carbon Reduction				1711.15	

17 17



## ROUTE / TRUCK ASSIGNMENT

OCT 2023

OCTOBER	Distance	Litre	Fuel Eff (km/l)	Fuel Cons (l/km)	Total Carb	Carb Rate
BPF6316	4812.40	1747.80	2.75	0.363	4684.10	0.97
WA4314G	3492.80	1305.80	2.67	0.374	3499.54	1.00
WYR2942	6710.20	1590.64	4.22	0.237	4262.92	0.64
NBK9957	7518.90	2324.20	3.24	0.309	6228.86	0.83
BJV4101	3196.10	1097.90	2.91	0.344	2942.37	0.92
BPF6318	6074.40	1739.18	3.49	0.286	4661.00	0.77
W5044Q	9822.20	3451.43	2.85	0.351	9249.83	0.94
BPF6317	15088.90	3618.20	4.17	0.240	9696.78	0.64
BPF6319	6140.60	1809.40	3.39	0.295	4849.19	0.79
W3087A	7761.10	2763.40	2.81	0.356	7405.91	0.95
DEE9884	5683.10	1518.70	3.74	0.267	4070.12	0.72
Total Carbon Emitted					61550.62	

OCTOBER	Fuel Eff (km/l)	Fuel Cons (l/km)	Distance	Total Carb	Carb Rate
WYR2942	4.22	0.237	15088.90	9585.81	0.635
BPF6317	4.17	0.240	9822.20	6312.17	0.643
DEE9884	3.74	0.267	7761.10	5558.34	0.716
BPF6318	3.49	0.286	7518.90	5769.39	0.767
BPF6319	3.39	0.295	6710.20	5299.00	0.790
NBK9957	3.24	0.309	6140.60	5087.04	0.828
BJV4101	2.91	0.344	6074.40	5592.17	0.921
W5044Q	2.85	0.351	5683.10	5351.93	0.942
W3087A	2.81	0.356	4812.40	4592.16	0.954
BPF6316	2.75	0.363	3492.80	3399.68	0.973
WA4314G	2.67	0.374	3196.10	3202.27	1.002
Total Carbon Emitted				59749.96	
Carbon Reduction				1800.66	

18 18

20-22 November, 2023, UTM KUALA LUMPUR, Malaysia



## CONCLUSION

- Scope data
  - 10 tonnes trucks,
  - Sept and Oct data.
- Age of vehicle does not correlate with carbon emission based on current data. Will be needing more data to see the correlation between age of vehicle and carbon emissions.
- Higher efficiency (km/l) – lower carbon footprint
- Driving style plays important part (lots of idle time, braking)
- Road condition – highway / federal (state) road.



## RECOMMENDATION

- Training and awareness
  - Awareness and training for drivers about fuel consumption
  - Inform impact of not reducing carbon emission to the drivers.
  - Inform how much km the drivers can drive / fuel to maintain efficiency
  - Awareness and incentives based on driving efficiency.
  - Maintain current training for driving behaviour.
- Improve truck / driver assignment problem
  - Rotational basis for driver's route.
  - Assign newer vehicle or more efficient vehicle for longer distance route.
  - Categorize types of driver.
- Maintenance
  - Periodical maintenance must be continued.
  - Do not remove catalytic converter in the truck
  - Check the condition catalytic converter (backflush and clean up)
  - Ensure no injector problem
- Data envelopment (rank)
- Hungarian method (assignment based on factors)
- More data to compare the performances
- After intervention by TLS, can compare the difference

21 21



22

*Price Forecasting Model for Main Vegetables in Malaysia*

- Industry Representatives : Aimi Athirah Ahmad<sup>8</sup>  
(MYHIMS SOLUTION LLP)
- Study Group Contributors : Shariffah Suhaila Syed Jamaludin<sup>1</sup>, Fadhilah Yusof<sup>8</sup>,  
Roslinazairimah Zakaria<sup>5</sup>, Mohd Mahayaudin Mansor<sup>3</sup>,  
Nor Hamizah Miswan<sup>2</sup>, Siti Rahayu Mohd Hashim<sup>7</sup>,  
Siti Mariam Norrulashikin<sup>1</sup>, Siti Rohani Mohd Nor<sup>1</sup>,  
Hanita Daud<sup>13</sup>, Razik Ridzuan Mohd Tajuddin<sup>2</sup>,  
Syahrizal Salleh<sup>5</sup>, Ruzaini Zulhusni Puslan<sup>1</sup>

**1.1 Introduction**

Monitoring the volatility of commodity prices, especially agricultural commodities, can be essential in evaluating the country's economic performance. Commodity price forecasts can help the government to make and develop appropriate economic policies and strategies in the future. Therefore, price forecasting is an alternative approach for reducing the negative effects of uncertainty, which can further decrease the risk of the producers' agricultural commodities.

Shahizan et al. (2023) investigated the effectiveness of the seasonal regression and the quadratic trend models with seasonal indices in predicting the price of red chili in Johor, Malaysia, using historical price data from 2018 to 2022. The results revealed that the seasonal regression model outperformed the quadratic trend model, with seasonal indices predicting red chili prices. Lestari et al. (2022) mentioned that red chili is an agricultural commodity with high price volatility. Their research aimed to analyze the price volatility of red chili in Semarang Regency from January 2019 to February 2020. They applied the ARCH-GARCH method, showing that the price volatility of red chili occurred at the beginning, middle, and end of the year due to climate change, changes in public consumption patterns on religious holidays, and oversupply.

On the other hand, Basnayake et al. (2022) forecasted the prices of green chili peppers in Sri Lanka using artificial neural networks. The Time Delay Neural Network (TDNN), Feedforward Neural Network (FFNN) with Levenberg-Marquardt (LM) algorithm, and FFNN with Scaled Conjugate Gradient (SCG) algorithm were employed on weekly average retail prices of green chili in Sri Lanka from the 1st week of January 2011 to the 4th week of December 2018. Based on the Mean Squared Error (MSE), Mean Absolute Error (MAE), and Normalized Mean Squared Error (NMSE), FFNN with the LM algorithm gave the best performance compared to other methods.

In general, fluctuations in the price of agricultural commodities occur mainly due to shocks in supply. These disturbances, combined with demand elasticity and short-term

supply, cause sudden price instability, which can cause farmers and consumers to experience uncertainty, risk, and commodity price fluctuations. Pratiwi and Rosyid (2020) used the time series data price of large red and curly red chili from July 2016 to October 2019 in Yogyakarta, Indonesia. They forecasted chili prices using Autoregressive Integrated Moving Average (ARIMA) for 12 periods, beginning in November 2019 and ending in October 2020. Putriasari et al. (2022) forecasted a weekly red chili price in Bengkulu City using the ARIMA and Singular Spectrum Analysis (SSA) Methods. They found that ARIMA performed better than SSA.

ARIMA was observed to be the most accurate forecasting model for curly red chili prices in Indonesia (Sukiyono and Janah 2019). Their study applied five forecasting models: Moving Average, Single Exponential Smoothing, Double Exponential Smoothing, Decomposition, and ARIMA. Despite focusing on univariate ARIMA, external regressors are recommended to improve the accuracy of the forecasting model. Hamjah (2014) developed the best Box-Jenkins Auto-Regressive Integrated Moving Average with external regressor, that is, the ARIMAX model, for measuring the temperature and rainfall effects on major spice crops productions in Bangladesh and forecasting the output using the same model. Their study found that ARIMAX (2,1,2), ARIMAX (2,0,1), and ARIMAX (2,1,1) are the best models for chili, garlic, and ginger crops, respectively. The finding contributes to agricultural forecasting by emphasizing the importance of comparing different models for price prediction and considering multiple crops in the analysis.

Given the substantial allocation of household income towards food expenditures, the assessment of price volatility through forecasting is deemed particularly crucial in developing nations. This significance arises from the direct impact of uncertainties surrounding food prices on overall well-being. Furthermore, the repercussions of instability in food prices extend to affect individuals of low-income status and small-scale agricultural producers who rely on the sales of their crops.

As acknowledged, the price of chili exhibits inherent instability and fluctuation, posing challenges for stakeholders in arriving at consistent and reliable decisions regarding chili pricing. Additionally, chili production is susceptible to threats arising from agricultural issues, potentially leading to a decrease in supply. The consequential decline in supply and increased demand results in a corresponding rise in chili prices. Consequently, there is a pertinent need for information concerning projected fluctuations in chili price trends to ascertain market demand.

Furthermore, a comprehensive analysis of chili price volatility and the impact of shocks on chili price fluctuations, attributed to factors such as production dynamics, input prices, the pricing and quantity of imported chili, climate, the Movement Control Order (PKP), and festive demands, is imperative. This analytical pursuit aims to examine the trend of chili prices, elucidate the multifaceted determinants influencing chili prices and analyzing chili price volatility in Johor using a time series approach. Consequently, a heightened interest emerges in comparing various forecasting models, seeking to identify those that yield the most accurate forecasted values. The envisaged outcomes include the enhancement of decision-making processes in both crop production strategies and market

interventions. Adopting a robust forecasting model is anticipated to alleviate uncertainties surrounding chili prices, thereby contributing to more informed decision-making within agriculture and market interventions.

## 1.2 Data and Methods

### 1.2.1 Data

Federal Agricultural Marketing Authority (FAMA) is a governmental authority under the Ministry of Agriculture and Food Industries that oversees the marketing of agricultural products. There is a responsibility on the part of FAMA to enhance the marketing of agro-food items such as fruits, vegetables, and other products that are derived from the agricultural industry. FAMA is responsible for expanding the market size of agro-food products and increasing the number of products produced by agriculture and agro-based industries. This is done to ensure that agriculture and agro-based products are readily available and can be purchased by consumers at prices within their financial means.

The prices of chilies were obtained from FAMA based on the market prices. The prices are taken monthly with a duration of 5 years, starting from 2018 to 2022. The life span of chili is between 6 and 12 months, while the maturity time is between 60 and 120 days. Table 1 lists all the variables in the analysis.

Table 1: Predictor variables

Type of variables	Notation
<b>Total Production</b>	Prod
<b>Fertilizers</b>	DAP Potassium Chloride Phosphate Rock Super Phosphates Urea
<b>Climate</b>	Temperature Rainfall
<b>Fuel</b>	Fuel_Price
<b>Season</b>	Movement Control Order (PKP) Festives



For the analysis, chili prices are considered as the main variables. The other covariates are the total production, fertilizers (DAP, Potassium Chloride, Phosphate rock, super phosphates, urea), climate (temperature, rainfall), fuel price, and seasons (Movement Control Order (PKP), festive).

### 1.2.2 Multiple Linear Regression

A multiple linear regression model is an extension of the simple linear regression model for data with multiple predictor variables and one outcome,  $(x_1, x_2, \dots, x_n)$ , where  $n$  is the number of observations. It formalizes a simultaneous statistical relation between the single continuous outcome  $Y$  and the predictor variables,  $X_1, X_2, \dots, X_n$ .

$$\begin{aligned} Y_i &= \beta_0 + \beta_1 X_1 + \beta_2 X_2 + \dots + \beta_n X_n + \varepsilon_i \\ \varepsilon_i &\sim N(0, \sigma^2). \end{aligned} \quad (1)$$

where  $\beta_0$  represents the intercept, the mean of  $Y$  when the predictor variables  $X_1, X_2, \dots, X_n = 0$ , and  $\beta_1, \beta_2, \dots, \beta_n$  represents a slope with respect to  $X_1, X_2, \dots, X_n$ . The assumptions are thus the same as for simple linear regression:

- i.  $y_i$  are independent of each other;
- ii.  $y_i$  follows a normal distribution;
- iii. mean of that distribution is a linear function of  $x_1, x_2, \dots, x_n$ ;
- iv. variance of that distribution is the same for all  $y$  (constant variance, or homoscedasticity).

### 1.2.3 Structural Equation Modelling

In structural equation modeling (SEM) applications, a critical step is to evaluate the goodness of fit of the proposed model with the data. The comparative fit index (CFI) and the Tucker–Lewis index (TLI) are commonly used indices. The CFI measures the relative improvement in fit from the baseline to the postulated model, while the TFI measures a relative reduction in misfit per degree of freedom. CFI and TFI have a normed fit index that ranges between 0 and 1, with higher values indicating a better fit.

### 1.2.4 ARIMAX Modelling

ARIMAX is a statistical modeling technique used in time series analysis and forecasting. It is an extension of the ARIMA (Auto-Regressive Integrated Moving Average) model, which is designed to capture and predict patterns in time series data. The only difference between ARIMA and ARIMAX is the addition of an exogenous (external) variable. The ARIMA model works on a single time series data (univariate) whereas ARIMAX uses multiple variables to include the external feature.

ARIMAX  $(m, n, k+p)$  stands for Autoregressive Integrated Moving Average process with exogenous input. The model can be written as

$$y(t) = a_1y(t-1) + \dots + a_my(t-m) + e(t) + \dots + c_n e(t-n) + b_0u(t-k) + b_1u(t-k-1) + b_pu(t-k-p) \quad (2)$$

$e(t) \sim w_n(\mu, \lambda^2)$  where  $e(t)$  is white noise (with mean  $\mu$  and variance  $\lambda^2$ ),  $c_0, c_1, \dots, c_n \in \mathbb{R}$  are the MA model's parameters,  $a_1, \dots, a_m \in \mathbb{R}$  are the AR model's parameters,  $n$  is the order of the MA portion,  $m$  is the order of the AR portion,  $u(t)$  is the exogenous input,  $b_0, b_1, \dots, b_p$  are the input portion parameters,  $p$  is the order of the exogenous portion, and  $k$  is the positive input delay.

If we Zeta transforms the process in the time domain,

$$\begin{aligned} Y(z) &= (a_1z^{-1} + \dots + a_mz^{-m})Y(z) + (1 + c_1z^{-1} + \dots + c_nz^{-n})E(z) \\ &\quad + (b_0 + b_1z^{-1} + \dots + b_pz^{-p})z^{-k}U(z) \\ Y(z) &= \frac{z^{-n}}{z^{-m}} \frac{z^n + c_1z^{n-1} + \dots + c_n}{z^m - a_1z^{m-1} - \dots - a_m} E(z) + \frac{z^{-p}}{z^{-m}} \frac{b_0z^p + b_1z^{p-1} + \dots + b_p}{z^m - a_1z^{m-1} - \dots - a_m} z^{-k}U(z) \\ Y(z) &= z^{m-n} \frac{z^n + c_1z^{n-1} + \dots + c_n}{z^m - a_1z^{m-1} - \dots - a_m} E(z) + z^{m-p-k} \frac{b_0z^p + b_1z^{p-1} + \dots + b_p}{z^m - a_1z^{m-1} - \dots - a_m} U(z) \\ Y(z) &= W(z)E(z) + G(z)U(z) \end{aligned} \quad (3)$$

$W(z)$  and  $G(z)$  are asymptotically stable if their poles (roots of the denominator) are inside the unit circle. So, the stationarity of an ARIMAX depends on the inputs as well.

Let  $y(t)$  be an ARIMAX process. Then  $y(t)$  is stationary if:

The poles of  $W(z)$  are inside the unit circle  $u(t)$  is stationary, this happens when  $u(t) = U$  constant for all  $t$ . In general, an ARIMAX process is not stationary, however, its stochastic portion (ARMA) is stationary. The nonstationary derives from the input  $u(t)$ .

An equivalent form of representing an ARIMAX is

$$y(t) = \frac{C(z)}{A(z)} e(t) + \frac{B(z)}{A(z)} z^{-k} u(t), \quad e(t) \sim w_n(\mu, \lambda^2) \quad (4)$$

where

$$\begin{aligned} C(z) &= 1 + c_1z^{-1} + \dots + c_nz^{-n} \\ A(z) &= 1 - a_1z^{-1} - \dots - a_mz^{-m} \\ B(z) &= b_0 + b_1z^{-1} + \dots + b_pz^{-p} \end{aligned} \quad (5)$$

Note that applying the superposition principle

$$\begin{aligned}
 y_e(t) &= \frac{C(z)}{A(z)} e(t), \\
 y_u(t) &= \frac{B(z)}{A(z)} z^{-k} u(t) \\
 \therefore y(t) &= y_e(t) + y_u(t)
 \end{aligned} \tag{6}$$

We can analyze  $y_e(t)$  as an ARMA process and  $y_u(t)$  as a dynamic system.

### 1.2.5 Machine Learning Model

- Machine Learning (ML) algorithms enable automatic learning from data to identify patterns for predictions with an iterative process. Four ML models are considered for time series data.
- Support Vector Regression (SVR) aims to reduce the error by determining the hyperplane (decision boundary) and minimizing the range between the predicted and observed values as shown in Figure 1.

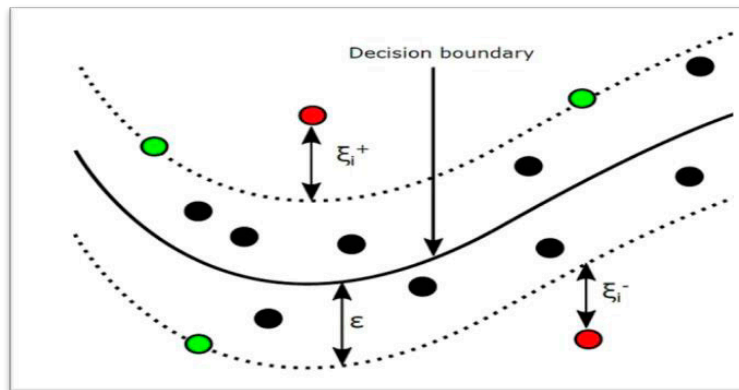


**Figure 1:** Support Vector Regression

- Random Forest Regression (RFR) aims to combine multiple decision trees, and the final output is the mean of all the outputs from these multiple trees as shown in Figure 2.

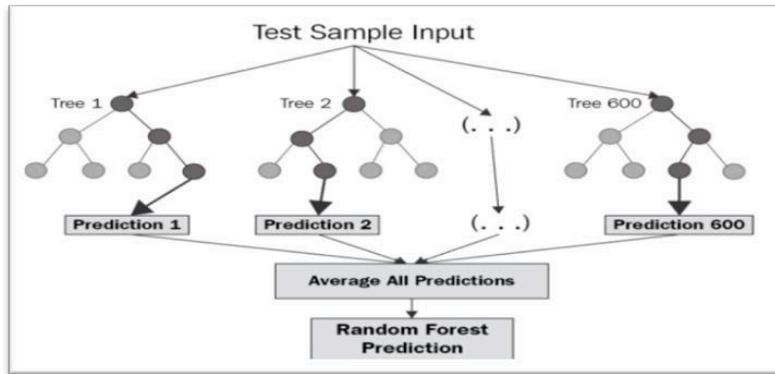


**Figure 2:** Random Forest Regression

- Artificial Neural Network (ANN) comprises node layers containing an input layer, hidden layers, and an output layer. Each node connects to another and has an associated weight and threshold as shown in Figure 3.

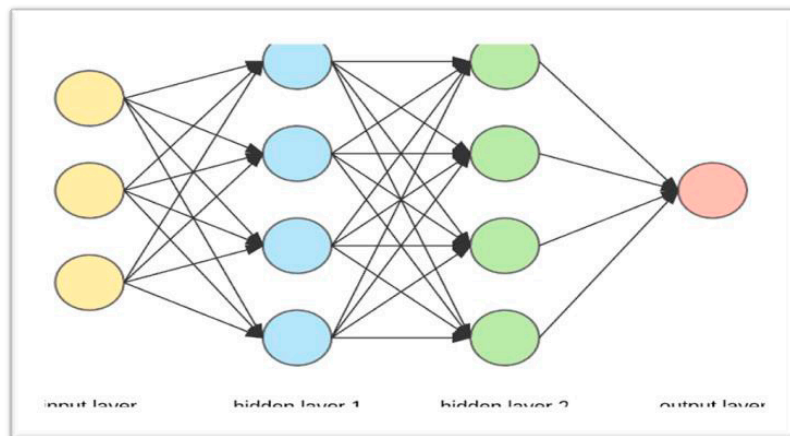


**Figure 3:** Artificial Neural Network (ANN)

- Long Short-Term Memory (LSTM) is a variant of RNN capable of learning long-time dependencies. It has the form of a chain of repeating modules of neural networks as shown in Figure 4.

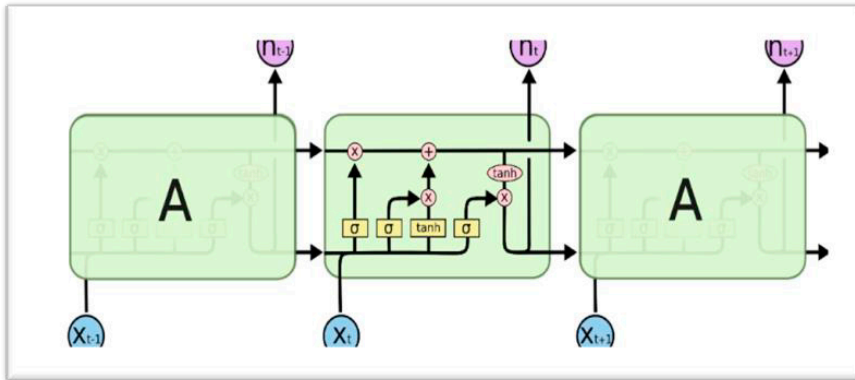


Figure 4: Long Short-Term Memory (LSTM)

### 1.3 Results and Discussion

#### 1.3.1 Trends and changes in Chili prices

The monthly chili prices from January 2018 to December 2022 are plotted as shown in Figure 5. The series exhibits cyclical effects, and no long-term linear trend or seasonality is identified from the plot. The stationarity assumption of the time series is tested by the Augmented-Dickey-Fuller (ADF) and Kwiatkowski-Phillips-Schmidt-Shin (KPSS) tests. Although the ADF ( $p$ -value=0.14) accepts the null hypothesis, the KPSS ( $p$ -value= 0.1) confirms the time series has stationary trend.

20-22 November, 2023, UTM KUALA LUMPUR, Malaysia

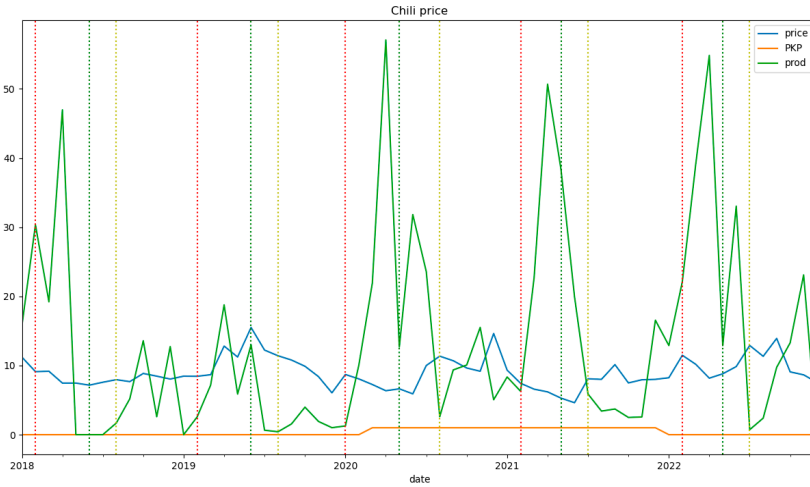


**Figure 5:** Time series plot of chili prices and production from 2018 to 2022.

Referring to Figure 5, it was observed that the chili price and chili production have opposite relationship. When there is more production, the price will decrease. Chili production is higher during movement control order (PKP) and after PKP compared to before PKP. It is also observed that the production peak happens between Chinese New Year and Aidil Fitri seasons. On the other hand, the price of fertilizer significantly increased after PKP but had little overall effect on the price of chili, as shown in Figure 6.



**Figure 6:** Effect of fertilizer on chili prices from 2018 to 2022.

### 1.3.2 Identifying significant factors that influence chili prices

In general, the inclusion of lag variables in a time series model is a remedial approach to the autocorrelation problem presented in the residuals. In this study, the lag-predictor variables are included in the modeling. The visual and numerical assessments supported the intuitive approach based on the red chili plantation experience, which shows that planting chilies are not seasonal. The harvesting could be done when chili plants reach three months old in addition to the effects of the fertilizer components added by the rainfall and temperature from the surrounding area.

Multiple Linear Regression (MLR) is implemented to determine the factors that significantly influence the price of chili. The model with the highest adjusted  $R^2$  is chosen as the best model. The results are presented in Table 2. In this case, Model 3 is chosen as the best model, indicating that chili prices and fertilizer components show significant relationships at least at lag 2. It can be summarized that the variables that significantly contribute to the chili price are Production, PKP versus non-PKP period, and the price of fertilizer, namely DAP, Potassium Chloride, Phosphate Rock, and Super Phosphate.

Table 2: Multiple Linear Regression based on Analysis of Variance (ANOVA)

MODEL	RESPONSE VARIABLE	PREDICTORS	ANOVA	$R^2$	Adjusted $R^2$
1	Prices	Production Fertilizer_Potassium Chloride Fertilizer_Phosphate Rock Fertilizer_Super Phosphate PKP	$p=0.003$	45.4%	30.5%
2	Prices	Production Lag1_Phosphate Rock Lag1_Super Phosphate	$p=0.003$	45.7%	30.9%
3	Prices	Production PKP Lag2_Fertilizer_DAP Lag2_Fertilizer_Potassium Chloride Lag2_Fertilizer_Phosphate Rock Lag2_Fertilizer_Super Phosphate	$p=0.002$	<b>46.8%</b>	<b>32.3%</b>

20-22 November, 2023, UTM KUALA LUMPUR, Malaysia

4	Prices	Production	$p=0.003$	45.7%	30.9%
		Lag3_Fertilizer_DAP			
		Lag3_Fertilizer_Potassium Chloride			
		Lag3_Fertilizer_Phosphate Rock			
		Lag3_Fertilizer_Super Phosphate			

$$\hat{Y}_t = \hat{\beta}_0 + \hat{\beta}_1.Production_t + \hat{\beta}_2.PKP_{t,j} + \hat{\beta}_3.(Fertilizer\_DAP)_{t-2} + \hat{\beta}_4.(Fertilizer\_PotassiumChloride)_{t-2} + \hat{\beta}_5.(Fertilizer\_PhosphateRock)_{t-2} + \hat{\beta}_4.(Fertilizer\_SuperPhosphate)_{t-2}$$

$$\hat{Y}_t = 10.381 - 0.048 Production_t - 1.084 PKP_{t,j} + 0.006 (Fertilizer\_DAP)_{t-2} + 0.001 (Fertilizer\_PotassiumChloride)_{t-2} + 0.004 (Fertilizer\_PhosphateRock)_{t-2} - 0.009 (Fertilizer\_SuperPhosphate)_{t-2}$$

where

$$PKP_j = \begin{cases} 1, j \text{ during PKP} \\ 0, j \text{ before or after PKP} \end{cases}$$

(7)

Another approach for identifying significant factors is using Structural Equation Modelling (SEM). Two models have been identified. The first model (Model 1) shown in Figure 7 indicates that the significant variables contributing to chili price are fertilizers (F1, F2, F3, F4, Urea) and production. Fertilizer has positive effects, while production has slightly negative effects since the chili price will decrease whenever the production increases. Referring to the second model, fertilizers and production become significant variables and mediator variables to chili price. Hence, based on the CFI and TLI values, the first model is chosen and supports the MLR results.

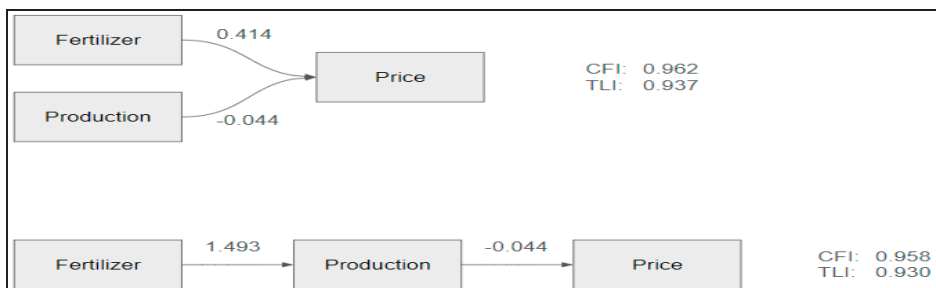
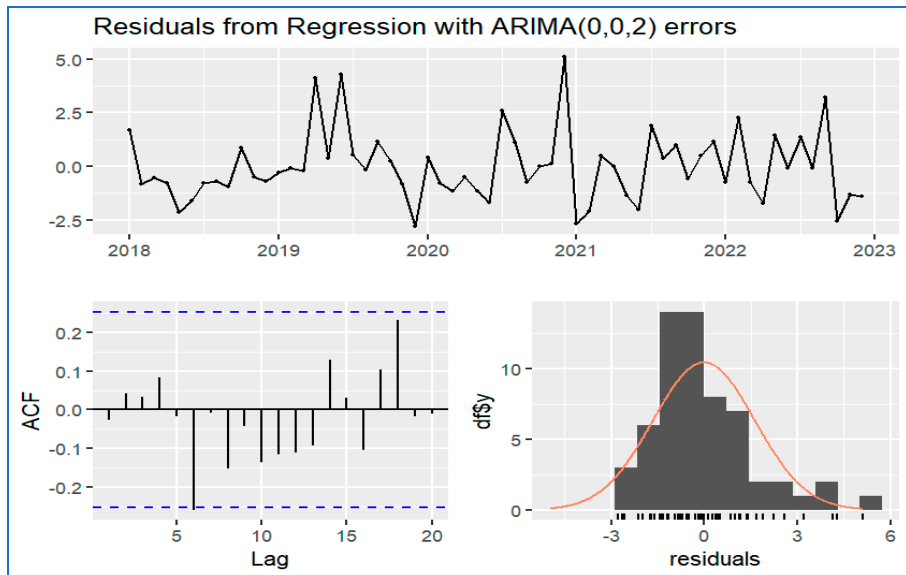


Figure 7: Significant factors using SEM



### 1.3.3 Chili price modelling using ARIMAX

ARIMAX model, or regression with ARIMA errors, generally conducts a time series regression with covariates. The remainder (error values) between the observed  $y_t$  and the fitted  $\hat{y}_t$  from the time series, regression is then remodelled using the ARIMA model, as shown in Figure 8.



**Figure 8:** Residuals analysis with ARIMA (0,0,2)

Based on the MLR and SEM approaches, the selected factors, i.e. fertilizers, production, and PKP season, act as the regressor, and the remainder terms are best fitted with the MA (2) model, hence ARIMAX (0, 0, 2) is the best model. The fitted model is written as:

$$\hat{Y}(t) = 9.8821 + \varepsilon_t + 0.4487\varepsilon_{t-1} + 0.4232\varepsilon_{t-2} - 0.02297P_t - 0.7888K_j + 0.0064F_{1t} + 0.0006F_{2t} + 0.0027F_{3t} - 0.0084F_{4t} \quad (8)$$

Production negatively affects the chili price and further supports the findings from MLR and SEM. Similarly, the effect of the fertilizer on chili prices is similar to those found in MLR. The Ljung-Box diagnostic test yields a  $p$ -value of 0.4002, which is greater than 0.05, supporting the fact that the ARIMAX(0, 0, 2) has no autocorrelation and can be considered adequate.

### 1.3.4 Models comparison

All tested models were compared and analyzed. Standard ML models such as Support Vector Regression (SVR) and Random Forest (RF) exhibit good model fitting for small-scale data. However, there is a less significant difference between the performances of the top three models, as shown in Table 3. Due to limited training data for machine learning algorithms, it is recommended to employ ARIMAX in forecasting chili prices.

Table 3. Error measurements using MLR, ARIMAX and ML

Measures	MLR	ARIMAX	SVR	RF	ANN	LSTM
RMSE	1.9244	1.6332	1.6757	<b>1.5691</b>	2.1791	1.9694
MAE	1.4192	1.2263	<b>1.1052</b>	1.2250	1.7102	1.4595
MAPE	16.2779	13.7654	<b>12.1057</b>	14.0159	19.9761	16.0156
Rank	4	3	1	2	6	5

Referring to Table 3, ARIMAX demonstrates superior statistical modeling compared to Multiple Linear Regression (MLR). The ARIMAX models can capture the patterns and follow the trend effectively by incorporating significant exogenous variables as shown in Figure 9. Fig. 9 compares the observed and fitted chili prices using all tested models.

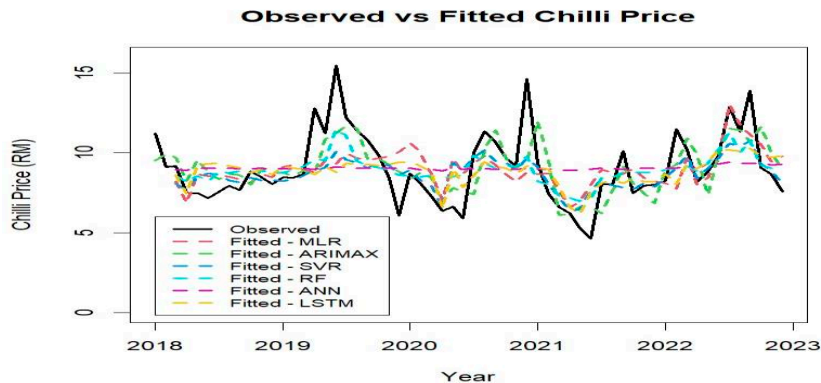


Figure 9: Comparison between the observed and fitted chili price

## 1.4 Conclusion and Recommendations

Forecasting chili prices in Malaysia is important for various stakeholders and the overall economic landscape. The identified model (ARIMAX) can be the foundation for future price simulations. Notably, predictor variables encompassing chili production, periods of Movement Control Order (PKP), and the type of fertilizers employed have a consequential influence on chili prices. If the model proves effective in determining future price trends over an extended period, farmers can plan vegetable production according to the appropriate season. A prospective inquiry may focus on specific proximate markets,

elucidating geographical interdependencies. Integrating these interdependencies into the evolving model is directed towards appraising whether a discernible enhancement in predictive accuracy can be realized. In conclusion, forecasting chili prices in Malaysia is essential for ensuring food security, supporting the agricultural sector, promoting economic stability, and facilitating informed decision-making across the entire chili supply chain.

### 1.6 Acknowledgement

This work was supported by Institute of Mathematics for Industry, Joint Usage/Research Center in Kyushu University. (FY2023 Workshop (I) “MMISG2023” (2023b003).)

## REFERENCES

- Basnayake, B.R.P.M., Kaushalya, K.D., Wickramaratne, R.H.M., Kushan, M.A.K., Chandrasekara, N.V. 2022. An Approach for Prediction of Weekly Prices of Green Chili in Sri Lanka: Application of Artificial Neural Network Techniques. *The Journal of Agricultural Sciences - Sri Lanka* 17(2): 333-349. <http://doi.org/10.4038/jas.v17i2.9746>
- Hamjah, M.A. 2014. Temperature and Rainfall Effects on Spice Crops Production and Forecasting the Production in Bangladesh: An Application of Box-Jenkins ARIMAX Model. *Mathematical Theory and Modeling* 4(10):149-159.
- Putriasari, N., Nugroho, S., Rachmawati, R., Agwil, W., and Sitohang, Y.O. 2022. Forecasting A Weekly Red Chilli Price in Bengkulu City Using Autoregressive Integrated Moving Average (ARIMA) and Singular Spectrum Analysis (SSA) Methods. *JSDS: Journal Of Statistics and Data Science* 1(1). <https://ejournal.unib.ac.id/index.php/jsds/index>.
- Shahizan, S., Balasubramaniam, K., Bakar, N. A., Masrom, M. 2023. Price Forecasting Analysis of Red Chilli Using Seasonal Regression and Quadratic Trend Models. *International Journal of Advanced Research in Technology and Innovation* 5(3): 21-31. <http://myjims.mohe.gov.my/index.php/ijarti>.
- Lestari, E.P., Prajanti, S.D.W., Wibawanto, W., Adzim, F. 2022. ARCH-GARCH Analysis: An Approach to Determine the Price Volatility of Red Chili. *AGRARIS: Journal of Agribusiness and Rural Development Research* 8(1): 90 – 105.
- Sukiyono, K., and Janah, M. 2019. Forecasting Model Selection of Curly Red Chili Price at Retail Level. *Indonesian Journal of Agricultural Research* 2(01): 1-12.

INDUSTRY PRESENTATION SLIDES

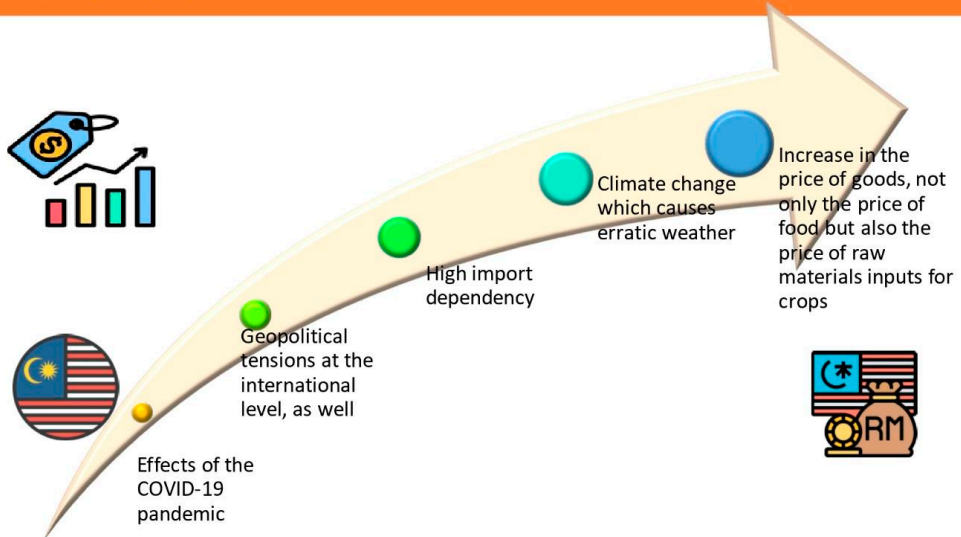


## Development of a Price Forecasting Model for the Main Vegetables in Malaysia

Aimi Athirah Ahmad<sup>1</sup>, Dr Syahrin Suhaimee<sup>1</sup>, Dr Teoh Chin Chuang<sup>2</sup> and Hafidha Azmon<sup>2</sup>

<sup>1</sup>Socio-Economic, Market Intelligence and Agribusiness Research Centre, MARDI-HQ, 43400 Serdang, Selangor, Malaysia  
<sup>2</sup>Engineering Research Centre, MARDI-HQ, 43400 Serdang, Selangor, Malaysia

### Introduction



## Introduction: Agricultural commodity

- Lack of supply and sudden demand
- Increase logistic cost and transportation
- Increase in labor cost
- Supply chain sources such as country of origin or the number of intermediaries and resellers
- High cost of raw materials
- Uncertain production
- Climate change



## Justification

Price forecasting is important in evaluating country's economic performance

- Help government agencies in making and developing appropriate economic policies and strategies in the future

Commodity prices experience high levels of volatility.

- Price forecasting is seen as one of the methods to reduce the negative effects of uncertainty

Fluctuations due to shocks in supply. These disturbances, combined with demand elasticity and short-term supply, cause sudden price instability.

- The impact of this can cause both farmers and consumers to experience uncertainty and risk and commodity price fluctuations

Forecasting price volatility is seen as a more critical method in developing countries

- uncertainty about food prices has a direct impact on well-being. The impact of food price instability also affects low-income people and small agricultural producers who are dependent on the sale of their crops

## Justification

- From the above problems, a model that is most suitable for assessing the fluctuation of exported crops needs to be identified through data analysis approach using statistical methods.
- **Therefore, this study aims to predict the price of the vegetable commodity that is chilli using the Statistical Modelling approach. This study uses chilli price data in the state of Johor.**
- The selection of Johor state is because Johor is the largest chilli producer in Malaysia.



## Objective

1. To examine the changes and trend of chilli price.
2. To analyze chili price volatility in Johor using time series analysis approach.
3. To analyze the effect of shock on chili price fluctuations from factors such as production, input prices, price and quantity of imported chili, climate (such as rain and temperature) and festival season.
4. To identify significant factors that affect chili prices.



## Methodology

- Data exploration
- Trend analysis
- Time series analysis



Mean	Std Dev	Median	Min	Max	Skewness	Kurtosis	CV
9.01	2.46	8.5	4	19	0.89	1.03	27.34%

OUTPUT PRESENTATION SLIDES



**MALAYSIA MATHEMATICS IN INDUSTRY STUDY GROUP 2023 (MMISG 2023)**  
PRICE FORECASTING MODEL FOR MAIN VEGETABLES IN MALAYSIA

*Innovating Solutions*



**INDUSTRY**

DR. AIMI ATHIRAH AHMAD  
MALAYSIAN AGRICULTURAL RESEARCH AND DEVELOPMENT INSTITUTE (MARDI)

**MODERATOR**

ASSOC. PROF. DR. SHARIFAH SUHAILA  
SYED JAMALUDIN  
UNIVERSITI TEKNOLOGI MALAYSIA

**DOMAIN ADVISOR**

PROF. DR. FADHILAH YUSOF  
UNIVERSITI TEKNOLOGI MALAYSIA  
ASSOC. PROF. DR. ROSLINAZAIRIMAH ZAKARIA  
UNIVERSITI MALAYSIA PAHANG AL-SULTAN ABDULLAH

**CONTRIBUTOR**

ASSOC. PROF. TS. DR. HANITA DAUD  
UNIVERSITI TEKNOLOGI PETRONAS  
TS. DR. MOHD MAHAYAUDIN MANSOR  
UNIVERSITI TEKNOLOGI MARA  
DR. NOR HAMIZAH MISWAN  
UNIVERSITI KEBANGSAAN MALAYSIA  
DR. SITI RAHAYU MOHD HASHIM  
UNIVERSITI MALAYSIA SABAH  
DR. SITI MARIAM NORRULASHIKIN  
UNIVERSITI TEKNOLOGI MALAYSIA  
DR. SITI ROHANI MOHD NOR  
UNIVERSITI TEKNOLOGI MALAYSIA  
DR. RAZIK RIDZUAN MOHD TAJUDDIN  
UNIVERSITI KEBANGSAAN MALAYSIA  
MR. SYAHRIZAL SALLEH  
UNIVERSITI MALAYSIA PAHANG AL-SULTAN ABDULLAH  
MR. RUZAINI ZULHUSNI PUSLAN  
UNIVERSITI TEKNOLOGI MALAYSIA



*innovative • entrepreneurial • global*



20-22 November, 2023, UTM KUALA LUMPUR, Malaysia



## PROJECT DESCRIPTION

- **Monitoring the volatility of commodity prices** can play an important role in evaluating the country's economic performance.
- Thus, **commodity price forecasts** can help government agencies make and develop appropriate economic policies and strategies in the future.
- Commodity prices, especially agricultural commodity prices, experience high levels of volatility.
- Therefore, **price forecasting** is seen as one of the methods for reducing the negative effects of uncertainty, which can further decrease the risk of the producers' agricultural commodities.



innovative • entrepreneurial • global



## PROJECT DESCRIPTION

- In general, fluctuations in the price of agricultural commodities occur mainly due to shocks in supply.
- These disturbances, **combined with demand elasticity and short-term supply**, cause **sudden price instability**.
- This can cause farmers and consumers to experience uncertainty, risk, and commodity price fluctuations.
- Hence, **forecasting price volatility** is seen as a more critical method in developing countries because a large portion of household income is spent on food.
- This is because the uncertainty about food prices has a direct impact on well-being.
- Moreover, the impact of food price instability can also affect low-income people and small agricultural producers dependent on their crops' sales.



innovative • entrepreneurial • global





## PROBLEM STATEMENT

- The vegetable commodity selected in this research is chili.
- As acknowledged, the chili price is **unstable** and **fluctuating**.
- This has made it difficult for the stakeholders to make a consistent and reliable decision on the chili price.
- In addition, chili production is sometimes threatened due to agriculture problems, and this will cause supply to decrease.
- When supply decreases while demand increases, the price will rise as well.
- Therefore, information is needed regarding the **predicted fluctuations in chili price trends** so that market demand for chili can be known.
- In addition, the chili price volatility and the effect of shock on chili price fluctuations from factors such as production, input prices, price and quantity of imported chili, climate, and festive needs to be analyzed.

innovative • entrepreneurial • global



## CHILI PLANT

Chili plant characteristics

Maturity duration: 60-120 days

Life span: 6 – 12 months

Data scale: monthly

Duration: 2018-2022 (5 years, 60 data)

Data source: Market price (FAMA,2023)

Other data:

Total production, fertilizers (DAP, Potassium Chloride, Phosphate rock, super phosphates, urea), climate (temperature, rainfall), fuel price, season (PKP, festives)



innovative • entrepreneurial • global



# OBJECTIVES

- 1 To examine the change and trend of chili prices
- 2 To determine significant factors contribute to chili prices
- 3 To analyze chili prices volatility in Johor using time series approach

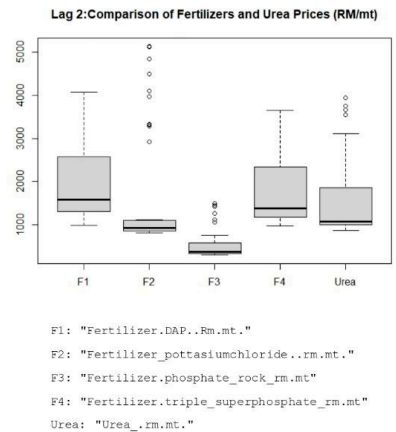
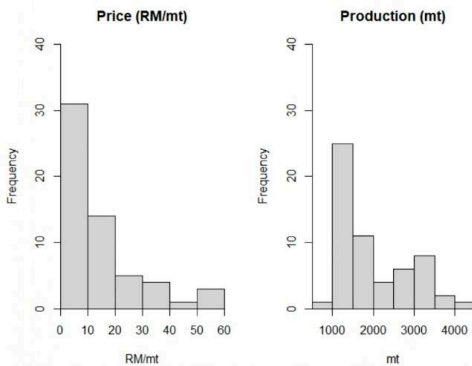
innovative • entrepreneurial • global



## TREND OF CHILI PRICE

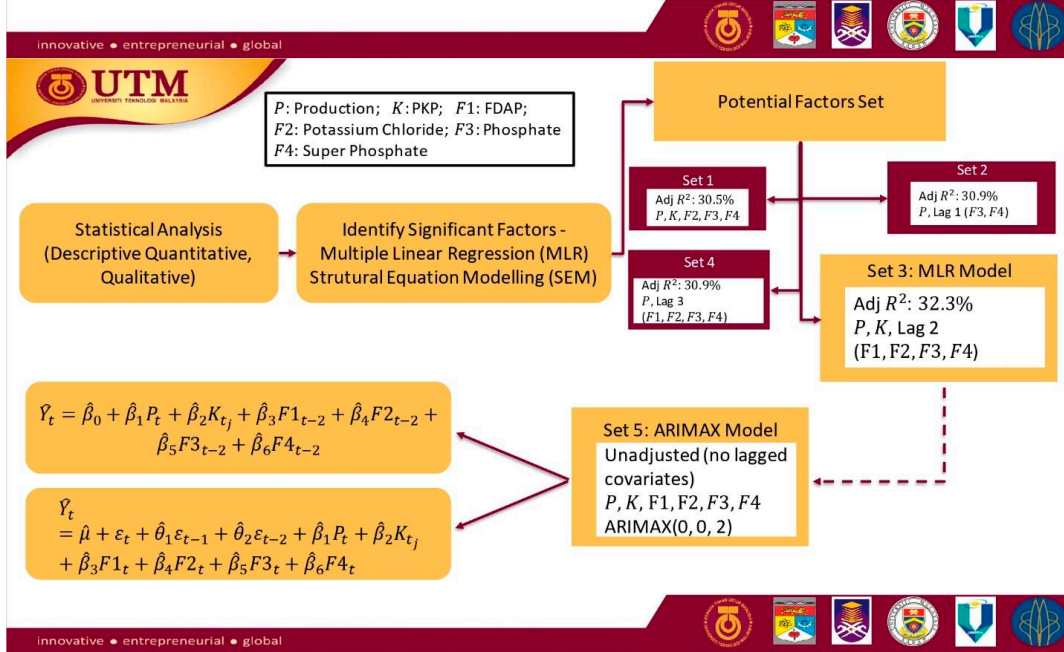
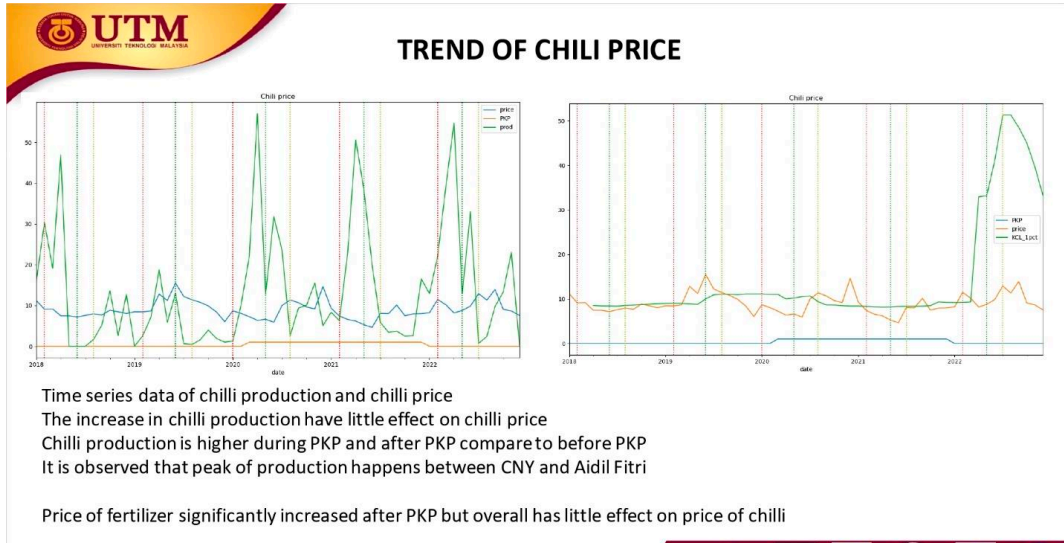
It is observed that the chili price and production of chili has opposite relationship. When the production is more the price will be decreased.

The price of fertilizers also has an effect to the chili price. It is found that the price of potassiumchloride has reached the highest price has compared to other fertilizers.



innovative • entrepreneurial • global







## MODELLING

1. Multiple Linear Regression Model – to identify significant factors
2. Structural Equation Modelling (SEM) – to identify significant factors
3. ARIMAX (Dynamic regression model) – Time series (lagged variables combine with covariates)
4. Machine Learning:
  - (i) Support Vector Regression (SVR)
  - (ii) Random Forest Regression (RFR)
  - (iii) Artificial Neural Network (ANN)
  - (iv) Long Short Term Memory (LSTM)

innovative • entrepreneurial • global



### MULTIPLE LINEAR REGRESSION (MLR)

MODEL	RESPONSE VARIABLE	PREDICTORS	ANOVA	R <sup>2</sup>	Adjusted R <sup>2</sup>
1	Prices	Production Fertilizer_Potassium Chloride Fertilizer_Phosphate Rock Fertilizer_Super Phosphate PKP	$p=0.003$	45.4%	30.5%
2	Prices	Production Lag1_Phosphate Rock Lag1_Super Phosphate	$p=0.003$	45.7%	30.9%
3	Prices	Production PKP Lag2_Fertilizer_DAP Lag2_Fertilizer_Potassium Chloride Lag2_Fertilizer_Phosphate Rock Lag2_Fertilizer_Super Phosphate	$p=0.002$	46.8%	32.3%
4	Prices	Production Lag3_Fertilizer_DAP Lag3_Fertilizer_Potassium Chloride Lag3_Fertilizer_Phosphate Rock Lag3_Fertilizer_Super Phosphate	$p=0.003$	45.7%	30.9%


All variables are considered in the multiple linear regression analyses and tested using ENTER method.

Only significant models are shortlisted based on the  $p$ -values of the ANOVA tests and the significant variables are identified based on the  $p$ -values ( $<\alpha=5\%$ ) obtained from the coefficient tests.

The model with the highest Adjusted  $R^2$  is chosen as the best model. In this case, Model 3 is chosen as the best model.

innovative • entrepreneurial • global





## MULTIPLE LINEAR REGRESSION (MLR)

$$\hat{Y}_t = \beta_0 + \beta_1 \cdot Production_t + \beta_2 \cdot PKP_{t,j} + \beta_3 \cdot (Fertilizer(DAP))_{t-2} + \beta_4 \cdot (Fertilizer(Potassium Chloride))_{t-2} + \beta_5 \cdot (Fertilizer(Phosphate Rock))_{t-2} + \beta_6 \cdot (Fertilizer(Super Phosphate))_{t-2}$$


$$\hat{Y}_t = 10.381 - 0.048 (Production)_t - 1.084 (PKP)_{t,j} + 0.006 (Fertilizer(DAP))_{t-2} + 0.001 (Fertilizer(Potassium Chloride))_{t-2} + 0.004 (Fertilizer(Phosphate Rock))_{t-2} - 0.009 (Fertilizer(Super Phosphate))_{t-2}$$


where;

$$PKP_j = \begin{cases} 1, & j \text{ during PKP} \\ 0, & j \text{ before or after PKP} \end{cases}$$

Based on Model 3, the variables that significantly contribute to the Price are Production, PKP vs Non-PKP period, the price of fertilizer namely DAP, Potassium Chloride, Phosphate Rock and Super Phosphate.

innovative • entrepreneurial • global



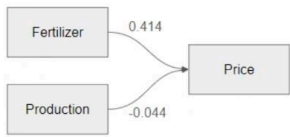


## STRUCTURAL EQUATION MODELLING (SEM)

In applications of structural equation modeling (SEM), a critical step is to evaluate the goodness of fit of the proposed model with the data. Two commonly used fit indices: the comparative fit index (CFI) and the Tucker–Lewis index (TLI). The CFI measures the relative improvement in fit going from the baseline model to the postulated model, while the TFI measures a relative reduction in misfit per degree of freedom. Both CFI and TFI is a normed fit index in the sense that it ranges between 0 and 1, with higher values indicating a better fit.


Two models are identified. **Model 1:** Significant variables contributing to chili price are fertilizers (F1,F2,F3,F4,Urea) and production. Fertilizer has positive effects while production has slightly negative effects since whenever the production increased, the chili price will be decreased. **Model 2:** Significant variables are fertilizers and production become mediator variable to chili price. Hence, based on the CFI and TLI values, **Model 1** is chosen and these support the MLR results.

### Model 1




CFI: 0.962  
TLI: 0.937

### Model 2



CFI: 0.958  
TLI: 0.930

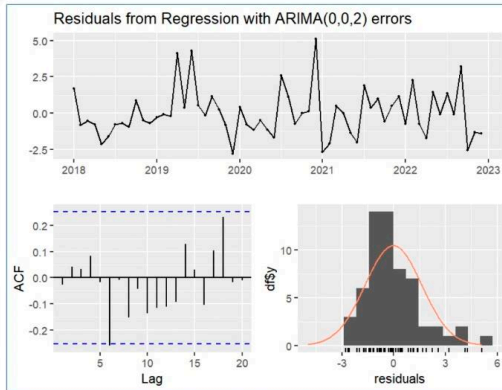
innovative • entrepreneurial • global



20-22 November, 2023, UTM KUALA LUMPUR, Malaysia



### ARIMAX model



ARIMAX model or also known as regression with ARIMA errors, generally conduct a time series regression with covariates. The remainder (error values) between the observed  $y_t$  and the fitted  $\hat{y}_t$  from the time series regression is then remodelled using ARIMA model.

Based on the MLR and SEM approaches, the selected factors, i.e. fertilizers, production and PKP season act as the regressor and the remainder terms are best fitted with MA(2) model, hence ARIMAX(0, 0, 2) is the best model. The fitted model is written as:

$$\begin{aligned} \hat{Y}_t &= 9.8821 + \varepsilon_t + 0.4487\varepsilon_{t-1} + 0.4232\varepsilon_{t-2} - 0.0297P_t \\ &\quad - 0.7888K_t + 0.0064F1_t + 0.0006F2_t + 0.0027F3_t \\ &\quad - 0.0084F4_t \end{aligned}$$

Production negatively affects the chili price and further support the findings from MLR and SEM. Similarly, the effect of the fertilizer towards chili price is similar to those found in MLR.

The Ljung-Box diagnostic test yields p-value of 0.4002, which is greater than 0.05, hence supporting that the ARIMAX(0, 0, 2) has no autocorrelation and can be considered adequate.

innovative • entrepreneurial • global

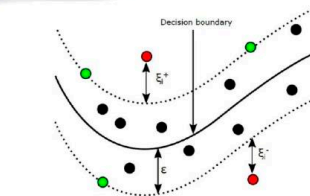


### MACHINE LEARNING MODEL

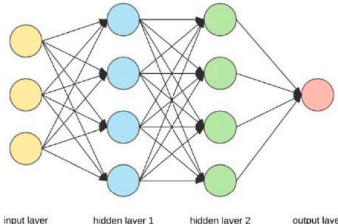
Machine Learning (ML) algorithms enable to automatically learn from data to identify patterns for predictions with an iterative process. Four ML models considered for time series data:

- Support Vector Regression (SVR) – aims at reducing the error by determine the hyperplane (decision boundary) and minimizing the range between predicted and observed value.
- Random Forest Regression (RFR) – aims to combine multiple decision trees and the final output is the mean of all the outputs from these multiple trees.
- Artificial Neural Network (ANN) – consists of a node layers containing an input layer, hidden layers and an output layer. Each node connects to another and has associated weight and threshold.
- Long Short Term Memory (LSTM) – a variant of RNN that are capable of learning long time dependencies. It has the form of chain of repeating modules of neural networks.

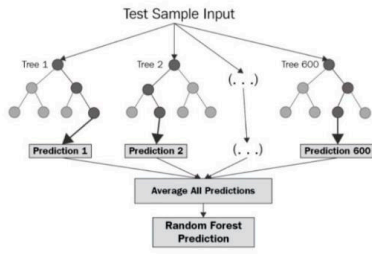
innovative • entrepreneurial • global



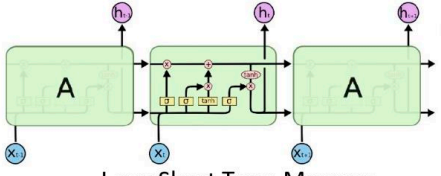
**Support Vector Regression**



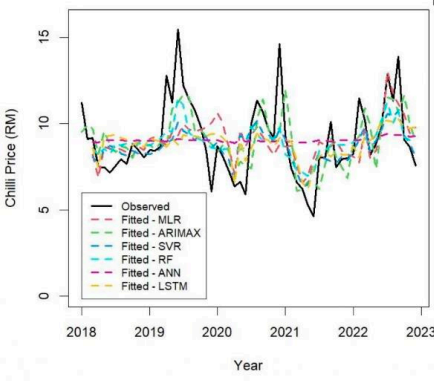
**Artificial Neural Network**



**Random Forest Regression**



**Long Short Term Memory**



**Observed vs Fitted Chilli Price**

Measures	MLR	ARIMAX	SVR	RF	ANN	LSTM
RMSE	1.9244	1.6332	1.6757	<b>1.5691</b>	2.1791	1.9694
MAE	1.4192	1.2263	<b>1.1052</b>	1.2250	1.7102	1.4595
MAPE	16.2779	13.7654	<b>12.1057</b>	14.0159	19.9761	16.0156
Rank	4	3	1	2	6	5

**Comments:**

- For small-scale data, standard ML models such as Support Vector Regression (SVR) and Random Forest (RF) exhibit good model fitting. However, there is a less significant difference between the performances of the top three models.
- ARIMAX demonstrates superior statistical modeling compared to Multiple Linear Regression (MLR). The ARIMAX models effectively capture and predict patterns by incorporating significant exogenous variables.
- Complicated ML models underperformed others, potentially due to a lack of training data and challenges in obtaining optimal hyperparameter values.
- The trade-off between accuracy and interpretability is an important consideration for both approaches (statistical and ML modeling). While ML models lack interpretability but excel in accuracy, the statistical approach provides good interpretability insight. Hence, ML models require a model diagnostic approach to include interpretability insight





## RECOMMENDATION

1. Chili is a commodity that contributes to inflation, particularly in the category of volatile food. The statistical modeling approach has the capability to predict chili prices in the future.
2. The identified model can serve as the foundation for future price simulations.
3. If this model proves effective in determining future price trends over an extended period, farmers can plan vegetable production according to the appropriate season.
4. The model application can be expanded to encompass different commodity prices and locations, considering the variations in commodity prices across the country.
5. In a future study, specific neighboring markets may be selected for analyzing geographical dependencies. Incorporating these dependencies into the developing model aims to assess whether there is a significant improvement in accuracy.
6. To capture the seasonality pattern in the data, a longer range of data or a higher frequency of data is necessary.



## MI レクチャーノートシリーズ刊行にあたり

本レクチャーノートシリーズは、文部科学省 21 世紀 COE プログラム「機能数理学の構築と展開」(H15-19 年度)において作成した COE Lecture Notes の続刊であり、文部科学省大学院教育改革支援プログラム「産業界が求める数学博士と新修士養成」(H19-21 年度)および、同グローバル COE プログラム「マス・フォア・インダストリ教育研究拠点」(H20-24 年度)において行われた講義の講義録として出版されてきた。平成 23 年 4 月のマス・フォア・インダストリ研究所 (IMI) 設立と平成 25 年 4 月の IMI の文部科学省共同利用・共同研究拠点として「産業数学の先進的・基礎的共同研究拠点」の認定を受け、今後、レクチャーノートは、マス・フォア・インダストリに関わる国内外の研究者による講義の講義録、会議録等として出版し、マス・フォア・インダストリの本格的な展開に資するものとする。

2022 年 10 月

マス・フォア・インダストリ研究所  
所長 梶原 健司

## International Project Research-Workshop (I)

# Proceedings of 4<sup>th</sup> Malaysia Mathematics in Industry Study Group (MMISG 2023)

発行 2024年3月28日  
編集長 Zaitul Marlizawati Zainuddin, Arifah Bahar  
編集 Shariffah Suhaila Syed Jamaludin, Zaiton Mat Isa, Nur Arina Bazilah Aziz,  
Taufiq Khairi Ahmad Khairuddin, Shaymaa M.H. Darwish, Ahmad Razin Zainal Abidin,  
Norhaiza Ahmad, Zainal Abdul Aziz, Hang See Pheng, Mohd Ali Khameini Ahmad  
発行 九州大学マス・フォア・インダストリ研究所  
九州大学大学院数理学府  
〒819-0395 福岡市西区元岡744  
九州大学数理・IMI 事務室  
TEL 092-802-4402 FAX 092-802-4405  
URL <https://www.imi.kyushu-u.ac.jp/>

印刷 城島印刷株式会社  
〒810-0012 福岡市中央区白金2丁目9番6号  
TEL 092-531-7102 FAX 092-524-4411

## シリーズ既刊

Issue	Author/Editor	Title	Published
COE Lecture Note	Mitsuhiro T. NAKAO Kazuhiro YOKOYAMA	Computer Assisted Proofs - Numeric and Symbolic Approaches - 199pages	August 22, 2006
COE Lecture Note	M.J.Shai HARAN	Arithmetical Investigations - Representation theory, Orthogonal polynomials and Quantum interpolations- 174pages	August 22, 2006
COE Lecture Note Vol.3	Michal BENES Masato KIMURA Tatsuyuki NAKAKI	Proceedings of Czech-Japanese Seminar in Applied Mathematics 2005 155pages	October 13, 2006
COE Lecture Note Vol.4	宮田 健治	辺要素有限要素法による磁界解析 - 機能数理学特別講義 21pages	May 15, 2007
COE Lecture Note Vol.5	Francois APERY	Univariate Elimination Subresultants - Bezout formula, Laurent series and vanishing conditions - 89pages	September 25, 2007
COE Lecture Note Vol.6	Michal BENES Masato KIMURA Tatsuyuki NAKAKI	Proceedings of Czech-Japanese Seminar in Applied Mathematics 2006 209pages	October 12, 2007
COE Lecture Note Vol.7	若山 正人 中尾 充宏	九州大学産業技術数理研究センター キックオフミーティング 138pages	October 15, 2007
COE Lecture Note Vol.8	Alberto PARMEGGIANI	Introduction to the Spectral Theory of Non-Commutative Harmonic Oscillators 233pages	January 31, 2008
COE Lecture Note Vol.9	Michael I.TRIBELSKY	Introduction to Mathematical modeling 23pages	February 15, 2008
COE Lecture Note Vol.10	Jacques FARAUT	Infinite Dimensional Spherical Analysis 74pages	March 14, 2008
COE Lecture Note Vol.11	Gerrit van DIJK	Gelfand Pairs And Beyond 60pages	August 25, 2008
COE Lecture Note Vol.12	Faculty of Mathematics, Kyushu University	Consortium "MATH for INDUSTRY" First Forum 87pages	September 16, 2008
COE Lecture Note Vol.13	九州大学大学院 数理学研究院	プロシーディング「損保数理に現れる確率モデル」 — 日新火災・九州大学 共同研究2008年11月 研究会 — 82pages	February 6, 2009

## シリーズ既刊

Issue	Author/Editor	Title	Published
COE Lecture Note Vol.14	Michal Beneš, Tohru Tsujikawa Shigetoshi Yazaki	Proceedings of Czech-Japanese Seminar in Applied Mathematics 2008 77pages	February 12, 2009
COE Lecture Note Vol.15	Faculty of Mathematics, Kyushu University	International Workshop on Verified Computations and Related Topics 129pages	February 23, 2009
COE Lecture Note Vol.16	Alexander Samokhin	Volume Integral Equation Method in Problems of Mathematical Physics 50pages	February 24, 2009
COE Lecture Note Vol.17	矢嶋 徹 及川 正行 梶原 健司 辻 英一 福本 康秀	非線形波動の数値と物理 66pages	February 27, 2009
COE Lecture Note Vol.18	Tim Hoffmann	Discrete Differential Geometry of Curves and Surfaces 75pages	April 21, 2009
COE Lecture Note Vol.19	Ichiro Suzuki	The Pattern Formation Problem for Autonomous Mobile Robots —Special Lecture in Functional Mathematics— 23pages	April 30, 2009
COE Lecture Note Vol.20	Yasuhide Fukumoto Yasunori Maekawa	Math-for-Industry Tutorial: Spectral theories of non-Hermitian operators and their application 184pages	June 19, 2009
COE Lecture Note Vol.21	Faculty of Mathematics, Kyushu University	Forum "Math-for-Industry" Casimir Force, Casimir Operators and the Riemann Hypothesis 95pages	November 9, 2009
COE Lecture Note Vol.22	Masakazu Suzuki Hoon Hong Hirokazu Anai Chee Yap Yousuke Sato Hiroshi Yoshida	The Joint Conference of ASCM 2009 and MACIS 2009: Asian Symposium on Computer Mathematics Mathematical Aspects of Computer and Information Sciences 436pages	December 14, 2009
COE Lecture Note Vol.23	荒川 恒男 金子 昌信	多重ゼータ値入門 111pages	February 15, 2010
COE Lecture Note Vol.24	Fulton B.Gonzalez	Notes on Integral Geometry and Harmonic Analysis 125pages	March 12, 2010
COE Lecture Note Vol.25	Wayne Rossman	Discrete Constant Mean Curvature Surfaces via Conserved Quantities 130pages	May 31, 2010
COE Lecture Note Vol.26	Mihai Ciucu	Perfect Matchings and Applications 66pages	July 2, 2010

## シリーズ既刊

Issue	Author/Editor	Title	Published
COE Lecture Note Vol.27	九州大学大学院 数理学研究院	Forum “Math-for-Industry” and Study Group Workshop Information security, visualization, and inverse problems, on the basis of optimization techniques 100pages	October 21, 2010
COE Lecture Note Vol.28	ANDREAS LANGER	MODULAR FORMS, ELLIPTIC AND MODULAR CURVES LECTURES AT KYUSHU UNIVERSITY 2010 62pages	November 26, 2010
COE Lecture Note Vol.29	木田 雅成 原田 昌晃 横山 俊一	Magma で広がる数学の世界 157pages	December 27, 2010
COE Lecture Note Vol.30	原 隆 松井 卓 廣島 文生	Mathematical Quantum Field Theory and Renormalization Theory 201pages	January 31, 2011
COE Lecture Note Vol.31	若山 正人 福本 康秀 高木 剛 山本 昌宏	Study Group Workshop 2010 Lecture & Report 128pages	February 8, 2011
COE Lecture Note Vol.32	Institute of Mathematics for Industry, Kyushu University	Forum “Math-for-Industry” 2011 “TSUNAMI-Mathematical Modelling” Using Mathematics for Natural Disaster Prediction, Recovery and Provision for the Future 90pages	September 30, 2011
COE Lecture Note Vol.33	若山 正人 福本 康秀 高木 剛 山本 昌宏	Study Group Workshop 2011 Lecture & Report 140pages	October 27, 2011
COE Lecture Note Vol.34	Adrian Muntean Vladimír Chalupecký	Homogenization Method and Multiscale Modeling 72pages	October 28, 2011
COE Lecture Note Vol.35	横山 俊一 夫 紀恵 林 卓也	計算機代数システムの進展 210pages	November 30, 2011
COE Lecture Note Vol.36	Michal Beneš Masato Kimura Shigetoshi Yazaki	Proceedings of Czech-Japanese Seminar in Applied Mathematics 2010 107pages	January 27, 2012
COE Lecture Note Vol.37	若山 正人 高木 剛 Kirill Morozov 平岡 裕章 木村 正人 白井 朋之 西井 龍映 柴 伸一郎 穴井 宏和 福本 康秀	平成23年度 数学・数理科学と諸科学・産業との連携研究ワーク ショップ 拡がっていく数学 ～期待される“見えない力”～ 154pages	February 20, 2012

## シリーズ既刊

Issue	Author/Editor	Title	Published
COE Lecture Note Vol.38	Fumio Hiroshima Itaru Sasaki Herbert Spohn Akito Suzuki	Enhanced Binding in Quantum Field Theory 204pages	March 12, 2012
COE Lecture Note Vol.39	Institute of Mathematics for Industry, Kyushu University	Multiscale Mathematics: Hierarchy of collective phenomena and interrelations between hierarchical structures 180pages	March 13, 2012
COE Lecture Note Vol.40	井ノ口順一 太田 泰広 寛 三郎 梶原 健司 松浦 望	離散可積分系・離散微分幾何チュートリアル2012 152pages	March 15, 2012
COE Lecture Note Vol.41	Institute of Mathematics for Industry, Kyushu University	Forum “Math-for-Industry” 2012 “Information Recovery and Discovery” 91pages	October 22, 2012
COE Lecture Note Vol.42	佐伯 修 若山 正人 山本 昌宏	Study Group Workshop 2012 Abstract, Lecture & Report 178pages	November 19, 2012
COE Lecture Note Vol.43	Institute of Mathematics for Industry, Kyushu University	Combinatorics and Numerical Analysis Joint Workshop 103pages	December 27, 2012
COE Lecture Note Vol.44	萩原 学	モダン符号理論からポストモダン符号理論への展望 107pages	January 30, 2013
COE Lecture Note Vol.45	金山 寛	Joint Research Workshop of Institute of Mathematics for Industry (IMI), Kyushu University “Propagation of Ultra-large-scale Computation by the Domain-decomposition-method for Industrial Problems (PUCDIP 2012)” 121pages	February 19, 2013
COE Lecture Note Vol.46	西井 龍映 栄 伸一郎 岡田 勘三 落合 啓之 小磯 深幸 斎藤 新悟 白井 朋之	科学・技術の研究課題への数学アプローチ —数学モデリングの基礎と展開— 325pages	February 28, 2013
COE Lecture Note Vol.47	SOO TECK LEE	BRANCHING RULES AND BRANCHING ALGEBRAS FOR THE COMPLEX CLASSICAL GROUPS 40pages	March 8, 2013
COE Lecture Note Vol.48	溝口 佳寛 脇 隼人 平坂 貢 谷口 哲至 鳥袋 修	博多ワークショップ「組み合わせとその応用」 124pages	March 28, 2013

## シリーズ既刊

Issue	Author/Editor	Title	Published
COE Lecture Note Vol.49	照井 章 小原 功任 濱田 龍義 横山 俊一 穴井 宏和 横田 博史	マス・フォア・インダストリ研究所 共同利用研究集会 II 数式処理研究と産学連携の新たな発展 137pages	August 9, 2013
MI Lecture Note Vol.50	Ken Anjyo Hiroyuki Ochiai Yoshinori Dobashi Yoshihiro Mizoguchi Shizuo Kaji	Symposium MEIS2013: Mathematical Progress in Expressive Image Synthesis 154pages	October 21, 2013
MI Lecture Note Vol.51	Institute of Mathematics for Industry, Kyushu University	Forum “Math-for-Industry” 2013 “The Impact of Applications on Mathematics” 97pages	October 30, 2013
MI Lecture Note Vol.52	佐伯 修 岡田 勘三 高木 剛 若山 正人 山本 昌宏	Study Group Workshop 2013 Abstract, Lecture & Report 142pages	November 15, 2013
MI Lecture Note Vol.53	四方 義啓 櫻井 幸一 安田 貴徳 Xavier Dahan	平成25年度 九州大学マス・フォア・インダストリ研究所 共同利用研究集会 安全・安心社会基盤構築のための代数構造 ～サイバー社会の信頼性確保のための数理学～ 158pages	December 26, 2013
MI Lecture Note Vol.54	Takashi Takiguchi Hiroshi Fujiwara	Inverse problems for practice, the present and the future 93pages	January 30, 2014
MI Lecture Note Vol.55	栄 伸一郎 溝口 佳寛 脇 隼人 洪田 敬史	Study Group Workshop 2013 数学協働プログラム Lecture & Report 98pages	February 10, 2014
MI Lecture Note Vol.56	Yoshihiro Mizoguchi Hayato Waki Takafumi Shibuta Tetsuji Taniguchi Osamu Shimabukuro Makoto Tagami Hirotake Kurihara Shuya Chiba	Hakata Workshop 2014 ~ Discrete Mathematics and its Applications ~ 141pages	March 28, 2014
MI Lecture Note Vol.57	Institute of Mathematics for Industry, Kyushu University	Forum “Math-for-Industry” 2014: “Applications + Practical Conceptualization + Mathematics = fruitful Innovation” 93pages	October 23, 2014
MI Lecture Note Vol.58	安生健一 落合啓之	Symposium MEIS2014: Mathematical Progress in Expressive Image Synthesis 135pages	November 12, 2014

## シリーズ既刊

Issue	Author/Editor	Title	Published
MI Lecture Note Vol.59	西井 龍映 岡田 勘三 梶原 健司 高木 剛 若山 正人 脇 隼人 山本 昌宏	Study Group Workshop 2014 数学協働プログラム Abstract, Lecture & Report 196pages	November 14, 2014
MI Lecture Note Vol.60	西浦 博	平成26年度九州大学 IMI 共同利用研究・研究集会 (I) 感染症数理モデルの実用化と産業及び政策での活用のための新たな展開 120pages	November 28, 2014
MI Lecture Note Vol.61	溝口 佳寛 Jacques Garrigue 萩原 学 Reynald Affeldt	研究集会 高信頼な理論と実装のための定理証明および定理証明器 Theorem proving and provers for reliable theory and implementations (TPP2014) 138pages	February 26, 2015
MI Lecture Note Vol.62	白井 朋之	Workshop on “ $\beta$ -transformation and related topics” 59pages	March 10, 2015
MI Lecture Note Vol.63	白井 朋之	Workshop on “Probabilistic models with determinantal structure” 107pages	August 20, 2015
MI Lecture Note Vol.64	落合 啓之 土橋 宜典	Symposium MEIS2015: Mathematical Progress in Expressive Image Synthesis 124pages	September 18, 2015
MI Lecture Note Vol.65	Institute of Mathematics for Industry, Kyushu University	Forum “Math-for-Industry” 2015 “The Role and Importance of Mathematics in Innovation” 74pages	October 23, 2015
MI Lecture Note Vol.66	岡田 勘三 藤澤 克己 白井 朋之 若山 正人 脇 隼人 Philip Broadbridge 山本 昌宏	Study Group Workshop 2015 Abstract, Lecture & Report 156pages	November 5, 2015
MI Lecture Note Vol.67	Institute of Mathematics for Industry, Kyushu University	IMI-La Trobe Joint Conference “Mathematics for Materials Science and Processing” 66pages	February 5, 2016
MI Lecture Note Vol.68	古庄 英和 小谷 久寿 新甫 洋史	結び目と Grothendieck-Teichmüller 群 116pages	February 22, 2016
MI Lecture Note Vol.69	土橋 宜典 鍛冶 静雄	Symposium MEIS2016: Mathematical Progress in Expressive Image Synthesis 82pages	October 24, 2016
MI Lecture Note Vol.70	Institute of Mathematics for Industry, Kyushu University	Forum “Math-for-Industry” 2016 “Agriculture as a metaphor for creativity in all human endeavors” 98pages	November 2, 2016
MI Lecture Note Vol.71	小磯 深幸 二宮 嘉行 山本 昌宏	Study Group Workshop 2016 Abstract, Lecture & Report 143pages	November 21, 2016



## シリーズ既刊

Issue	Author/Editor	Title	Published
MI Lecture Note Vol.72	新井 朝雄 小嶋 泉 廣島 文生	Mathematical quantum field theory and related topics 133pages	January 27, 2017
MI Lecture Note Vol.73	穴田 啓晃 Kirill Morozov 須賀 祐治 奥村 伸也 櫻井 幸一	Secret Sharing for Dependability, Usability and Security of Network Storage and Its Mathematical Modeling 211pages	March 15, 2017
MI Lecture Note Vol.74	QUISPEL, G. Reinout W. BADER, Philipp MCLAREN, David I. TAGAMI, Daisuke	IMI-La Trobe Joint Conference Geometric Numerical Integration and its Applications 71pages	March 31, 2017
MI Lecture Note Vol.75	手塚 集 田上 大助 山本 昌宏	Study Group Workshop 2017 Abstract, Lecture & Report 118pages	October 20, 2017
MI Lecture Note Vol.76	宇田川誠一	Tzitzéica 方程式の有限間隙解に付随した極小曲面の構成理論 —Tzitzéica 方程式の楕円関数解を出発点として— 68pages	August 4, 2017
MI Lecture Note Vol.77	松谷 茂樹 佐伯 修 中川 淳一 田上 大助 上坂 正晃 Pierluigi Cesana 濱田 裕康	平成29年度 九州大学マス・フォア・インダストリ研究所 共同利用研究会 (I) 結晶の界面, 転位, 構造の数理 148pages	December 20, 2017
MI Lecture Note Vol.78	瀧澤 重志 小林 和博 佐藤憲一郎 斎藤 努 清水 正明 間瀬 正啓 藤澤 克樹 神山 直之	平成29年度 九州大学マス・フォア・インダストリ研究所 プロジェクト研究 研究会 (I) 防災・避難計画の数理モデルの高度化と社会実装へ向けて 136pages	February 26, 2018
MI Lecture Note Vol.79	神山 直之 畔上 秀幸	平成29年度 AIMaP チュートリアル 最適化理論の基礎と応用 96pages	February 28, 2018
MI Lecture Note Vol.80	Kirill Morozov Hiroaki Anada Yuji Suga	IMI Workshop of the Joint Research Projects Cryptographic Technologies for Securing Network Storage and Their Mathematical Modeling 116pages	March 30, 2018
MI Lecture Note Vol.81	Tsuyoshi Takagi Masato Wakayama Keisuke Tanaka Noboru Kunihiro Kazufumi Kimoto Yasuhiko Ikematsu	IMI Workshop of the Joint Research Projects International Symposium on Mathematics, Quantum Theory, and Cryptography 246pages	September 25, 2019
MI Lecture Note Vol.82	池森 俊文	令和2年度 AIMaP チュートリアル 新型コロナウイルス感染症にかかわる諸問題の数理 145pages	March 22, 2021

## シリーズ既刊

Issue	Author/Editor	Title	Published
MI Lecture Note Vol.83	早川健太郎 軸丸 芳揮 横須賀洋平 可香谷 隆 林 和希 堺 雄亮	シェル理論・膜理論への微分幾何学からのアプローチと その建築曲面設計への応用 49pages	July 28, 2021
MI Lecture Note Vol.84	Taketoshi Kawabe Yoshihiro Mizoguchi Junichi Kako Masakazu Mukai Yuji Yasui	SICE-JSAE-AIMaP Tutorial Advanced Automotive Control and Mathematics 110pages	December 27, 2021
MI Lecture Note Vol.85	Hiroaki Anada Yasuhiko Ikematsu Koji Nuida Satsuya Ohata Yuntao Wang	IMI Workshop of the Joint Usage Research Projects Exploring Mathematical and Practical Principles of Secure Computation and Secret Sharing 114pages	February 9, 2022
MI Lecture Note Vol.86	濱田 直希 穴井 宏和 梅田 裕平 千葉 一永 佐藤 寛之 能島 裕介 加藤田雄太朗 一木 俊助 早野 健太 佐伯 修	2020年度採択分 九州大学マス・フォア・インダストリ研究所 共同利用研究集会 進化計算の数理 135pages	February 22, 2022
MI Lecture Note Vol.87	Osamu Saeki, Ho Tu Bao, Shizuo Kaji, Kenji Kajiwara, Nguyen Ha Nam, Ta Hai Tung, Melanie Roberts, Masato Wakayama, Le Minh Ha, Philip Broadbridge	Proceedings of Forum “Math-for-Industry” 2021 -Mathematics for Digital Economy- 122pages	March 28, 2022
MI Lecture Note Vol.88	Daniel PACKWOOD Pierluigi CESANA, Shigenori FUJIKAWA, Yasuhide FUKUMOTO, Petros SOFRONIS, Alex STAYKOV	Perspectives on Artificial Intelligence and Machine Learning in Materials Science, February 4-6, 2022 74pages	November 8, 2022

## シリーズ既刊

Issue	Author/Editor	Title	Published
MI Lecture Note Vol.89	松谷 茂樹 落合 啓之 井上 和俊 小磯 深幸 佐伯 修 白井 朋之 垂水 竜一 内藤 久資 中川 淳一 濱田 裕康 松江 要 加葉田雄太郎	2022年度採択分 九州大学マス・フォア・インダストリ研究所 共同利用研究集会 材料科学における幾何と代数 III 356pages	December 7, 2022
MI Lecture Note Vol.90	中山 尚子 谷川 拓司 品野 勇治 近藤 正章 石原 亨 鍛冶 静雄 藤澤 克樹	2022年度採択分 九州大学マス・フォア・インダストリ研究所 共同利用研究集会 データ格付けサービス実現のための数理基盤の構築 58pages	December 12, 2022
MI Lecture Note Vol.91	Katsuki Fujisawa Shizuo Kaji Toru Ishihara Masaaki Kondo Yuji Shinano Takuji Tanigawa Naoko Nakayama	IMI Workshop of the Joint Usage Research Projects Construction of Mathematical Basis for Realizing Data Rating Service 610pages	December 27, 2022
MI Lecture Note Vol.92	丹田 聡 三宮 俊 廣島 文生	2022年度採択分 九州大学マス・フォア・インダストリ研究所 共同利用研究集会 時間・量子測定・準古典近似の理論と実験 ～古典論と量子論の境界～ 150pages	January 6, 2023
MI Lecture Note Vol.93	Philip Broadbridge Luke Bennetts Melanie Roberts Kenji Kajiwara	Proceedings of Forum “Math-for-Industry” 2022 -Mathematics of Public Health and Sustainability- 170pages	June 19, 2023
MI Lecture Note Vol.94	國廣 昇 池松 泰彦 伊豆 哲也 穴田 啓晃 縫田 光司	2023年度採択分 九州大学マス・フォア・インダストリ研究所 共同利用研究集会 現代暗号に対する安全性解析・攻撃の数理 260pages	January 11, 2024
MI Lecture Note Vol.95	Osamu Saeki Wojciech Domitrz Stanisław Janeczko Marcin Zubilewicz Michał Zwierzyński	International Project Research-Workshop (I) WORKSHOP on Mathematics for Industry 364pages	March 14, 2024
MI Lecture Note Vol.96	澤田 茉伊	2023年度採択分 九州大学マス・フォア・インダストリ研究所 共同利用研究集会 デジタル化時代に求められる斜面防災の思考法 70pages	March 18, 2024



Institute of Mathematics for Industry  
Kyushu University

九州大学マス・フォア・インダストリ研究所  
九州大学大学院 数理学府

〒819-0395 福岡市西区元岡744 TEL 092-802-4402 FAX 092-802-4405  
URL <http://www.imi.kyushu-u.ac.jp/>